早稲田大学大学院 環境・エネルギー研究科

博士学位論文

A Comprehensive Framework for Assessment and Design of Hybrid Renewable Energy Microgrid for Rural Agricultural Areas using GIS and Optimization Techniques

GIS と最適化技術による農村部の複合再エネ型マイクログリッド評価と設計の包括的な枠組み

2023 年 02 月

Tarife Rovick Pelos

早稲田大学大学院 環境・エネルギー研究科

博士学位論文

A Comprehensive Framework for Assessment and Design of Hybrid Renewable Energy Microgrid for Rural Agricultural Areas using GIS and Optimization Techniques

GIS と最適化技術による農村部の複合再エネ型マイクログリッド評価と設計の包括的な枠組み

2023 年 02 月

早稲田大学大学院 環境・エネルギー研究科
環境エネルギーネットワーク研究

Tarife Rovick Pelos

TABLE OF CONTENTS

LIST OF FIGURES

LIST OF TABLES

ABSTRACT

The Philippines faces several obstacles in electrifying its rural areas, including low population density and economic feasibility, which make connecting these areas to the grid impractical and difficult, and the negative effects of climate change, which can cause frequent power outages. The implementation of Hybrid Renewable Energy Microgrids is one solution to these challenges (HREMs). HREMs are localized power grids that can function independently of the main grid and provide electricity to small communities by utilizing renewable energy sources such as solar, wind, and hydropower, as well as a diesel generator and battery energy storage system. This combination addresses a single-type renewable energy systems' limitations by providing a consistent and stable supply of energy. By deploying HREMs in rural areas, the Philippines can improve electrification, boost economic and social development, and reduce its carbon footprint, paving the way for a more sustainable future. However, implementation of HREMs poses several challenges.

Using geographic information systems (GIS) as well as a variety of optimization strategies and models, the main objective of this study is to provide a comprehensive framework for the assessment and design of hybrid renewable energy microgrids (HREMs) for rural agricultural areas. The framework has a lot of potential applications in the Philippines, which has a lot of rural agricultural areas that haven't been electrified up to this day. These microgrids typically consist of multiple renewable energy sources, such as solar photovoltaic (PV), run-of-river (ROR) hydropower, and wind power systems, along with a backup diesel generator and a battery energy storage system (BESS). The framework attempts to address the common issues and challenges in siting, planning, and optimization of hybrid renewable energy microgrids.

In the first step of the proposed framework, a local scale assessment of multiple renewable energy sources (solar-photovoltaic, wind, and hydro power) using different GIS-based tools and algorithms is proposed. Solar resource assessment was done using the r.sun model and QGIS. For wind resource assessment, the Weather Research and Forecasting (WRF) model and ArcGIS were

used, while the Soil and Water Assessment Tool (SWAT) and head algorithm were used for hydro resource assessment. After the assessment, the renewable energy potential in the study area for different resources is mapped. Results from analysis and mapping are further evaluated and validated using data from the reconnaissance survey and secondary data.

The next stage after the assessment of renewable energies in an area is suitability analysis and site selection. To perform the suitability analysis, a method for locating hybrid wind-solar and hydro-solar renewable energy systems is presented in this thesis. Specific methodologies to determine the suitable sites for individual and hybrid renewable energy systems were also developed. The environmental acceptability and economic feasibility objectives are defined by reviewing relevant literature on renewable energy facility siting and suitability analysis, existing legislation and regulations regarding the planning and development of microgrids or any energy facilities in the Philippines, and consulting with experts in renewable energy and microgrid technology. These identified objectives/criteria are fuzzified and weighted. The weighted linear combination (WLC) technique is used to combine several targets to measure environmental acceptability and economic feasibility. Several indices that define the socio-environmental and techno-economic suitability were developed and used for the site selection.

After determining the suitable sites for hybrid renewable energy systems, another issue is addressed in this thesis, which is determining the specific locations of renewable energy generation and load demand and optimizing the electric transmission line routes between these locations. As a solution to this issue, an alternative electric transmission line (ETL) routing method for a renewable energy microgrid. The cost surface was created using a weighted ranking system and a geographic suitability index. The overall methodology is a modification of the Electric Power Research Institute-Georgia Transmission Corporation (EPRI-GTC) method for overhead electric transmission line siting based on the available data. The Analytic Hierarchy Process (AHP) was used to determine the weights of the criteria for routing. GIS-MCDA and the Least Cost Path (LCP) algorithm (Dijkstra's algorithm) produced three alternative routes based

on three perspectives: built, natural, and engineering. The final route is created by combining the alternative routes from a simple perspective.

Furthermore, in the proposed comprehensive framework, an integrated method for optimal sizing and operation of an HREM for rural agricultural communities is developed using multi-objective particle swarm optimization (MOPSO) and a multi-case power management strategy. The proposed HREM structure is composed of ROR hydropower, a solar PV system, a back-up diesel generator, and a battery energy storage system. The overall methodology for the sizing and operation optimization. The decision variables that are contained in a particle/feasible solution are the component sizes of the HREM. These variables represent the number of PV panels, capacity size of diesel generator (kW), and BESS (kWh). The three conflicting objective functions are the loss of power supply probability (LPSP), the levelized cost of energy (LCOE), and greenhouse gas emissions (GHG). The optimization produced 200 non-dominated or Pareto optimal options, four of which were selected.

Lastly, after solving the common technical issues in the design and planning of microgrids, another issue that was investigated in this thesis was improving the community's acceptance of HREM by the rural agricultural community. Several issues and factors that affect the microgrid's acceptability are investigated and studied. Based on the results of previous issues that were solved (suitable sites based on different criteria and restrictions, optimized routing, optimized component sizes, and operation of HREM), which form the "experts' opinion," a series of qualitative surveys was done in the study area, and the influence of such results on the social acceptance of HREM was analyzed.

In conclusion, important issues of the design and assessment of HREM are considered in this thesis for the sustainability, stability, and economic performance of the system. The overall framework for HREM design and assessment and the solution for each issue are proposed and applied to the rural agricultural area in the southern province of Lanao del Norte, Philippines. The results show the effectiveness of these solutions.

Chapter 1 Introduction

1.1. Background of the Study

Concerns about pollution and climate change caused by greenhouse gas emissions have generated a worldwide drive toward renewable energy and a shift away from fossil fuels. Renewable energy sources are predicted to account for a significant percentage of overall energy supply in the future, with a wide range of applications in both developed and developing countries [1-1]. The Philippines' shift to renewable energy is necessary for a variety of reasons. Due to the country's geographical peculiarities, it is especially sensitive to climate change's detrimental effects. Due to the country's archipelagic nature, which includes multiple coastal towns, increasing sea levels are a hazard, and numerous coastal communities may face flooding if the shoreline recedes due to increasing tides [1-2].

Despite the tremendous potential for renewable energy in the Philippines, renewable energy sources provided just 23.38 percent of the country's energy needs. These sources supplied just 23,326 GWh of electrical energy in 2018 against a total demand of 99,765 GWh [1-3]. For decades, the nation has been a net importer of fossil fuels to meet the country's increasing energy demand as a result of economic and population growth. The Philippine government has made efforts to advance green energy development and the use of renewable energy sources to ensure energy security. The country has hydropower, geothermal, solar photovoltaic, and other renewable energy system options [1-4].

The Philippine government has implemented several policies aimed at increasing the country's reliance on renewable energy. The Philippine Congress has enacted legislation to promote clean energy use. Among these laws are the 2001 Electric Power Industry Reform Act, the 2006 Biofuels Act, the 2008 Renewable Energy Act, and the 2008 Climate Change Act (2009). With 15.3 gigawatts (GW) of generation capacity, the Philippine government has committed to raising renewable energy's share of the energy mix to 50% by 2030 in order to achieve a 70% reduction in carbon emissions [1-5]. To facilitate and realize this transition, it is essential to evaluate renewable energy potential and renewable energy systems site suitability [1-6]- [1-7].

1.2. Motivation of the Study

The Philippines, being prone to adverse effects of climate change, needs to transition to renewable energy. Connecting rural agricultural areas to the grid is not economically feasible and the population density is sparse Since the target of this research is on the electrification of rural agricultural areas, the most feasible solution for this problem is the implementation of microgrid [1-8],[1-9]. The problem with single type is that it is prone to energy reliability issues (limitations of renewable energy due to intermittent nature, highly depended on climatic conditions). With HREM, the limitations of one type of renewable energy is being compensated with the other type of renewable energy (for example: PV only operates during daytime considering a sunny weather while hydropower and wind can operates/produce energy 24/7 [1-10]–[1-15].

With the rising demand for energy due to economic growth and increasing concerns over climate change caused by greenhouse gas emissions, the Philippine government has been pushing towards energy transition by planning to increase the share of renewable energy in the energy mix. Despite having vast renewable energy potential, only 22% of it is tapped [1-16]. Furthermore, in 2019, about five percent of the population or over 2.3 million households remain without electricity [1-17]. Most of which are in rural and remote areas where agriculture is one of the main livelihoods. To combat this issue, the Philippine government has considered the development of HREM for rural electrification, and implemented mechanisms to encourage the establishment of local energy communities [1-18], [1-19]. However, design, development and implementation of these microgrids poses several issues and challenges which are enumerated as following [1-20]–[1-27]:

1. Determining the local scale potential of multiple renewable energy sources
2. Identifying suitable sites for hybrid renewable energies
3. Optimal electric transmission line routing of identified renewable energy sites to serve local energy demand
4. Determining optimal operation and sizes of microgrid components for rural agricultural areas
5. Community participation and acceptance of microgrid

To address the aforementioned issues, this study presents a comprehensive framework for

assessment and design of HREM for rural agricultural areas using GIS and optimization techniques.

1.3. Statement of the Objectives

The general objective of this thesis is the development of a comprehensive framework for assessment and design of hybrid renewable energy microgrids for rural agricultural areas using GIS and various optimization techniques and models. Specifically, this thesis aims to achieve the following objectives:

1. To develop an integrated methodology for local scale assessment of solar energy, wind energy, and hydro energy using various GIS tools and models.
2. To create comprehensive framework for identifying suitable sites for hybrid renewable energies using GIS and Fuzzy-AHP
3. To construct an alternative optimal electric transmission line (ETL) routing of identified renewable energy sites to serve local energy demand using GIS-MCDA
4. To develop an integrated methodology for determining optimal operation and sizes of microgrid components for rural agricultural areas using MOPSO.
5. To analyze the implication of the experts' opinion on the social acceptance of microgrid by the community.

1.4. Thesis Outline

The overall comprehensive framework is shown in Figure 1.1 while the connections between chapters are shown in Figure 1.2. The outline of the thesis is as follows.

Chapter 1 describes the research problems, the background of the study, and the structure of each chapter. In this research, a comprehensive framework for assessment and design of hybrid renewable energy microgrids for rural agricultural areas is presented. The framework is composed of several processes further discussed in the following chapters:

In Chapter 2, multiple renewable energy sources at the local scale were assessed and mapped using various Geographic Information System (GIS) tools.

In Chapter 3, using GIS and Fuzzy-Analytic Hierarchy Process (AHP), a suitability analysis is performed to identify hybrid renewable energy sites.

Chapter 4 describes an optimal routing of electric transmission lines (ETL) for renewable-energy microgrids is accomplished using GIS-Multi-Criteria Decision Analysis (MCDA) and Least Cost Path (LCP) Analysis.

In Chapter 5, the sizing and operation of Hybrid Renewable Energy Microgrid (HREM) is optimized using Multi-Objective Particle Swarm Optimization (MOPSO).

Chapter 6 analyzes the implication of the experts' opinion on the social acceptance of the HREM by the community.

Lastly, Chapter 7 describes the conclusion of the whole research, future works and recommendations.

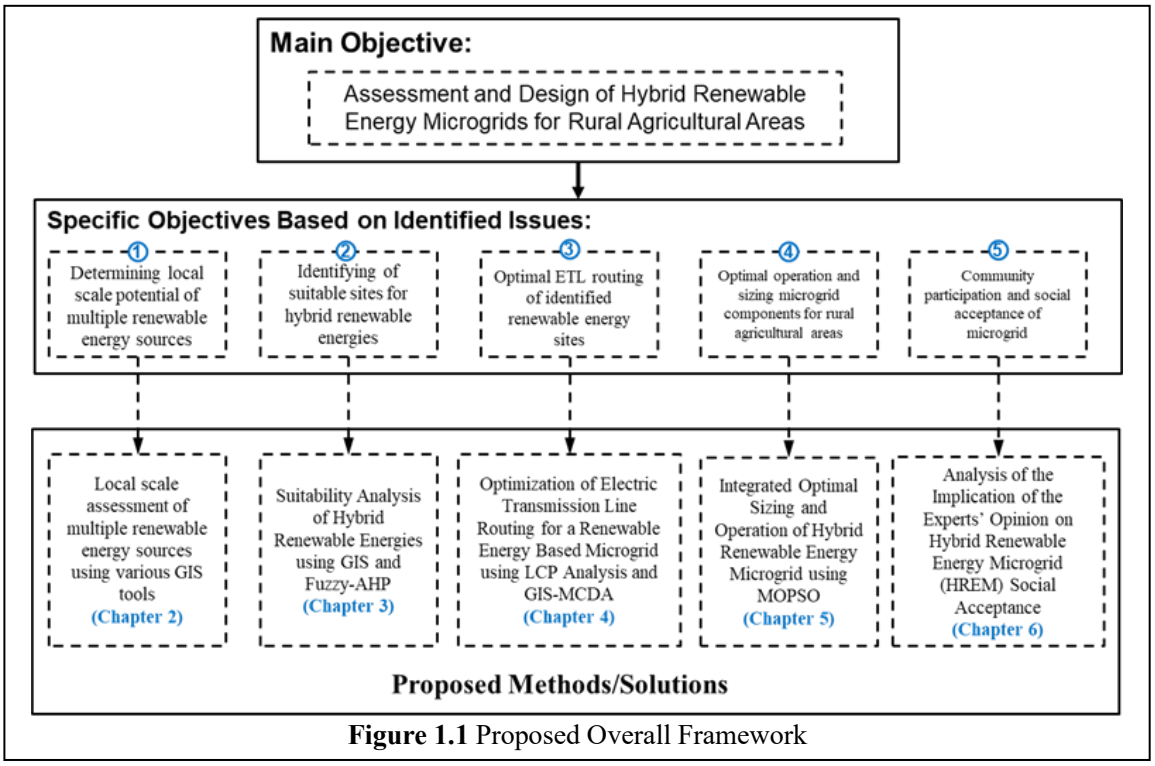

Figure 1.1 Proposed Overall Framework

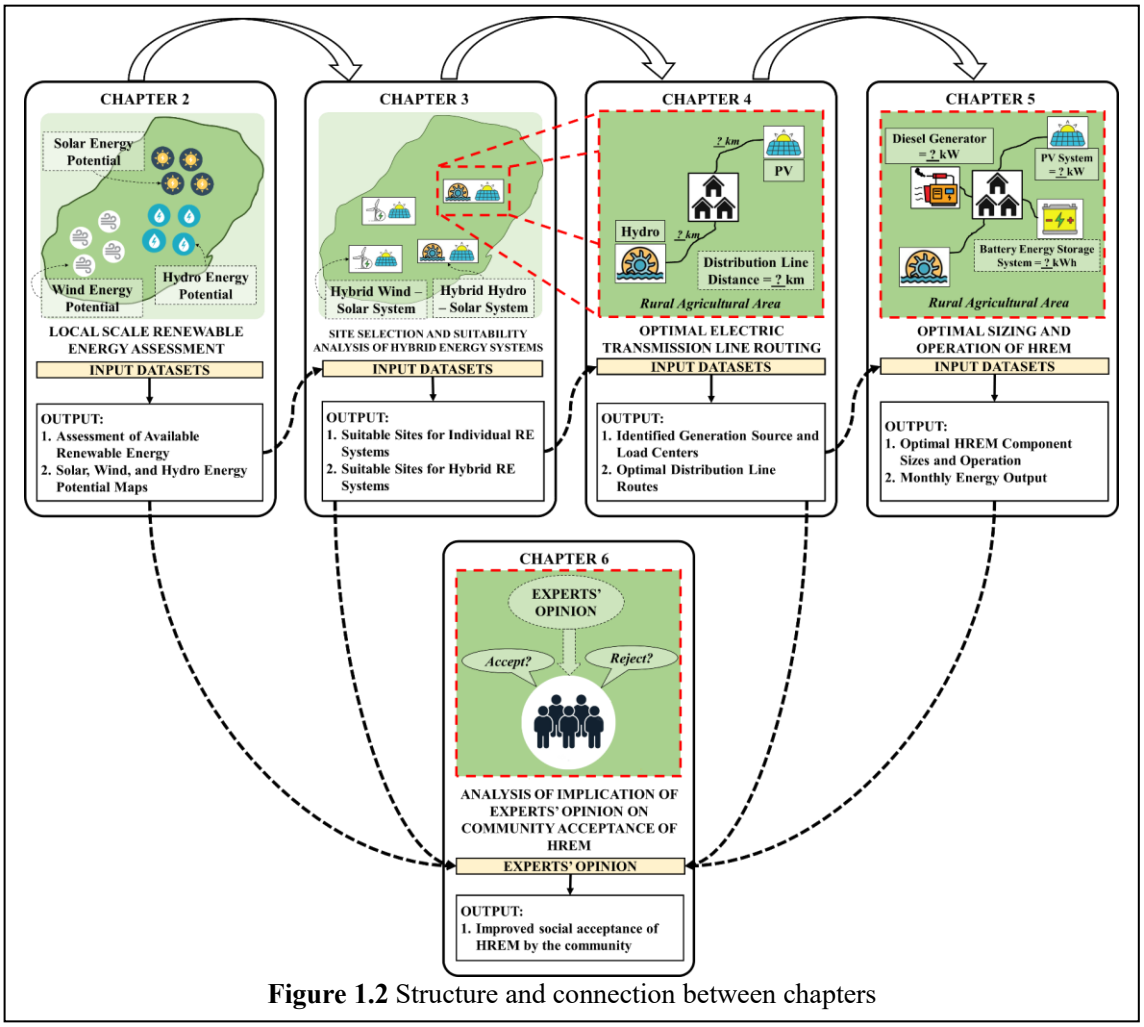

Figure 1.2 Structure and connection between chapters

Chapter 2 focuses on local scale assessment of different renewable energies using different datasets, geospatial tools and models and the output of the assessment are the renewable energy potential maps of the study area. These maps are then used as an input in the suitability analysis and site selection of hybrid energy systems using Fuzzy-AHP which is the focus of Chapter 3. The results from the suitability analysis are the sites for development of hybrid wind-solar and hybrid hydro-solar systems. One of the identified suitable sites is selected for designing HREM in a rural agricultural area and in Chapter 4, the specific locations of the renewable energy generation and the load demand are identified. The routes electric transmission line that connects the generation and load sites are optimized using AHP and LCP analysis. In Chapter 5, considering the identified available renewable energy resource, locations of the generation and load demand, the sizes of the components of the HREM and the operation are optimized using mathematical

modeling, MOPSO and a developed power management strategy. Based on the results of previous chapters (suitable sites based on different criteria and restrictions, optimized routing, optimized component sizes, and operation of HREM) which form the "experts' opinion", Chapter 6 analyzes the influence of such results to the social acceptance of HREM by the community members.

1.5. Main Contributions

The following research gaps from previous research on microgrid design, planning and assessment are addressed in this study:

1. The majority of existing studies on microgrid design and assessment only focus on one or two stages of the design process, resulting in an incomplete and fragmented understanding of the entire process. This research aims to provide a more thorough examination of the design and assessment methodology by examining multiple stages and their interrelationships.
2. Many previous studies on the modeling and design of microgrids have focused on a single type of renewable energy system, limiting their applicability and scope. This study, on the other hand, seeks to address this limitation by examining multiple renewable energy sources, which can contribute to a more diverse and resilient energy mix.
3. The majority of previous microgrid design models place an overemphasis on technical and mathematical approaches while ignoring crucial social and environmental factors. This study addressed this gap by examining the social and environmental impacts of microgrid design, which are essential for the long-term viability and sustainability of the systems.

The main contributions of this thesis are:

1. An integrated methodology for local scale assessment of solar energy, wind energy, and hydro energy using various GIS tools and models. The methodology is capable of creating local-scale and accurate maps that will aid the selection of suitable sites for renewable energy development.
2. Using a Geographic Information System (GIS) and the Fuzzy Analytic Hierarchy Process,

a complete framework for site selection of hybrid micro hydropower-solar and hybrid wind-solar energy systems has been developed (AHP). Given the constrained datasets, the created framework may be used to any sort of renewable energy.

3. An alternative ETL routing capable of optimizing distribution and transmission lines for hybrid renewable energy microgrids to serve local energy demands.
4. Comprehensive modeling and integrated methodology for optimal HREM sizing and operation using a modified multi-objective particle swarm optimization (MOPSO) algorithm capable of simultaneous optimization of multiple conflicting objectives with multiple constraints, as well as a proposed multi-case power management strategy. The datasets utilized in the optimization are real ones from a rural agricultural region, and they contain meteorological data as well as several sorts of load data from household surveys. The proposed HREM design and research methodology, which employs MOPSO optimization, is based on a cost-effective approach that aims to find the best microgrid configuration while also taking increased system reliability, operational cost minimization, and environmental impact into account through emission reduction into account.
5. Analysis of the implication of experts' opinion in improving the social acceptance of HREM by the community.

1.6. Publications

1.6.1. Journal Articles

1. **R. Tarife**, Y. Nakanishi, Y. Chen, Y. Zhou, N. Estoperez, and A. Tahud, "Optimization of Hybrid Renewable Energy Microgrid for Rural Agricultural Area in Southern Philippines," *Energies*, Volume 15, Issue No. 6, 19 March 2022. **[Chapter 5]**
2. **R. Tarife**, Y. Nakanishi,Y. Zhou, N. Estoperez, and A. Tahud, "Integrated GIS and Fuzzy-AHP Framework for Suitability Analysis of Hybrid Renewable Energy Systems: A Case in Southern Philippines," *Sustainability*, Volume 15, Issue No. 3, 28 January 2023. **[Chapter 3]**

1.6.2. Conference Papers/Oral Presentations

3. **R. Tarife**, R. Crampatanta, and W. dela Cerna, "A Sensitivity Analysis of the Weather Research and Forecasting (WRF) Model for Finding Wind Resource Potential," Asia-Pacific Journal of Science, Mathematics and Engineering (APJSME, Volume 5, Issue No. 2, pp. 23-27, 2019) **[Chapter 2]**
4. **R. Tarife**, A. Tahud, N. Estopoerez, M. Tatsuma, and Y. Nakanishi, "Integrated Geographic Information System (GIS) and Multi-Criteria Decision-Making (MCDM) for Renewable Energy Assessment and Site Suitability in Southern Philippines," in CIGRE-AORC Technical Meeting 2020 - Japan Web-Library Event 2020. **[Chapter 3]**
5. **R. Tarife**, Y. Nakanishi, J. Bondaug, R. Irosido, A. Tahud, and N. Estoperez, "Optimization of Electric Transmission Line Routing for a Renewable Energy Based Micro-Grid System using Geographic Information System (GIS) Spatial Analysis," in 2017 IEEE 6th International Conference on Renewable Energy Research and Applications (ICRERA), 2020, pp. 348 353. **[Chapter 4]**
6. Y. Chen, **R. Tarife,** Y. Nakanishi, J. Fukushima, and R. Minami, "Addressing Major Issue to Optimal Sizing and Operation of Microgrid Considering Multiple Run-of-River Hydropower", in IEEJ Power and Energy Division Conference 2022. **[Chapter 5]**

1.7. Chapter 1 References

[1-1] IRENA, "Global Energy Transformation: A roadmap to 2050," International Renewable Energy Agency, Abu Dhabi, Technical Report 978-92-9260-121-8, 2019.

[1-2] The World Bank and Asian Development Bank, "World Bank and Asian Development Bank - Climate Risk Country Profile: Philippines." Accessed: Aug. 10, 2021. [Online]. Available: https://www.adb.org/sites/default/files/publication/722241/climate-risk-country-profile-philippines.pdf

[1-3] DOST, "Department of Science and Technology: How reliant is the Philippines on renewable energy?," Department of Science and Technology, 2018. [Online]. Available:

https://www.dost.gov.ph/knowledge-resources/news/56-infographics/infographics-2018/1487-how-reliant-is-the-philippines-on-renewable-energy.html#:~:text=In%20the%20Philippines%2C%20about%2025,million%20MWh%20consumption%20from%202016.

[1-4] DOE, "Department of Energy Philippines - EMPOWERED: Renewable Energy Decade Report." Accessed: Jul. 15, 2021. [Online]. Available: https://www.doe.gov.ph/sites/default/files/pdf/renewable_energy/empowered-re-decade-report-2008-2018.pdf

[1-5] ADB, "Asian Development Bank - Philippines: Energy Sector Assessment, Strategy, and Road Map," Asian Development Bank, Aug. 2018. Accessed: May 16, 2021. [Online]. Available: http://dx.doi.org/10.22617 /TCS189616

[1-6] K. R. M. Supapo, L. Lozano, I. D. F. Tabañag, and E. M. Querikiol, "A Geospatial Approach to Energy Planning in Aid of Just Energy Transition in Small Island Communities in the Philippines," Appl. Sci., vol. 11, no. 24, p. 11955, Dec. 2021, doi: 10.3390/app112411955.

[1-7] M. Kuijpers, "How Geographic Information Systems (GIS) can fuel energy transition," Accenture, Nov. 2019. Accessed: Apr. 20, 2021. [Online]. Available: https://www.accenture.com/nl-en/blogs/insights/how-geographic-information-systems-gis-can-fuel-energy-transition

[1-8] E. I. Come Zebra, H. J. van der Windt, G. Nhumaio, and A. P. C. Faaij, "A review of hybrid renewable energy systems in mini-grids for off-grid electrification in developing countries," Renew. Sustain. Energy Rev., vol. 144, p. 111036, Jul. 2021, doi: 10.1016/j.rser.2021.111036.

[1-9] G. Falchetta, "Energy access investment, agricultural profitability, and rural development: time for an integrated approach," Environ. Res. Infrastruct. Sustain., vol. 1, no. 3, p. 033002, Dec. 2021, doi: 10.1088/2634-4505/ac3017.

[1-10] Y.-J. Choi, B.-C. Oh, M. A. Acquah, D.-M. Kim, and S.-Y. Kim, "Optimal Operation of a Hybrid Power System as an Island Microgrid in South-Korea," Sustainability, vol. 13, no. 9, p. 5022, Apr. 2021, doi: 10.3390/su13095022.

[1-11] F. Dawood, G. Shafiullah, and M. Anda, "Stand-Alone Microgrid with 100% Renewable Energy: A Case Study with Hybrid Solar PV-Battery-Hydrogen," Sustainability, vol. 12, no.

5, p. 2047, Mar. 2020, doi: 10.3390/su12052047.

[1-12] N. M. Kumar, S. S. Chopra, A. A. Chand, R. M. Elavarasan, and G. M. Shafiullah, "Hybrid Renewable Energy Microgrid for a Residential Community: A Techno-Economic and Environmental Perspective in the Context of the SDG7," Sustainability, vol. 12, no. 10, p. 3944, May 2020, doi: 10.3390/su12103944.

[1-13] J. Olmedo-González, G. Ramos-Sánchez, E. P. Garduño-Ruiz, and R. de G. González-Huerta, "Analysis of Stand-Alone Photovoltaic—Marine Current Hybrid System and the Influence on Daily and Seasonal Energy Storage," Energies, vol. 15, no. 2, p. 468, Jan. 2022, doi: 10.3390/en15020468.

[1-14] F. Canziani, R. Vargas, M. Castilla, and J. Miret, "Reliability and Energy Costs Analysis of a Rural Hybrid Microgrid Using Measured Data and Battery Dynamics: A Case Study in the Coast of Perú," Energies, vol. 14, no. 19, p. 6396, Oct. 2021, doi: 10.3390/en14196396.

[1-15] M. I. Nazir, I. Hussain, A. Ahmad, I. Khan, and A. Mallik, "System Modeling and Reliability Assessment of Microgrids: A Review," Sustainability, vol. 14, no. 1, p. 126, Dec. 2021, doi: 10.3390/su14010126.

[1-16] J. Enano, "Philippines, ASEAN must tap solar, wind to meet rising electricity demand — report," Institute for Climate and Sustainable Cities, Jul. 2022. [Online]. Available: https://icsc.ngo/philippines-asean-must-tap-solar-wind-to-meet-rising-electricity-demand-report/

[1-17] J. Peralta, "Over 2.3 million households remain without electricity – NEA," CNN Philippines, Aug. 27, 2019. Accessed: Mar. 27, 2022. [Online]. Available: https://www.cnnphilippines.com/news/2019/8/27/filipino-households-electricity-national-electrification-administration.html

[1-18] Electric Power Industry Management Bureau, "Missionary Electrification Development Plan for 2009-2013," Department of Energy, Dec. 2008. [Online]. Available: https://policy.asiapacificenergy.org/sites/default/files/2009%20MEDP%20fourth%20draft.pdf

[1-19] J. C. Altomonte and H. S. Guinto, "How can microgrids help the Philippines' energy transition? Adapting the Institutional Analysis and Development (IAD) framework for

microgrid development," IOP Conf. Ser. Earth Environ. Sci., vol. 997, no. 1, p. 012012, Feb. 2022, doi: 10.1088/1755-1315/997/1/012012.

[1-20] Wencong Su, Zhiyong Yuan, and Mo-Yuen Chow, "Microgrid planning and operation: Solar energy and wind energy," in IEEE PES General Meeting, Minneapolis, MN, Jul. 2010, pp. 1–7. doi: 10.1109/PES.2010.5589391.

[1-21] A. M. Rosso-Cerón and V. Kafarov, "Barriers to social acceptance of renewable energy systems in Colombia," Curr. Opin. Chem. Eng., vol. 10, pp. 103–110, Nov. 2015, doi: 10.1016/j.coche.2015.08.003.

[1-22] D. Akinyele, J. Belikov, and Y. Levron, "Challenges of Microgrids in Remote Communities: A STEEP Model Application," Energies, vol. 11, no. 2, p. 432, Feb. 2018, doi: 10.3390/en11020432.

[1-23] B. Resch et al., "GIS-Based Planning and Modeling for Renewable Energy: Challenges and Future Research Avenues," ISPRS Int. J. Geo-Inf., vol. 3, no. 2, pp. 662–692, May 2014, doi: 10.3390/ijgi3020662.

[1-24] D. R. Prathapaneni and K. P. Detroja, "An integrated framework for optimal planning and operation schedule of microgrid under uncertainty," Sustain. Energy Grids Netw., vol. 19, p. 100232, Sep. 2019, doi: 10.1016/j.segan.2019.100232.

[1-25] S. R. Sivarasu, E. Chandira Sekaran, and P. Karthik, "Development of renewable energy based microgrid project implementations for residential consumers in India: Scope, challenges and possibilities," Renew. Sustain. Energy Rev., vol. 50, pp. 256–269, Oct. 2015, doi: 10.1016/j.rser.2015.04.118.

[1-26] M. M. Kamal, I. Ashraf, and E. Fernandez, "Planning and optimization of microgrid for rural electrification with integration of renewable energy resources," J. Energy Storage, vol. 52, p. 104782, Aug. 2022, doi: 10.1016/j.est.2022.104782.

[1-27] S. Choudhury, "A comprehensive review on issues, investigations, control and protection trends, technical challenges and future directions for Microgrid technology," Int. Trans. Electr. Energy Syst., vol. 30, no. 9, Sep. 2020, doi: 10.1002/2050-7038.12446.

Chapter 2 Local-Scale Assessment of Multiple Renewable Energy Sources Using Various GIS Tools and Models

2.1. Introduction

For the Philippines' distant barangays in particular, exploiting micro-hydro resources to offer an alternate energy source is seen to be a feasible approach [2-1]. The creation of a framework for assessing possible locations for the aforementioned resource is necessary since the technology for harvesting micro-hydro is not yet well established [2-2]. A reliable, sustainable, and clean energy source is hydropower [2-3]. Most of this resource is off-grid, enabling rural populations to obtain electricity for the improvement of their means of subsistence and way of life. A potential answer to the country's economic problems is to provide communities and developers enough information about the location of the resource [2-4], [2-5].

The Philippines also aspires to become a powerhouse for solar production in Southeast Asia [2-6]. Recently, several solar power plants have been constructed all throughout the nation. Solar energy is a smooth-running, almost maintenance-free energy source. Electricity is produced utilizing radiant sunshine, which lowers pollutants and CO^2 emissions [2-7]. Data on solar energy illustrate the quantity of available solar energy in a certain region of the country at a particular moment [2-8]. It is required for precise financial analysis as well as the design and sizing of solar energy systems [2-9], [2-10]. Some models are also utilized in GIS and other softwares, like the Solar Analyst tool in ArcGIS, RETScreen and PVsyst [2-11]–[2-14].

The capacity to effectively analyze and characterize available wind resources is a critical component in the development, location, and operation of a wind farm [2-15]. Climate is one of numerous meteorological elements that should be addressed when developing a model for assessing wind resource [2-16], [2-17]. The Philippines has a tropical marine climate with rainy and dry seasons. It is influenced by three primary air masses: the Northeast Monsoon (Amihan), the North Pacific Trade, and the Southwest Monsoon. The wind resource of the nation is greatly impacted by its latitude, height, and archipelagic character. Despite the availability of wind energy as a potential renewable energy resource in the nation, wind power investment and development encounter several obstacles. These include high supply and equipment costs owing to a lack of

local manufacturers and suppliers, the need to develop technical expertise, and inadequate public awareness initiatives regarding the advantages of the community.

2.2. Overall Methodology for the Local-Scale Multiple Renewable Energy Assessment

The assessment of renewable energy resources on a smaller scale at a local level, using geospatial tools, methods, and models is one of the most important aspects of the entire methodology of this research. Because the objectives of this research include the development of a methodology and the creation of local-scale resource maps and maps of potential renewable energy development sites, the research workflow was supplemented by visualization of the results. This was done because the research workflow was supplemented by visualization of the results. The entire process for the evaluation of numerous renewable energy at a local scale is shown in Figure 2.1 below.

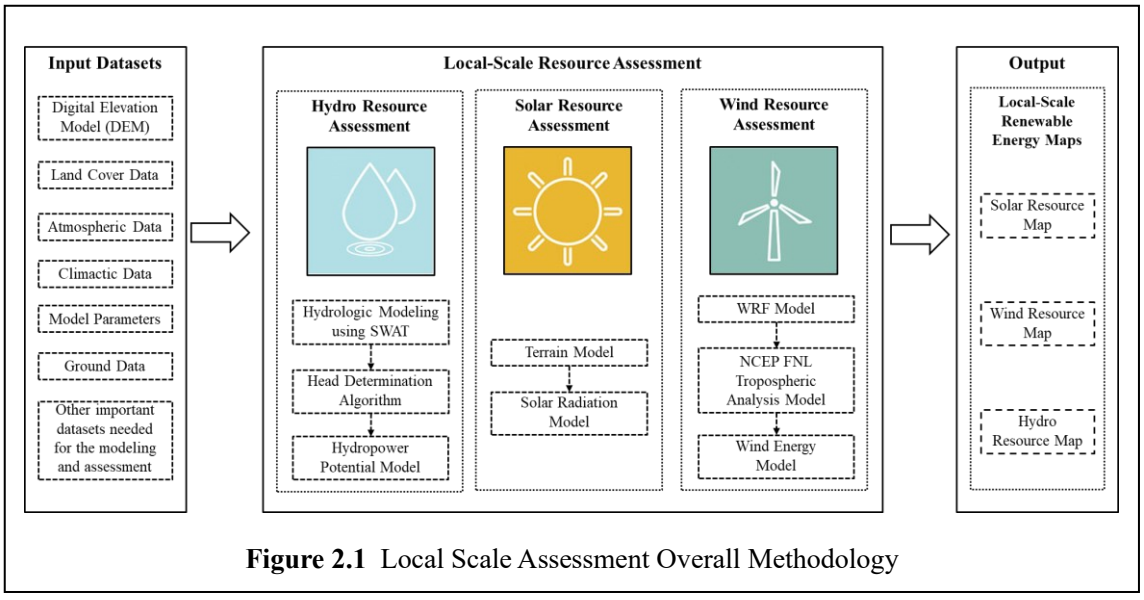

Figure 2.1 Local Scale Assessment Overall Methodology

The first goal of the research methodology was on gathering data and setting up the input datasets. The main input dataset for all the investigated renewable energy sources was the digital elevation model. There were numerous models used during the procedure. Each model has a different level of accuracy and spatial resolution. The technique includes selecting the appropriate elevation model for each assessment of a renewable energy resource. A number of datasets are

used to enhance the elevation model, depending on the renewable energy source.

A hydrologic model and a terrain analysis must be used in combination to identify the hydropower resource in order to compute hydropower. The hydrologic model uses soil data, high-resolution digital elevation models (DEMs), with spatial resolution of 30m x 30m, land use/land cover maps, and long-term climate data to generate the long-term anticipated discharge. The delineation of the river and the elevation model are required for a specifically developed technique to determine the head.

The solar energy model needs the high-resolution DEM from which the slope, aspect, and horizon data are generated. These topographical data are combined with Linke turbidity data and atmospheric factors to produce the solar radiation data.

The wind energy model requires a large amount of meteorological and tropospheric data in order to anticipate the wind speed from which the wind energy is derived. Then, high-resolution digital elevation models are used to simulate the site-specific urban wind energy potential in three dimensions.

Each renewable energy resource assessment model's input datasets are all georeferenced and standardized to fulfill the model's requirements. After the input datasets were prepared, each renewable energy source was assessed using the model that best described the surface where the resources were identified as well as outside data that influenced the resource's growth and renewal.

The topography of the physical-based hydrologic model for evaluating hydropower resources is determined by the definition of watersheds, rivers, and monitoring stations. The landscape is enhanced with land cover, soil, and slope data in order to depict the flow of water as it moves through the land surface, via water bodies, and into the sky. The hydrologic model describes the movement of water through the atmosphere using databases of long-term climate data. The hydrologic model was used to produce the discharge data.

The difference in elevation that the body of water drops via from the land is also determined using the head determination technique. A model of hydroelectric power is then created using the quantity of water that falls across river reaches.

A high-resolution DEM was used to provide the topographical elements of slope, aspect, and

horizon for the assessment of solar energy resource potential. Additional variables are added to the air's absorption and scattering of solar energy, which is represented by Linke turbidity, in order to use the solar radiation model. The model computes the global horizontal irradiance, which is the amount of energy the surface receives from the sun, under both clear-sky and real-sky conditions.

2.3. Study Area

The study area is the province of Lanao del Norte, Philippines shown in Figure 2.2. The province is located at 7.8722° N latitude and 123.8858° E longitude. It has a total population of 676,395 (as of 2015) and covers a total area of 4,159.94 square kilometres (1,606.16 sq mi) occupying the southwestern section of the Northern Mindanao region in Mindanao. The province is bordered by Lanao del Sur to the southeast, Zamboanga del Sur to the west, Illana Bay to the southwest, Iligan Bay to the north, Iligan City to the northeast, and the Panguil Bay to the northwest. Lanao del Norte comprises 22 municipalities and 1 highly urbanized city. It has diverse flora and fauna. Lanao del Norte is a rugged province that ranges from the coastal shorelines in the north to the high plateaus and mountains in the south. With regards to the electrification status of the province, the electrification rate under the two distribution utilities Iligan Light and Power Incorporated (ILPI) and Lanao del Norte Electric Cooperative (LANECO) is 73.89% as of 2018. Only 149,379 households are electrified out of 202,151 households.

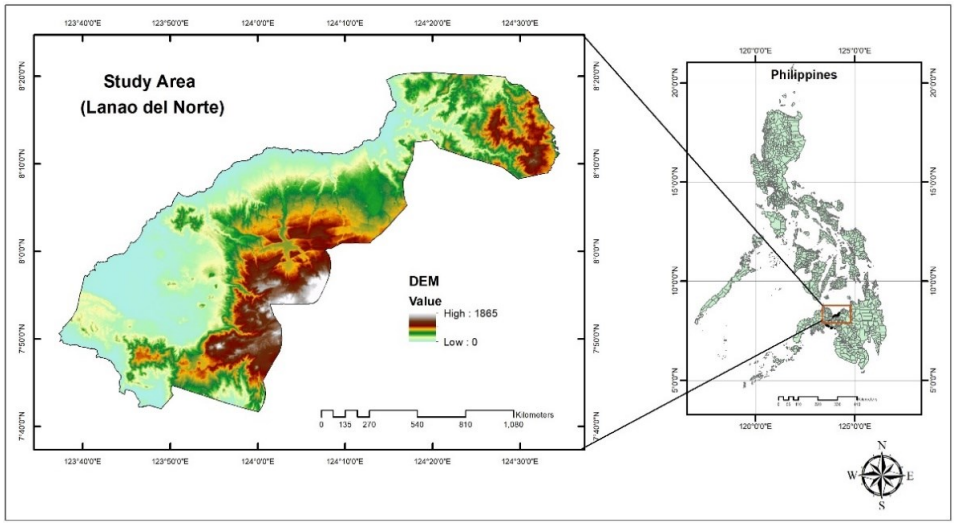

Figure 2.2 Study Area – Lanao del Norte, Philippines

2.4. Datasets and Pre-processing

ArcSWAT requires various inputs, each of which must be structured in databases and be comprehensive in order for ArcSWAT to accept the data for processing. The key input datasets for terrain characterisation are land use/land cover (LULC), soil, and slope. These three datasets are required for the development of the hydrologic response units (HRUs), which serve as the foundation for the equations guiding the hydrologic processes inherent in the model [2-18].

The LULC dataset was derived from NREL's GST developed for the DOE. The GST offers publicly accessible information; the data from the GST are necessary in decision-making for renewable energy development in the Philippines. The GST LULC dataset is provided by NAMRIA (as was stated in the metadata). As seen in Table 2.1, the land use shapefile comprises 14 land use indces. The soil dataset was collected from the Bureau of Soil and Water Management's (BSWM) Department of Agriculture-Bureau of Agricultural Research Spatial Analysis and Information Laboratory (DA-BARSAIL).

Data for the weather stations was given by PAGASA, the Advanced Science and Technology Institute (ASTI), and the NOAA. SWAT requires the following meteorological data: precipitation, temperature, relative humidity, sun radiation, and wind speed. The solar radiation data were obtained by analyzing the terrain using the r.sun model. The remaining datasets were produced using NCDC and ASTI information.

Table 2.1 Land use index for local land use/land cover data

Land Use Index	Land Use
1	Annual Crop
2	Built-up
3	Closed Forest
4	Fallow
5	Fishpond
6	Grassland
7	Inland Water
8	Mangrove Forest
9	Marshland/Swamp
10	Open/Barren
11	Open Forest
12	Perennial Crop
13	Shrubs
14	Wooded Grassland

2.5. Hydro Resource Assessment

The ArcSWAT model, namely the ArcGIS-based soil and water assessment tool, is used to compute theoretical hydropower potential. A python-based application is used in addition to the hydrologic model to determine the head or difference in elevation. Power is computed, classified, and mapped when these two parameters are obtained. The flowchart below shown in Figure 2.3 demonstrates the conventional method for evaluating hydropower resources in run-of-river systems.

The process's administrative boundary was given by the Global Administrative Areas (GADM), while the watershed delineation was provided by the Disaster Risk and Exposure Assessment for Mitigation (DREAM) Program. In this study, the discharge and head are the two essential variables being simulated for resource evaluation.

The SWAT hydrology model, which is included into the ArcGIS GIS platform, was used to analyze run-of-river hydropower resources. The simulations are run from 2000 to 2015, including three years of warm-up runs. Climate data, soil data, land cover data, and discharge data for the model are acquired from governmental bodies in charge of developing them. SAR was used to generate the DEM that was used in the method. The soil data is compiled from both local (from the Bureau of Soil and Water Management) and global sources (from the Digital Soil Map of the World). The land use/land cover data in the model is derived from the National Renewable Energy Laboratory's (NREL) Geospatial Toolkit (GST), which is made accessible via the National Mapping and Resource Information Authority (NAMRIA). Climate data is provided by the Philippine Atmospheric Geophysical and Astronomical Services Administration (PAGASA) in the form of monthly data derived from raw daily data gathered from existing weather stations.

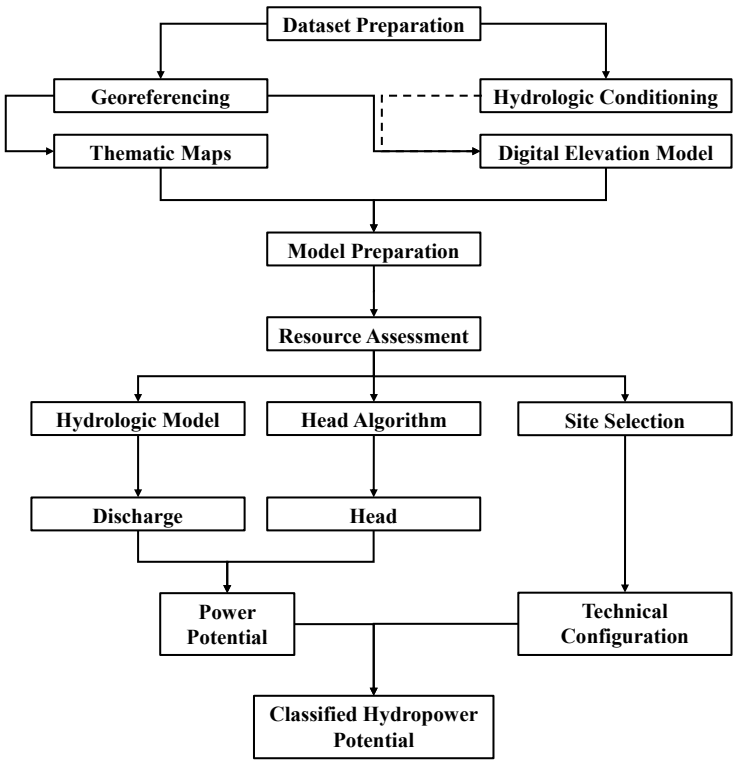

Figure 2.3 Hydro Resource Assessment Flowchart

Only sites with actual discharge data from DPWH gauging stations can use the flow validation. Few sites are used for field data collecting for flow measurements and validation, and the findings are instantaneous flow measurements. The head determination method based on algorithm by [2-19] is developed in Python and then turned into an ArcPy script for usage in an ArcGIS toolbox and an executable file for standalone use.

The input for the method is collected from the same DEM as the hydrologic model before any hydrologic conditioning. It is clarified which DEM is to be used in the head algorithm when hydrologic conditioning is applied to the original DEM, producing a reconditioned DEM of the same study area. Sample processing is finished, and the findings using the original and restored DEMs show significant differences.

However, using the original DEM for the head to get the genuine elevation values rather than the "filled" values for the depression areas is logically sounder. The program analyzes the landscape using a minimum height difference of 20 meters and horizontal lengths up to 1000 meters at intervals of 100 meters.

Maps that depict the locations of areas with potential development resources also display the hydropower resource assessment. The output of the maps is based on the head of the potential areas, which has a predicted flow of 80% exceedance and 80% cautious efficiency.

2.5.1 Hydrological Modeling, ArcSWAT and Head Determination Algorithm

The hydrologic model to predict flow and the head determination algorithm to identify a site with sufficient head to generate hydropower are the two main techniques used in the hydropower resource assessment process. To construct potential growth zones and display the results visually, the method is often integrated with GIS. The hydrologic model elements that were utilized to determine each river reach's discharge value are shown in Figure 2.4.

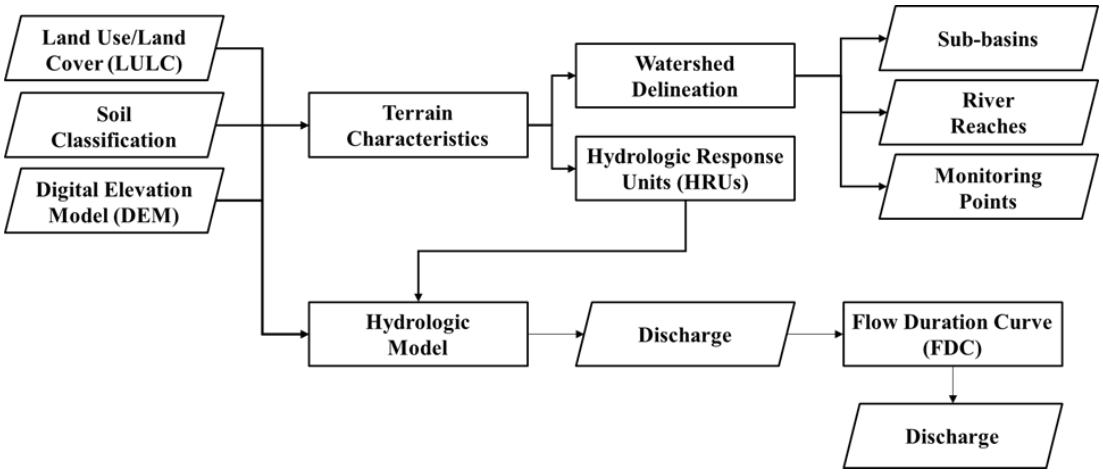

Figure 2.4 Hydrological Modeling Flowchart

The main model used in this study to assess the hydropower resources is ArcSWAT, a hydrologic Soil and Water Assessment Tool (SWAT) that is connected to GIS. The ArcSWAT modeling flowchart is shown in Figure 2.5.

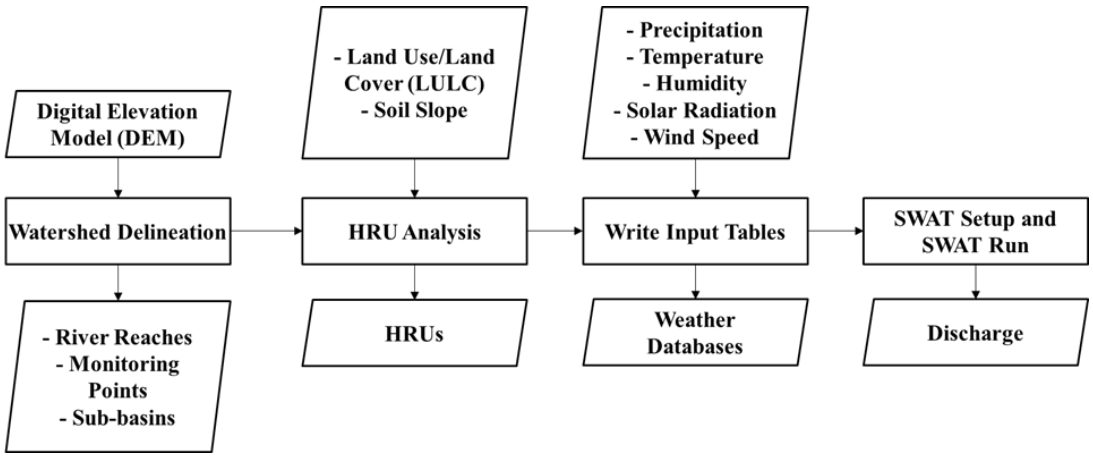

Figure 2.5 ArcSWAT Modeling Flowchart

The local watershed data layer's buffered extent must be used to reduce the DEM input for the watershed delineation module. This module uses ArcHydro, a hydrological program built on ArcGIS, to automate the stream delineation process. A stream is defined as the minimum number of cells that must accumulate in order for it to be deemed a stream, and the stream vector is defined in accordance with that specification. Filling sinks modifies abrupt changes in elevation to facilitate flow. Flow accumulation depicts areas where water will most likely accumulate based on the terrain. The sub-watersheds are then determined using the catchment areas of the identified streams. Finally, databases are built for SWAT to utilize after the run for each river reach.

Head is the term for the height difference at which water falls to produce hydropower. As shown in Figure 2.6, this quantity may be calculated as the difference between the virtual intake and the virtual powerhouse. To work with ArcGIS, the Head Determination Algorithm was first created in Python and then translated to an ArcPy script. The two primary inputs of the program are the DEM and the flow vector file from the ArcSWAT simulation.

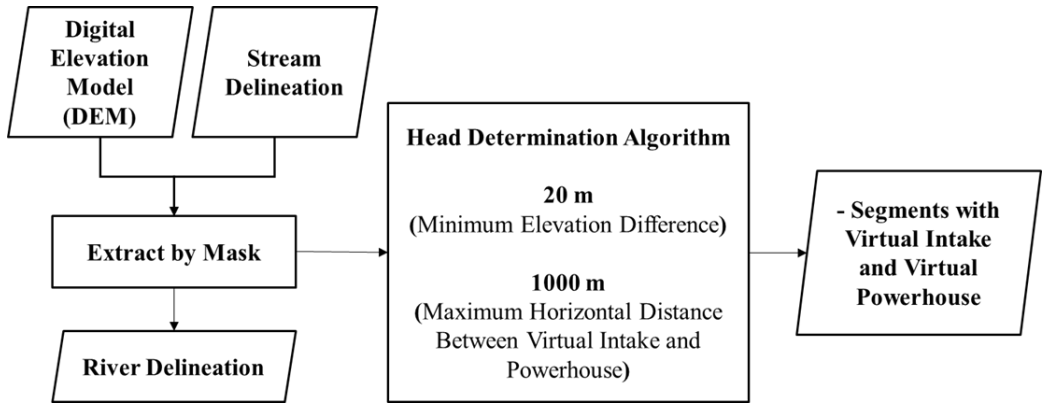

Figure 2.6 Head Determination Algorithm Flowchart

2.5.2 Hydropower Potential Computation and Classification

As shown in Figure 2.7, GIS is used to obtain river segments with hydropower potential. By adding a property that includes the flow of the river reach to the head segments, the river flow values that geographically match the head dataset are merged. A second property is added to hold the power that is calculated by dividing the head value by the corresponding flow, accounting for gravitational pull and conservative efficiency. All of the disconnected portions are disregarded. The matching categorization is then included as an extra property to the final vector file once the theoretical power potential has been determined.

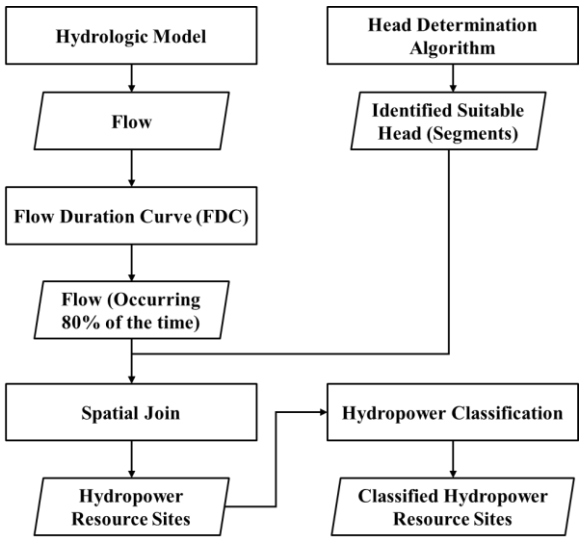

Figure 2.7 Hydropower Potential Computation and Classification Flowchart

2.6. Solar Resource Assessment

For solar resource assessment, using the r.sun model, the theoretical solar energy potential was calculated at the local scale. The open-source GRASS GIS-based r.sun model was used to estimate solar energy availability. This model of solar radiation and irradiance computes solar irradiation raster maps for a particular day, latitude, surface conditions, and air conditions. The map history file stores solar parameters, such as dawn and sunset timings, declination, extraterrestrial irradiance, and daylight duration. For the purpose of calculating the sun incidence angle and/or irradiance raster maps, a local time and the topographic shadowing effect are included [2-20]. The primary inputs for the model were DEMs produced from SAR and DSMs acquired from LiDAR. The tools in GRASS GIS were used for pre-processing. Figure 2.8 shows the overall process for assessment of the solar energy resource.

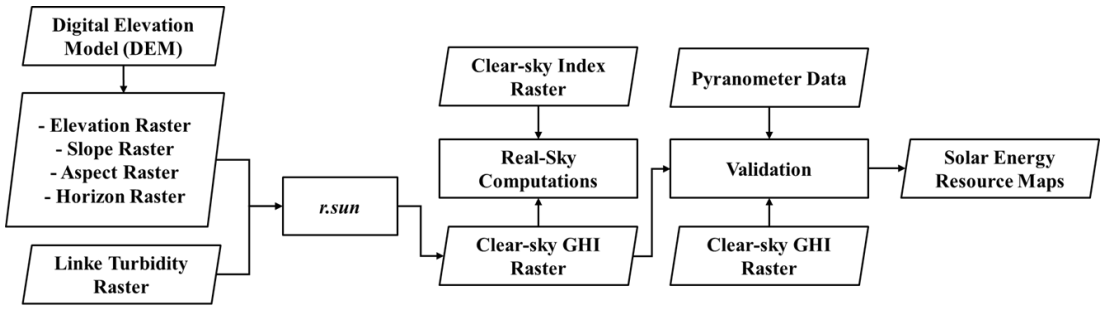

Figure 2.8 Solar Resource Assessment Flowchart

The steps taken in assessing the solar energy resource included data collection and pre-processing, computation of clear-sky radiation components, computation and interpolation of the clear-sky index, computation of real-sky solar radiation components, and validation of computed real-sky radiation components using ground truth data.

DEM and linke turbidity values made up the data that were gathered. The Linke Turbidity values were interpolated using the Regularized Spline with Tension method, and the slope, aspect, and horizon rasters were produced using the DEM (r.vol.rst in GRASS GIS). These pre-processed data were used as inputs for the r.sun model in GRASS GIS.

The clear-sky index (Kc) is a value that contrasts simulated and real clear-sky radiation observed from the ground. The clear-sky index for this study was calculated using the ratio of observed to simulated solar radiation.

$$K_C = \left(\frac{radiation_{measured}}{radiation_{modeled}}\right) \quad (2-1)$$

Shown in Figure 2.9, the clear-sky index raster are then produced by combining satellite images, long-term beam and diffused solar radiation data, and other sources. Data on solar radiation obtained from the ground are used to construct the clear-sky index. Then, these values were interpolated using GRASS GIS's Regularized Spline with Tension tool (v.surf.rst). As a result, the Clear-sky Index raster was produced.

Figure 2.9 Flowchart for Generating Clear-sky Index Raster

2.7. Wind Resource Assessment

For the assessment of the wind resource, the mesoscale assessment approach was used which is a modification of the framework done by [2-21]. The processing at the mesoscale was carried out using WRF. It is more confined on a smaller scale. To simulate the wind speed resource accessible in the whole Philippines and local-scale settings, a mesoscale wind resource assessment using the WRF Model version 3.6.1 was conducted. The Philippines option featured a spatial and temporal resolution of 4 km and 3 hours, compared to 1 km and hourly for the local-scale setting. Both setups used the same vertical resolution, meteorological and geographic information, setup of the parameterization system, and nesting mechanism. The flowchart for the local scale wind resource assessment is shown in Figure 2.10.

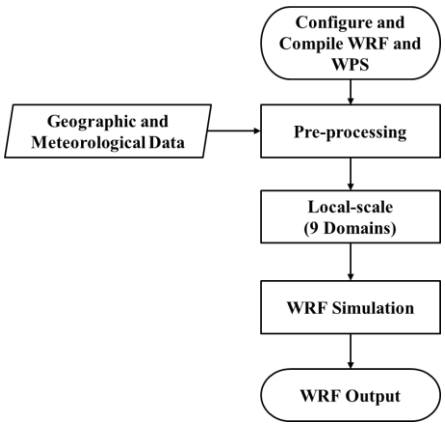

Figure 2.10 Wind Resource Assessment Flowchart

2.7.1. WRF Output Extraction

There are several techniques to extract and modify data from the WRF output. Consequently, the Python programming language was used in this study. The two most often used modules were TkInter and Netcdf4-python. While the second module creates a program interface, the first module developed by Phil-LiDAR 2 Project provides a Python interface for the netCDF C library. The application that was designed supports both single point extraction and multi-point extraction. The values are taken from a single point by a single point for each iteration (latitude and longitude). All of the extracted variables for the single point extraction type were at a height of 10 meters, with the exception of temperature (2 m above the ground). This will serve to verify the information that has been gathered. The temperature, latitude, longitude, x- and y-wind speeds, wind direction (degrees), wind speed (vector magnitude), and wind speed (vector magnitude) were all obtained. The flowchart for WRF output extraction is shown in Figure 2.11.

The wind resource assessment will use the output, while the multi-point averages data from all points in a domain from the input start date to the output end date. Longitude, latitude, scalar and vector average wind speeds, wind power density (at 80 and 100 meters), temperature, and the number of occurrences were all gathered (80- and 100-m height).

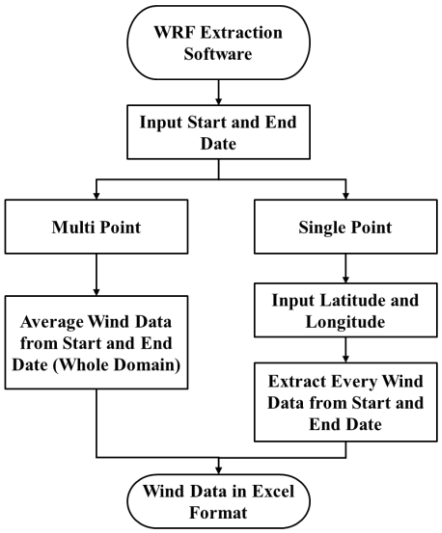

Figure 2.11 WRF Extraction Flowchart

2.8. Results and Discussion

This section discusses all the results of the local scale assessment of multiple renewable energies.

2.8.1. Hydro Resource Assessment Results

The primary result of the assessment of the hydropower resource is the surface discharge, which is the output of the hydrologic model. The SWAT model is a physical-based model that incorporates each procedure in the corresponding theoretical model of the water cycle. The input database includes local land cover, soil, topography, and climatic data in order to reflect plant growth, infiltration rate, and other processes necessary to estimate water flow within the study area. The output database stores the surface flow, groundwater flow, sedimentation, and other discoveries.

A vector file comprising sites with an elevation difference of at least 20 meters and a horizontal distance difference of at least one kilometer is produced when the Head Determination Algorithm is applied to river elevation data (separated into ten vector files for each distance range). Each feature in the generated vector file is a linear feature that connects the associated

virtual powerhouse downstream with the virtual intake upstream, fulfilling the requirements for the right head to generate adequate hydropower. Figure 2.12 displays the zoomed-in sample result, whereas Figure 2.13 displays sample output from the head determination algorithm overlayed on ArcGIS Earth.

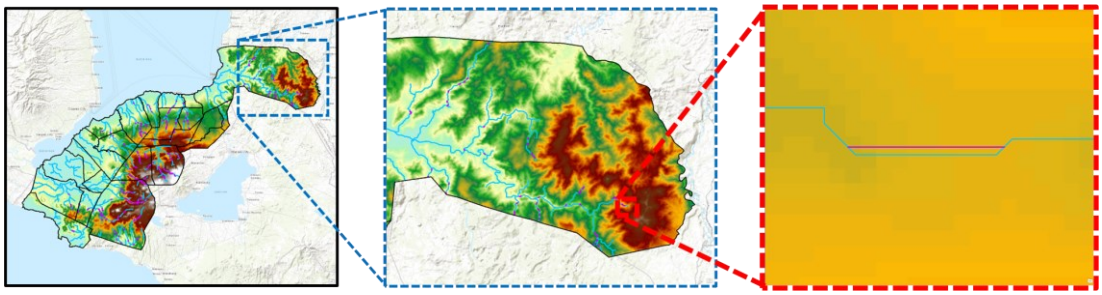

Figure 2.12 Sample Output from Head Determination Algorithm Zoomed-in

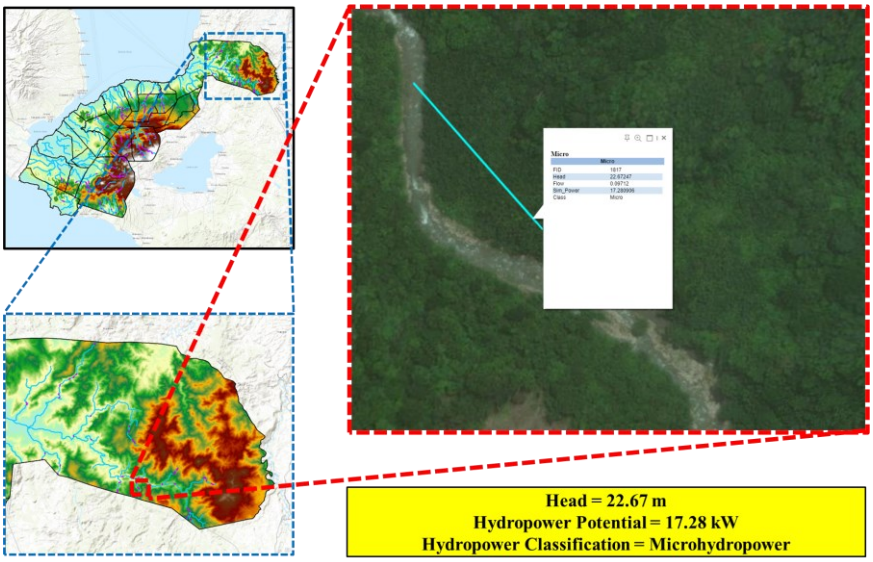

Figure 2.13 Sample Output from Head Determination Algorithm Overlayed on ArcGIS Earth

The hydropower resource assessment result illustrates potential sites for hydropower production based on the theoretical potential of the river reach for a run-of-river system. The controlling mathematical model is used to determine the theoretical potential given the river flow and the associated head value.

The flow that happens 80% of the time during simulation and the associated outcome of the

head determination technique utilizing the simulated flow from the hydrologic model, as previously mentioned, are used to create the hydropower potential. The theoretical potential estimate includes an 80 percent technical efficiency as specified by the DOE. Combining the head vector data with the simulated flow vector data produces overlapped zones from which the hydropower potential may be computed. The hydropower potential sites also include ten vector files since the head determination method produces ten of them. The result maps for the hydro resource assessment for various penstock lengths are shown in Figure 2.14 to Figure 2.16.

Power_100			
			Reach
Minimum Power	0.015	kW	172
Maximum Power	432.443	kW	230

Power Distribution	Count	Percentage
Pico	266	10%
Micro	1,975	77%
Mini	320	12%
Small	0	0%
Medium	0	0%
Large	0	0%

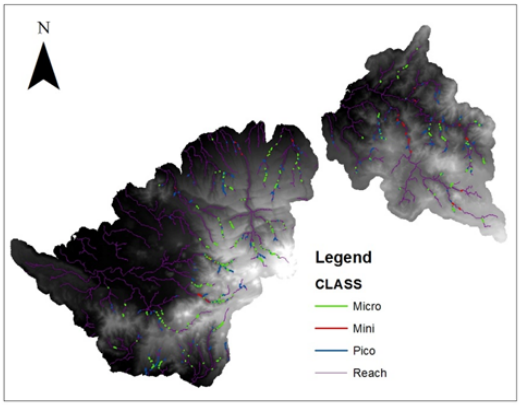

Figure 2.14 Hydro Resource Map of Lanao del Norte – 100m Penstock Length

Power_500			
			Reach
Minimum Power	0.018894	kw	182
Maximum Power	1739.836	kw	41

Power Distribution	Count	Percentage
Pico	2750	7%
Micro	24745	65%
Mini	10558	28%
Small	34	1%
Medium	0	0%
Large	0	0%

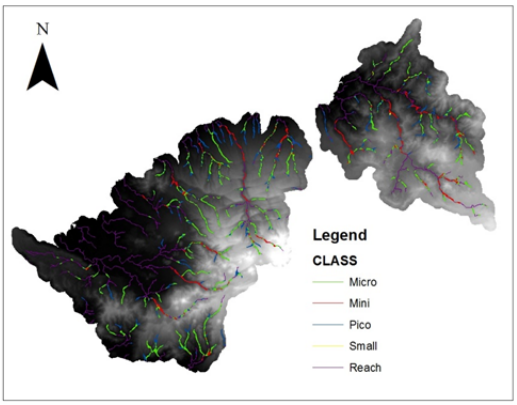

Figure 2.15 Hydro Resource Map of Lanao del Norte – 500m Penstock Length

Power_1000		
		Reach
Minimum Power	0.047139 kW	182
Maximum Power	2373.49 kW	41

Power Distribution	Count	Percentage
Pico	2486	4%
Micro	30953	52%
Mini	26281	44%
Small	310	1%
Medium	0	0%
Large	0	0%

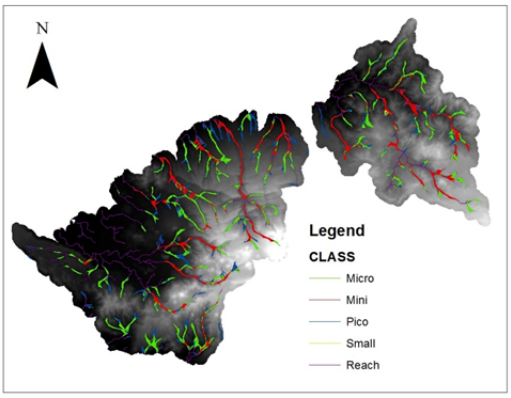

Figure 2.16 Hydro Resource Map of Lanao del Norte – 1000m Penstock Length

2.8.2. Solar Resource Assessment Results

Using the aforementioned techniques and approaches, monthly clear-sky GHI rasters were constructed for the study area. It was unnecessary to construct a yearly clear-sky GHI raster since it is the first outcome of the procedure and is not yet relevant in terms of judging the site's potential because calculated monthly values are still for perfect circumstances. The lowest value, 565.636 Wh/m^2/day, was recorded in January, while the highest value, 9,349.52 Wh/m^2/day, was also recorded in January. From January through May, the monthly average GHI readings show an upward trend. In June, the value drops, then gradually rises until September. Following that, the levels gradually decline until December. Figure 2.17 shows the trend of monthly average values, as well as the trend of the values of the lowest and highest monthly values. The high average values seen in clear-sky circumstances are indicative of the country's solar resource.

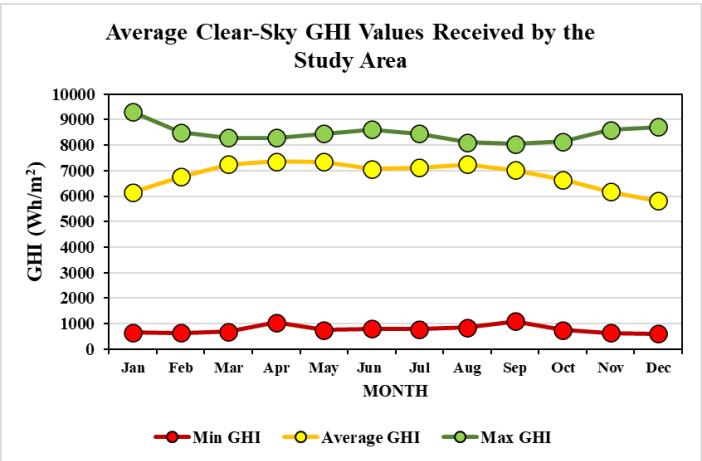

Figure 2.17 Trend of the minimum, maximum, and mean monthly values for the study area

To determine whether the sky is clear or cloudy, the clear-sky index, or Kc, was utilized. A Kc value of approximately 1.0 indicates either a relatively clear sky or a model value that is quite close to the ground-based solar radiation measurement. In the majority of the country, this is accurate during the months of April, May, and August. In other months, kc values of approximately 0.5 and overcast skies are typical. With the highest mean values of 5462.10 Wh/m^2/day and 5190.03 Wh/m^2/day in the summer months of April and May and the lowest mean value of 3226.70 Wh/m^2/day in the winter months of January and February, the estimated available solar energy fluctuated seasonally. The highest anticipated solar energy is for the month of February, at 7366.86 Wh/m^2/day, while the lowest is for the month of January, at 283.13 Wh/m^2/day. The average GHI monthly values are shown in Figure 2.18.

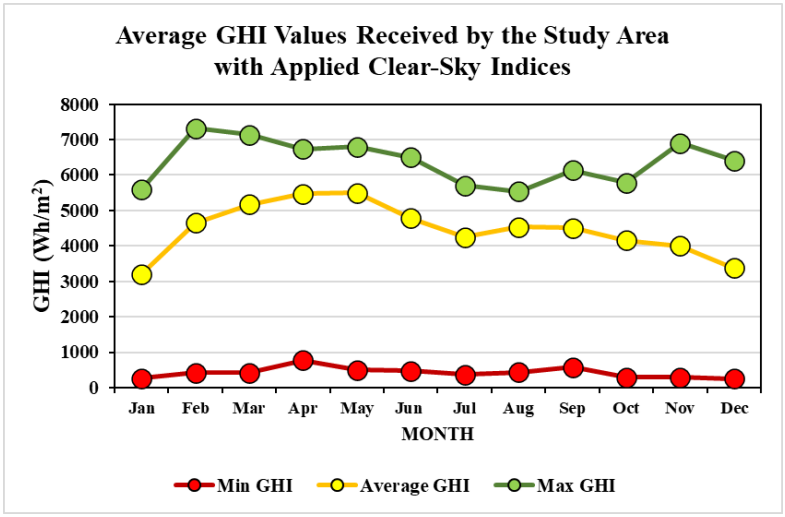

Figure 2.18 Monthly average GHI values of the study area with applied K_C

The map's higher detail in Figure 2.19 shows that Lanao Del Norte could get up to 8261.68 kWh/m2/day of irradiation on a clear day. Additionally, it can be seen that places facing south get more radiation, as shown by the reddish areas, while those facing north receive less radiation, as shown by the blue areas.

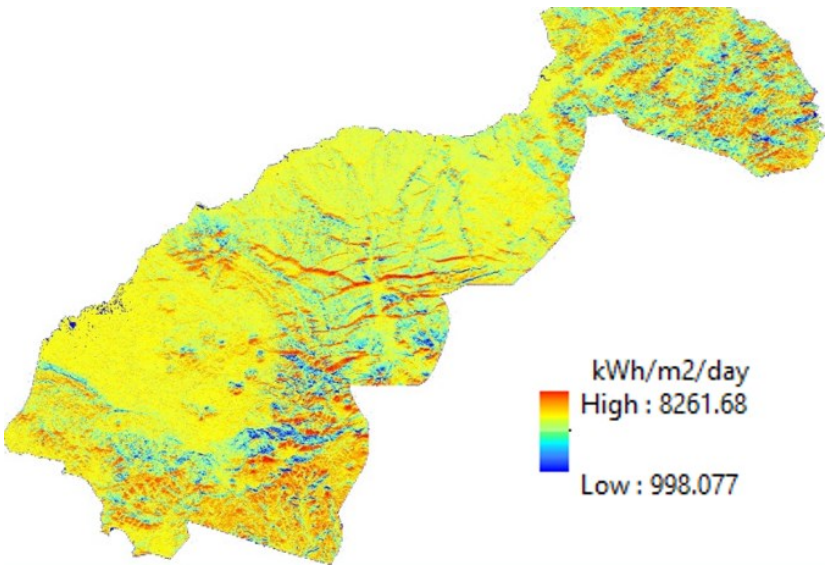

Figure 2.19 Clear-sky GHI of Lanao del Norte for the month of January

Real-sky GHI are raster mapsets that combine clear-sky GHI with cloud attenuation to create an accurate estimation of the solar irradiance that will really reach the earth's surface. As shown in Figure 2.20 The maximum solar irradiation values for the study region range from 4500 to 5000 kWh/m^2/day with an index value of 0.57 for the month of January.

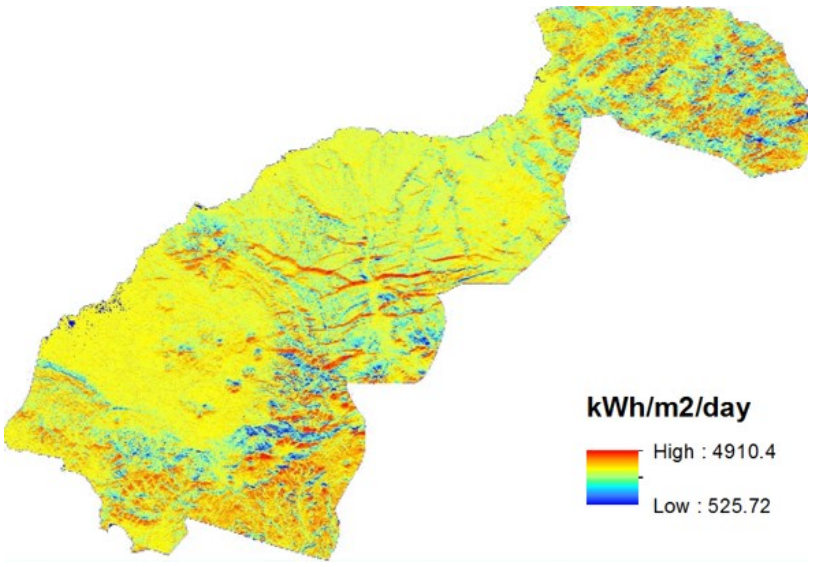

Figure 2.20 Real-sky GHI of Lanao del Norte for the month of January

Annual real-sky GHI shown in Figure 2.21 is the total average solar irradiance of Lanao Del Norte. It is computed based on the monthly solar irradiance output in kWh/m^2/day average for 365 days.

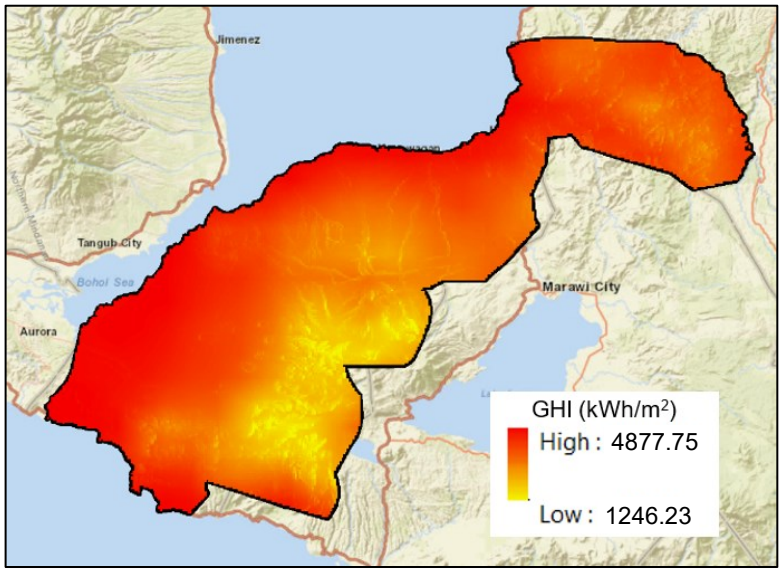

Figure 2.21 Annual Real-sky GHI of Lanao del Norte

2.8.3. Wind Resource Assessment Results

The simulation domains are shown in Figure 2.22. The WRF model was built over the parent domain (D1) with 25 km spatial resolution covering all of Mindanao, Philippines. The first nested domain (D2), with a spatial resolution of 5 km. The innermost domain (D3) covers the province of Lanao del Norte and some parts of Misamis Oriental. The vertical structure of the model contains 35 vertical levels with 10 m, 5 m and 2 m geographic resolution for the 3 domains. The sensitivity test is divided into different categories: seasonal representation, physical options, simulation domain resolution and validation of the model. Two different months were considered that represent the two seasons in the Philippines: the wet and dry seasons. The months of July and January were chosen for the wet and dry season, respectively.

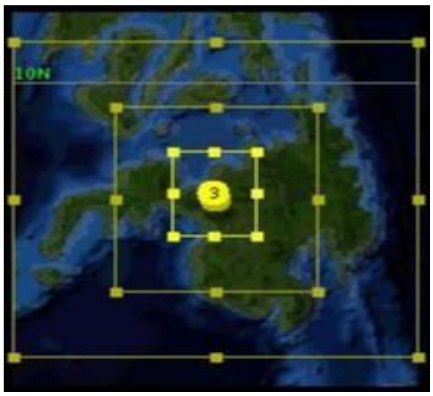

Figure 2.22 Simulation domain projection.

For physical options, the adaptive time step was used to facilitate faster runtime in the simulation. Since the focus of this study is to simulate near-surface winds, physical options that deal with the interaction of the atmosphere and the land surface were utilized. The available parameter options which were used for simulating two different cases for the simulation are shown in Table 2.2 and Table 2.3. The physical options related to the boundary processes parameterization (Surface Land (SL), Planetary Boundary Layer (PBL), and Land Surface Model (LSM)) are the ones that will have a larger influence on an accurate near-surface wind simulation. Although more physical options are available in the model (for cumulus, radiation, microphysics, etc.), it is not feasible to include them in the sensitivity analysis. Other options were set to default values in the configuration of the WRF Model Version 3.6.1 ARW core.

Table 2.2 Parametrization schemes

Parametrization	Available Schemes
Surface Land (SL) MM5, ETA, Pleim-Xiu	Surface Land (SL) MM5, ETA, Pleim-Xiu
Planetary Boundary Layer (PBL) Yonsei University,	Planetary Boundary Layer (PBL) Yonsei University,
Mellor-Yamada-Janjic, ACM2,	Mellor-Yamada-Janjic, ACM2,
RUC	RUC
Land Surface Model (LSM) Noah, RUC, 5-layer, Pleim-Xiu	Land Surface Model (LSM) Noah, RUC, 5-layer, Pleim-Xiu
Long-wave Radiation Rapid Radiative Transfer Model	Long-wave Radiation Rapid Radiative Transfer Model
Short-wave Radiation Dudhai	Short-wave Radiation Dudhai

Table 2.3 First Case and Second Case Parameters

Parametrization	First Case Parameters	Second Case Parameters
Surface Land (SL) MM5 Pleim-Xiu	Surface Land (SL) MM5 Pleim-Xiu	Surface Land (SL) MM5 Pleim-Xiu
Planetary Boundary	Planetary Boundary	Planetary Boundary
Layer (PBL)	Layer (PBL)	Layer (PBL)
Yonsei University ACM2	Yonsei University ACM2	Yonsei University ACM2
Land Surface Model	Land Surface Model	Land Surface Model
(LSM)	(LSM)	(LSM)
Noah Pleim-Xiu	Noah Pleim-Xiu	Noah Pleim-Xiu

An output file in netCDF format is produced by the simulation using the WRF Model. This format represents scientific variables in data that is array-oriented. The output of the WRF model is meteorological data. The wind speed and wind direction were two scientific variables that were taken from the output data in this investigation.

Open-source GIS-based software was be utilized for visualization while creating a wind resource map. The data were projected onto WGS 1984 and displayed using the extracted wind speed. To create raster data that was smooth, interpolation was utilized. Identification of the region with high wind speeds is the last step.

With 8 logical processors and an adjustable time step, the simulation lasted around a month. Each case's simulation with its matching month took around 5 days. Figure 2.23 and Figure 2.24 illustrate the comparison of the actual data with the simulated wind speed data. For the months of January and July, each case is presented differently.

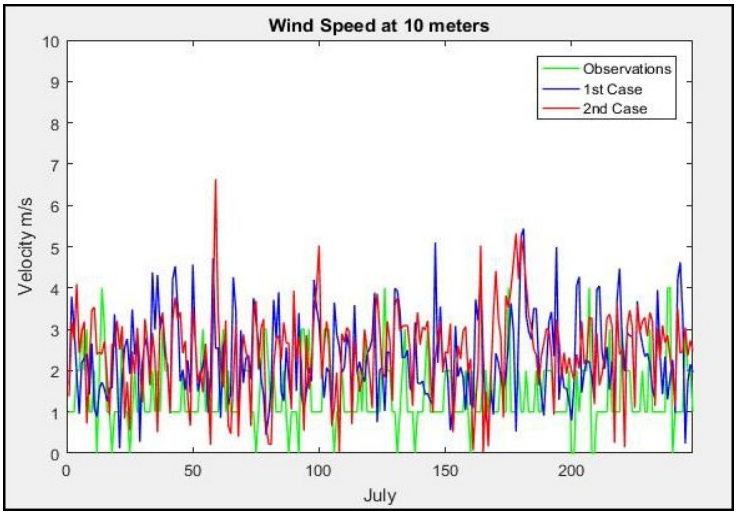

Figure 2.23 Wind speed plot for January.

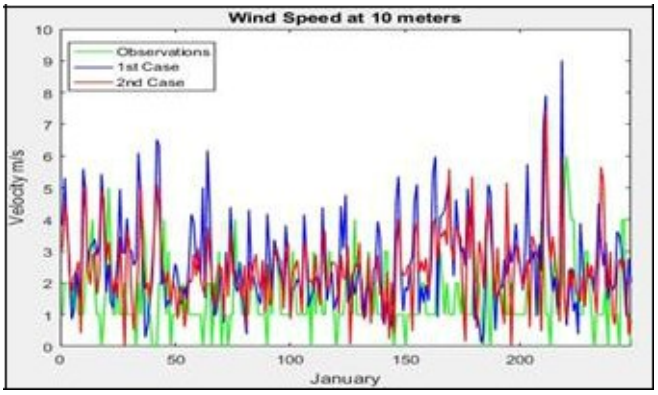

Figure 2.24 Wind speed plot for July.

Using statistical methods, the value of MAE is 0.87096, RMSE is 13.716, Bias is -0.87096, and STDE is 13.688 for the month of January's second case parameter, which has lower values than the first case parameter for the same month. This demonstrates that the model parameters used in the second instance outperformed the model parameters used in the first example. For the month of July, the first case parameter outperforms the second case parameters. The values for the first instance statistical parameters are as follows: MAE = 0.88699, RMSE = 13.968, Bias = -0.88699, and STDE = 13.94. As can be seen, the Bias value is negative, indicating that the model underestimated the expected wind speed values.

Figure 2.25 shows the wind rise plot of each example for each month. Plots for the month of January called Wind Rose (a) and (b) demonstrate that the majority of the time the wind comes

from the west. The frequency of wind blowing from a certain direction per unit of time is correlated with the length of each "spoke" around the circle. The two wind roses show that 6 percent of the time the wind comes from the west and blows between 2 and 3 m/s. This demonstrates that the wind seldom blows from the north or south and that the eastern and western areas have faster wind speeds.

The wind rise plot for the month of July is shown in wind rose (c) and (d). Similar results are seen in the first and second cases since the wind is mostly from the west. This outcome is consistent with the southwest monsoon's impact on the nation this month.

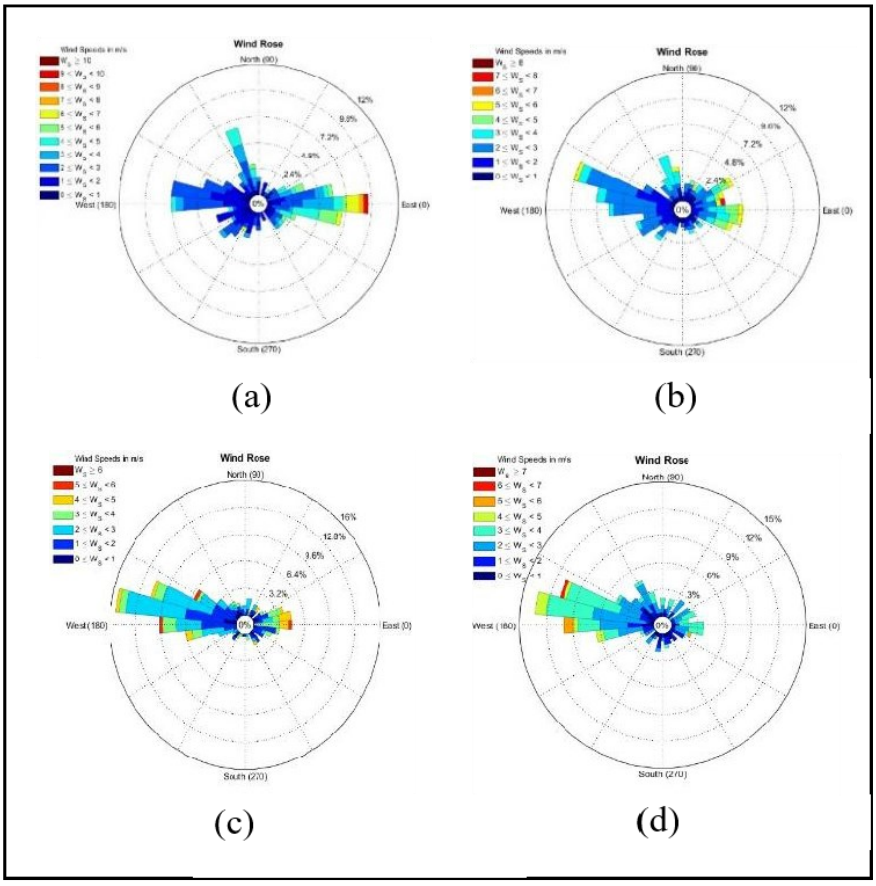

Figure 2.25 Wind Rose Plot.

The different wind power maps are shown in Figure 2.26 to Figure 2.29. Projection of the simulated data using GIS environment shows the specific places in Mindanao which exhibits larger wind speeds. The data is projected in WGS 1984 and employed raster smoothing technique to acquire a better visualization of the output data. From the map, the area extracted which exhibits

viable potential for wind project is the area of Panguil Bay. Funneling effect occurs in the bay which shows large wind speed values. This simulation replicated the phenomenon.

Wind Power calculation of the area is based in the output wind speed at 80m and 100m. Wind power varies for a specific wind turbine design. Notable area in the municipality of Tubod, Lanao del Norte and in the bay area of Ozamiz city. The highest simulated wind speed in this area is 7.90791 m/s.

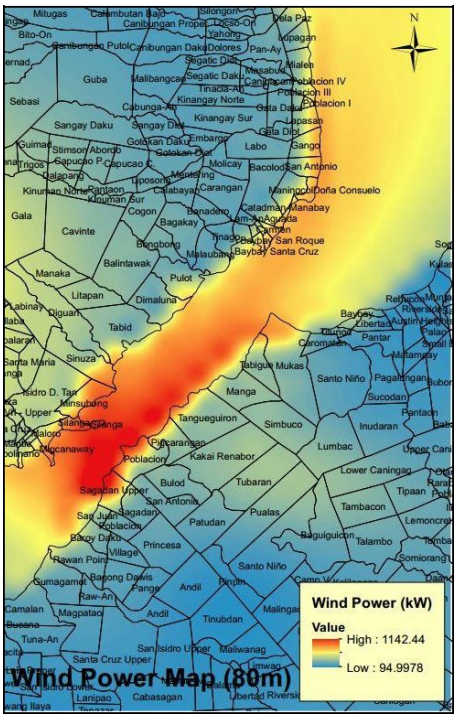

Figure 2.26 Wind Power Map at 80m for January.

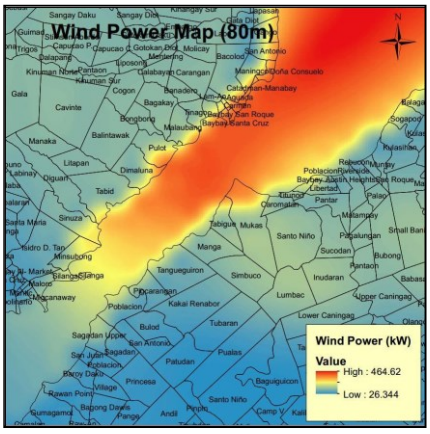

Figure 2.27 Wind Power Map at 80m for July.

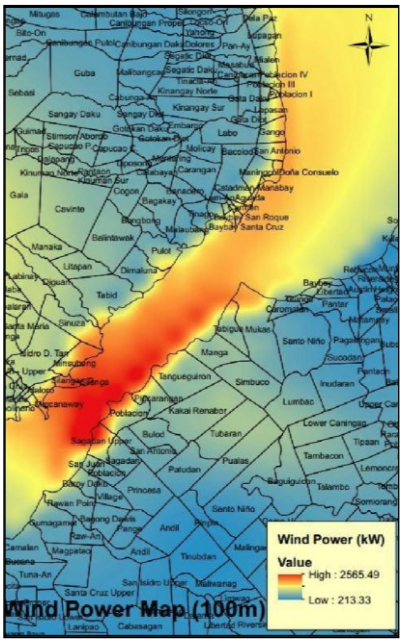

Figure 2.28 Wind Power Map at 100m for January.

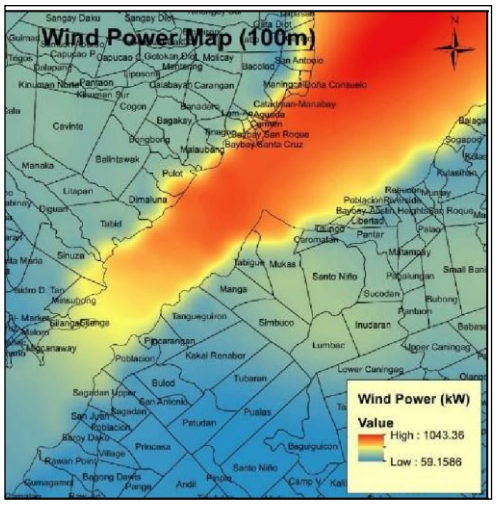

Figure 2.29 Wind Power Map at 100m for July.

2.9. Summary

This chapter used a combination of geographic information systems (GIS), models, and algorithms to evaluate various renewable energy resources (solar, wind, and hydro) at the local scale. R.sun, SWAT, the head algorithm, and WRF were some of the tools and algorithms used. The results show that the region under study has a lot of potential for solar energy, especially

along the shore. The research's westernmost area has a considerable potential for wind energy, and various prospective hydroelectric power sites have been discovered, according to the results.

In order to evaluate their potential for rural electrification, run-of-river systems are the main focus of hydropower research. A geographic information system platform was employed in the study to include spatial analysis into the resource assessment. When assessing potential sites based on resource potential, both theoretical and practical, the use of geographic data was advantageous. Using topographic and climatic data, high-resolution digital elevation models were used to generate probable hydropower development sites.

The two primary variables in the mathematical model for theoretical hydropower potential are discharge and head, which work in conjunction with gravitational force to generate energy from falling water. The model provided direction for the study's methodology and produced spatial data models for the two relevant variables. The study determined the amount of the surface flow using a hydrologic model tied to a GIS. The SWAT is a physically grounded continuous-event hydrologic model that was developed to predict how land management practices would affect water, sediment, and agricultural chemical yields over the course of extended time periods in vast, intricate watersheds with a variety of soil types, land uses, and management conditions. The dynamic datasets, which included rainfall datasets, temperature records, and long-term statistics on other meteorological variables like solar radiation, wind speed, and relative humidity, were required as inputs, in addition to the digital elevation model, soil layer model, land use layer, and dynamic datasets. The model's smallest mapping unit was the hydrologic response units, which are determined by certain combinations of land cover type, soil type, and slope classification. Each step of the water cycle was simulated by the model utilizing a unique collection of mathematical models.

Inputs crucial for estimating the amount of solar energy available were a solar radiation model and DEMs. The topography-based solar radiation model r.sun accounts for the effects of terrain in the inquiry. LiDAR DEM has a resolution of one meter compared to SAR DEM's ten-meter resolution. By more accurately simulating the effects of topography on insolation, high-resolution DEMs provide more detailed and exact information that may be utilized to assess the solar resource potential. The SAR DEM was used to assess the potential of solar energy resources

on a national scale. The size of the country is shown on provincial maps. LiDAR DEMs were used for urban-scale solar resource evaluation because they show building characteristics and are useful for assessing rooftop PV installation sites. This was carried out in a few areas where pyranometers and LiDAR DSM were installed.

Any sky condition may be used to compute solar radiation using the r.sun model. Given the country's meteorological conditions, where clouds and rain are an inescapable occurrence, it is crucial to take the effects of the clouds into account. This was achieved by employing the clear-sky index, which was created by combining expected clear-sky values with information from the BSWM's solar sensors.

To examine wind sources, a python-based user interface called WRF Extraction Software was used. Using this program, wind data is retrieved from the WRF output. There are two extraction types in the software: multi point and single point. The first was an input file for the wind resource map, and the second was a tool for validation. The single point outputs wind speed, wind direction, and wind power density at a single coordinate at a certain moment, whereas the multi point produces scalar and vector average wind speed, wind power density, and the number of occurrences throughout the whole domain.

Overall, the renewable energy maps developed in this study have higher accuracy (30m x 30m) compared to maps available online (NASA, SolarGIS with 1 km x 1 km). This research was able to pinpoint Tubod, Lanao del Norte as a viable wind project location, which was in line with other studies about its potential. By experimenting with different model configurations for the area of interest, one may minimize errors in wind simulations. The simulation grid's properties should strike a balance between the computing resources that may be used and the resolution that is selected.

2.10. Chapter 2 References

[2-1] IRENA, “Renewables Readiness Assessment: The Philippines,” *Int. Renew. Energy Agency Abu Dhabi*, p. 64, 2017.

[2-2] J. Domínguez and I. Pinedo-Pascua, “GIS Tool for Rural Electrification with Renewable Energies in Latin America,” in *2009 International Conference on Advanced Geographic*

Information Systems & Web Services, Cancun, Mexico, Feb. 2009, pp. 171–176. doi: 10.1109/GEOWS.2009.25.

[2-3] S. Murni, J. Whale, T. Urmee, J. Davis, and D. Harries, "The Role of Micro Hydro Power Systems in Remote Rural Electrification: A Case Study in The Bawan Valley, Borneo," *Procedia Eng.*, vol. 49, pp. 189–196, 2012, doi: 10.1016/j.proeng.2012.10.127.

[2-4] P. Costa, T. Simões, and A. Estanqueiro, "A GIS Methodology for Planning Sustainable Renewable Energy Deployment in Portugal," *Energy Power Eng.*, vol. 11, no. 12, pp. 379–391, 2019, doi: 10.4236/epe.2019.1112025.

[2-5] K. Calvert, J. M. Pearce, and W. E. Mabee, "Toward renewable energy geo-information infrastructures: Applications of GIScience and remote sensing that build institutional capacity," *Renew. Sustain. Energy Rev.*, vol. 18, pp. 416–429, Feb. 2013, doi: 10.1016/j.rser.2012.10.024.

[2-6] ASEAN Briefing, "Solar Power Industry in the Philippines," Jun. 27, 2017. https://www.aseanbriefing.com/news/solar-power-industry-philippines/

[2-7] J. Nelson, A. Gambhir, and N. Ekins-Daukes, "Solar power for CO2 mitigation," no. 11, p. 16, 2014.

[2-8] M. I. Al-Najideen and S. S. Alrwashdeh, "Design of a solar photovoltaic system to cover the electricity demand for the faculty of Engineering- Mu'tah University in Jordan," *Resour.-Effic. Technol.*, vol. 3, no. 4, pp. 440–445, Dec. 2017, doi: 10.1016/j.reffit.2017.04.005.

[2-9] K. Ronay and C. D. Dumitru, "Technical and Economical Analysis of a Solar Power System Supplying a Residential Consumer," *Procedia Technol.*, vol. 22, pp. 829–835, 2016, doi: 10.1016/j.protcy.2016.01.056.

[2-10] Akpolat, Dursun, Kuzucuoğlu, Yang, Blaabjerg, and Baba, "Performance Analysis of a Grid-Connected Rooftop Solar Photovoltaic System," *Electronics*, vol. 8, no. 8, p. 905, Aug. 2019, doi: 10.3390/electronics8080905.

[2-11] P. Fu and P. Rich, "Design and Implementation of the Solar Analyst: an ArcView Extension for Modeling Solar Radiation at Landscape Scales," p. 34.

[2-12] B. Kausika and W. van Sark, "Calibration and Validation of ArcGIS Solar Radiation Tool

for Photovoltaic Potential Determination in the Netherlands," *Energies*, vol. 14, no. 7, p. 1865, Mar. 2021, doi: 10.3390/en14071865.

[2-13] M. Tamoor, A. R. Bhatti, M. Farhan, S. Miran, F. Raza, and M. A. Zaka, "Designing of a Hybrid Photovoltaic Structure for an Energy-Efficient Street Lightning System Using PVsyst Software," in *The 1st International Conference on Energy, Power and Environment*, Dec. 2021, p. 45. doi: 10.3390/engproc2021012045.

[2-14] D. González-Peña, I. García-Ruiz, M. Díez-Mediavilla, M. I. Dieste-Velasco, and C. Alonso-Tristán, "Photovoltaic Prediction Software: Evaluation with Real Data from Northern Spain," *Appl. Sci.*, vol. 11, no. 11, p. 5025, May 2021, doi: 10.3390/app11115025.

[2-15] M. Al-Addous, M. Saidan, M. Bdour, Z. Dalala, A. Albatayneh, and C. B. Class, "Key aspects and feasibility assessment of a proposed wind farm in Jordan," *Int. J. Low-Carbon Technol.*, vol. 15, no. 1, pp. 97–105, Feb. 2020, doi: 10.1093/ijlct/ctz062.

[2-16] A. Yamaguchi, T. Ishihara, and Y. Fujino, "An Assessment of Offshore Wind Energy Potential Using Mesoscale Model and GIS," p. 5.

[2-17] S. Ahmad *et al.*, "Offshore wind resource assessment using reanalysis data," *Wind Eng.*, vol. 46, no. 4, pp. 1173–1186, Aug. 2022, doi: 10.1177/0309524X211069384.

[2-18] M. Winchell, R. Srinivasan, and M. D. Luzio, "ARCSWAT INTERFACE FOR SWAT2009 USER'S GUIDE," p. 489.

[2-19] D. Bergström and C. Malmros, "Finding Potential Sites for Small-Scale Hydro Power in Uganda: a Step to Assist the Rural Electrification by the Use of GIS.," p. 95.

[2-20] H. T. Nguyen and J. M. Pearce, "Estimating potential photovoltaic yield with r.sun and the open source Geographical Resources Analysis Support System," *Sol. Energy*, vol. 84, no. 5, pp. 831–843, May 2010, doi: 10.1016/j.solener.2010.02.009.

[2-21] J. T. Tolentino, M. V. Rejuso, J. K. Villanueva, L. C. Inocencio, and M. R. C. O. Ang, "Development of a Wind Resource Assessment Framework Using Weather Research and Forecasting (WRF) Model, Python Scripting and Geographic Information Systems," *Open Sci. Index Comput. Syst. Eng.*, vol. 9, no. 12, pp. 1348–1351, 2015, doi: 10.5281/zenodo.1110329.

Chapter 3 Suitability Analysis of Hybrid Renewable Energy Systems using GIS and Fuzzy-AHP

3.1. Introduction

Finding a suitable location for renewable energy generation development poses several challenges. In the traditional approach, a comprehensive ground survey is required. Furthermore, It is not feasible to conduct a large-scale survey due to the costs, manpower, and security restrictions [3-1], [3-2]. Several factors are involved in the operation which impacts include the well-being of individuals, society, and the environment. Geographic Information System (GIS) has developed into a rapidly growing technological field that is increasingly being used to assess real-world problems. It is capable of performing a wide variety of tasks, ranging from simple mapping to complex spatial modeling. Consequently, research on renewable energy resource suitability and site selection has increased dramatically in the last decade.

Numerous studies conducted in different countries investigated the use of GIS technology in the field of renewable energy [3-3], [3-4]. Sammartano et al. [3-5] combined GIS and Soil and Water Assessment Tool (SWAT) to identify optimal potential locations for a run-of-river plant in South West England while Guiamel and Lee [3-6] used the same combined tools to estimate the potential hydropower generation for the Mindanao River Basin in the Philippines and proposed potential mini and small-scale hydropower sites for sustainable energy development in the island. Alcala et al. [3-7] used Mesh Sweeping Approach (MSA) based in GIS for automated assessment of Small Hydro-Power (SHP) potential for a run-of-river (RoR) scheme in Huazuntlan River Watershed, Mexico.

Various studies were also conducted using GIS for assessment, suitability analysis, and site selection for the development and construction of solar energy projects such as solar photovoltaic (PV) farms. Using a combination of GIS and AHP, Albraheem and Alabdulkarim [3-8] In the West Kalimantan Province of Borneo, Sunarso et al. [3-9] conducted an analysis to determine whether or not utility-scale solar photovoltaic (PV) plants are technically and economically feasible. They proposed A GIS-integrated analytical tool was used to determine yearly energy output and electricity cost for the assessment of the technical and economic viability.In Iran's Markazi

Province, Yousefi et al.[3-10] developed a GIS-based boolean-fuzzy logic model and used it in the process of finding suitable locations for solar power facilities while taking into account the economic, technical, and environmental criteria and constraints. In order to simulate, investigate, and evaluate the amount of solar power produced in East Africa, Palmer and Blanchard [3-11] made use of a variety of high-resolution GHI datasets. Their findings were verified by utilizing data collected from field measurements and statistical analysis. Noorollahi et al.[3-12]created a two-step framework using GIS and Fuzzy Analytic Hierarchy Process (FAHP) to identify the suitability and feasibility of various places in Iran for the use of solar energy based on various technical, topographical, and economic parameters. Several studies were also conducted on finding suitable locations for onshore and offshore wind farms using various methods in different countries such as Spain, Sudan and Greece [3-13]–[3-15].

In the process of planning and evaluating projects including renewable energy sources, GIS and Multi-Criteria Decision-Making (MCDM) are both used extensively [3-16]–[3-19]. This is due to the vast potential that GIS has to offer in terms of the processing, administration, and analysis of geographical information. GIS also makes it possible to include a large number of social, economic, technical, and environmental criteria and constraints and facilitates the straightforward and practical use of multi-criteria analysis. Because of this, one develops a wide range of abilities for spatial analysis, which can then be applied to decision-making and site-selection problems.

Although several methods for analyzing the suitability of different single renewable energy systems have been developed over the last decade in the aforementioned studies, only a few have focused on hybrid energy systems [3-20]–[3-22]. Furthermore, to the best of the authors' knowledge, there is no published research yet on suitability analysis for hybrid renewable energy systems that includes land suitability for the development of hydroelectric facilities. There is also currently no research has been carried out in the Philippines that determines suitable sites for hybrid renewable energy systems. Thus, in this chapter, an integrated framework is presented and developed for suitability analysis and site selection for single (wind, solar, hydro) and hybrid (wind-solar and hydro-solar) renewable energy systems using a Geographic Information System (GIS) and the Fuzzy Analytic Hierarchy Process (AHP), an MCDM method. The developed framework can be applied to any type of renewable energy, considering the limited datasets. The

proposed framework is applied to the study area, which is Lanao del Norte, a southern province in the Philippines.

3.2. Overall Methodology for the Suitability Analysis and Site Selection

The proposed integrated framework for the suitability analysis and site selection of single and hybrid renewable energy systems using GIS and Fuzzy-AHP is shown in Figure 3.1. Throughout this research, suitable locations for wind energy (wind farms), solar energy (solar–photovoltaic power plants), and hydro energy (run-of-river hydropower) systems are identified separately; these suitable locations are then stacked to give feasible locations for hybrid renewable energy (wind–solar and hydro–solar) energy systems. The framework is composed of six steps, and the details of each step are discussed in detail in the succeeding subsections.

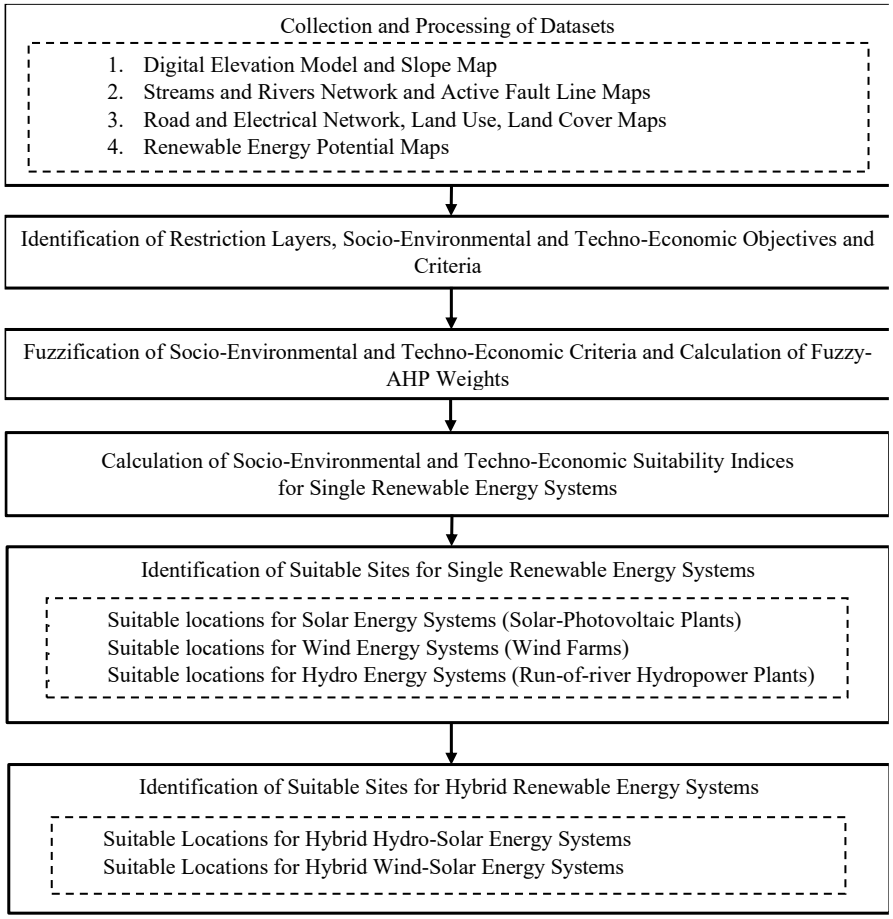

Figure 3.1 Overall Methodology for Site Selection and Suitability Analysis of Hybrid Energy Systems

3.2.1. Study Area

The case study area is situated in Lanao del Norte, a southern province in the Philippines, as shown in Figure 3.2 Study area map (Lanao del Norte, Philippines). It was chosen as the study area since it has high solar energy potential and hydropower potential. Despite this, the whole province hasn't been assessed for the suitability of hybrid renewable energy systems [3-23]. It is located at 7.87 degrees north latitude and 123.89 degrees east longitude and has a population of 722,902 (as of 2020) and a land area of 4,159.94 square kilometers (1,606.16 square miles). The province is composed of 22 municipalities and a highly urbanized city. It is rich in natural resources, with different water bodies such as streams, rivers, and waterfalls. The province has hilly topography that stretches from the coast to high plateaus and mountains in the south. It also has a Type III climate with no clearly defined maximum rain period and a relatively brief dry

season that lasts one to three months from March to May. As of 2020, electricity is provided to 73.89 percent of the province's residents by two distribution companies, Iligan Light and Power Incorporated (ILPI) and Lanao del Norte Electric Cooperative (LANECO). However, only 149,379 houses out of 202,151 have access to electricity [3-23].

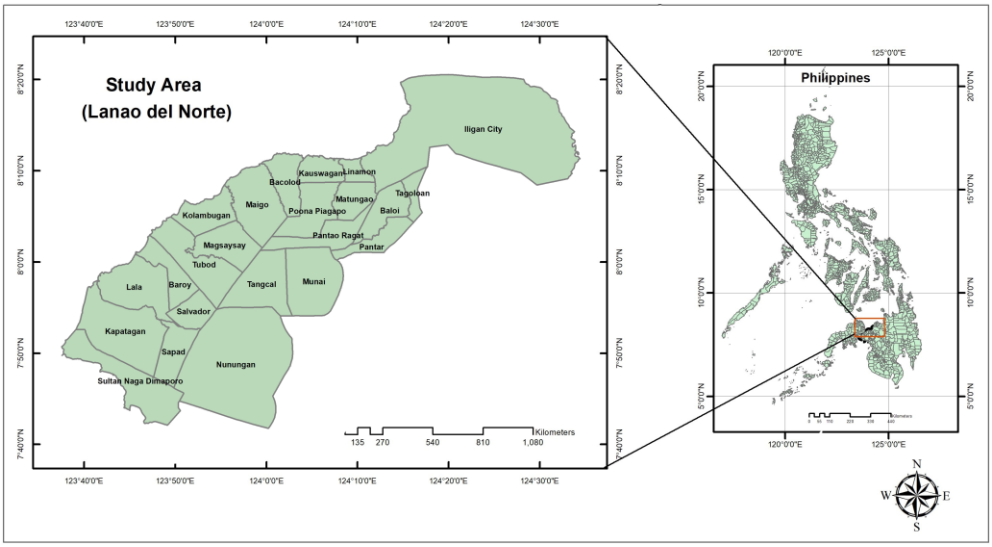

Figure 3.2 Study area map (Lanao del Norte, Philippines)

3.2.2. Collection and Processing of Datasets

To perform suitability analysis, significant datasets from various sources were assembled. The ASTER Global Digital Elevation Model (ASTER GDEM), which has a spatial resolution of 30 meters, was used to construct the digital elevation model (DEM) for this study [3-24]. For the renewable energy resource data, Global Solar Atlas, an online platform operated by the Energy Sector Management Assistance Program, was used to extract the long-term (2007-2018) annual average of global horizontal irradiation (GHI) in kilowatt-hour per square meters [3-25]. The wind speed data that was used for the analysis was extracted from the Global Wind Atlas [3-26]. Furthermore, the TIF raster format was used for both wind speed and GHI data. The Phil-LiDAR 2 tool was used to calculate the province's hydropower resource data [3-27]. Phil-LiDAR 2 used a run-of-river setup with a minimum head of 20 meters and a penstock length of 100 meters to perform this resource assessment.

Land use, hazard maps, land cover, and local political boundaries vector data were collected using PhilGIS [3-28] while hazard maps were obtained from Philippine Institute of Volcanology and Seismology (PHIVOLCS) [3-29]. Data on road networks, rivers, lakes, and population centers were extracted from OpenStreetMap [3-30] while the data on transmission and distribution networks were from the Department of Energy (DOE) of the Philippines [3-31]. Both raster and vector datasets utilize the GCS_WGS_1984 geographic coordinate system. Figure 3.3 and Figure 3.4 show the input raster and vector layers used for the suitability analysis. Furthermore, the study area was divided into mesh grids of 300 meters by 300 meters, with each grid representing a separate potential installation site for single (hydro, solar, and wind) and hybrid (wind-solar and hybrid hydro-solar) energy systems. The mesh grid size selected allows for the consolidation of individual cells into a land area large enough to support the development of a specific plant.

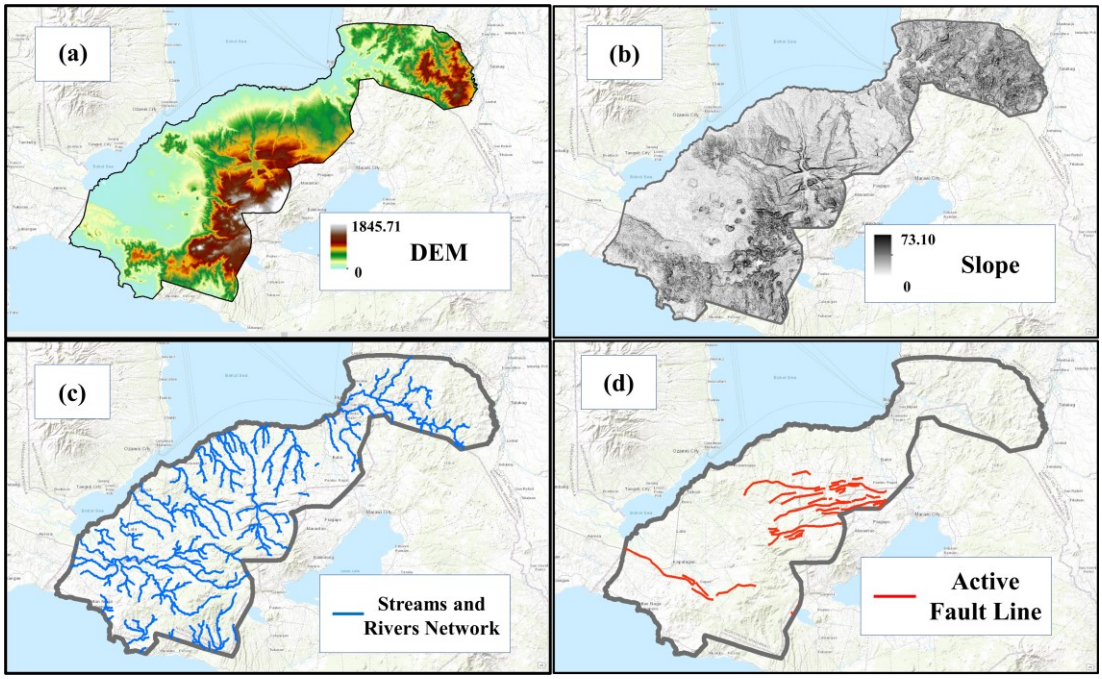

Figure 3.3 (a) DEM; (b) slope; (c) streams and river network; and (d) active fault lines

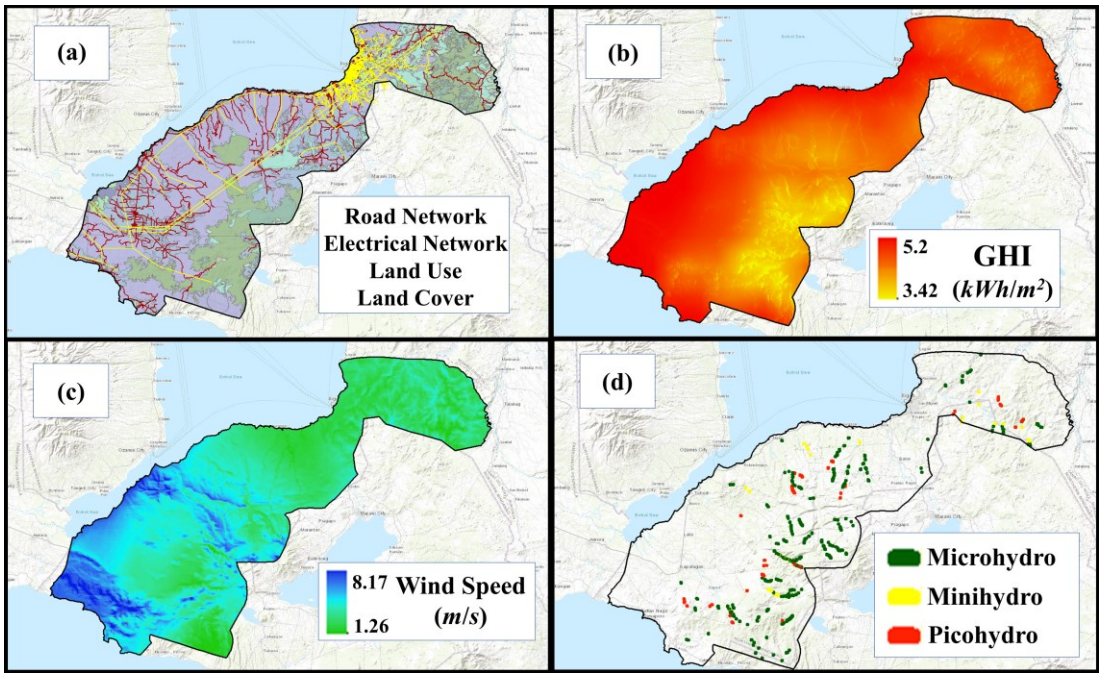

Figure 3.4 (a) Land use, land cover, electrical network, road network (b) annual average global horizontal radiation (GHI); (c) average annual wind speed at 50 m of altitude; and (d) identified hydropower potential sites

3.2.3. Identification of Restriction Layers, Socio-Environmental and Techno-Economic Objectives and Criteria

Suitability analysis of single and hybrid renewable energy systems requires the identification of different social. environmental, technical, and economic restrictions, objectives, and criteria. Prior to the selection of these restrictions, objectives, and criteria, existing laws and regulations regarding the installation of renewable energy facilities such as wind farms, solar-PV plants, and small run-of-river hydropower plants in the Philippines and other previously published related research from other countries were examined and considered. Experts in renewable energy technology and microgrid design and installation from academe and industry were also interviewed to filter out and narrow down the set of restrictions, objectives, and criteria that were used in the study.

Table 3.1 shows the restriction layers used for the site selection and suitability analysis. For example, R01, which is the layer containing the active fault lines in the study area, was given a buffer distance of 100 meters to be avoided in the analysis based on the guidelines from

PHILVOLCS. Other prohibited areas, such as ancestral domains and protected areas in R02, were given a 1 km buffer. All of the restriction layers, with the exception of R04, were applied to the suitability analysis and site selection of wind, solar, and hydro energy systems. These buffered, restricted areas were given a Boolean value of "0" so they can be excluded from the site selection. For R04, areas that were more than 2 km away from the streams and rivers were excluded from the land suitability analysis and from finding areas that are suitable for hydro energy and hybrid hydro-solar systems.

Socio-environmental objectives and criteria for wind, solar, and hydro energy systems derived from legislation and previous studies are shown in Table 3.2 to Table 3.4, respectively. These lists of objectives and criteria are the combined social and environmental factors that were considered for the construction of renewable energy systems. For example, in C01, which is the "distance from airports" criteria, previous studies dictate that, pertaining to flight protection, shiny structures such as PV farms are prohibited in the first 3 km zone. Although they have some similarities, the socio-environmental objectives for solar energy systems have some differences from those for wind energy systems. Philippine renewable energy regulations, for example, permit the building of wind turbines nearby agricultural areas. Solar power plants, on the other hand, necessitate vast installation areas. This means that the construction of solar power plants would result in the loss of large areas for agriculture.

When determining where to construct and develop hybrid renewable energy systems, the techno-economic feasibility of wind, solar, and hydropower projects must be considered in addition to socio-environmental concerns. For renewable energy projects to have feasible operation, technical and economic factors should be considered prior to development and installation. These two types of factors were fused and termed "Techno-Economic Objectives" in this study. Table 3.5 to Table 3.7 list all the techno-economic objectives and criteria for wind, solar, and hydro energy systems, respectively.

The availability of suitable wind speed and solar energy generation within the study area is one of the most important techno-economic suitability objectives since techno-economic feasibility is strongly reliant on energy potential. Furthermore, previous literature identify adequate hydro, solar, and wind energy potential as highly if not most important criteria to be

considered in the site selection and suitability analysis. Areas must have average wind speed greater than 4.5 meters per second to be suitable for installation wind farms while for solar-PV farms, suitable areas must have a yearly solar energy generation based on global horizontal irradiance (GHI) greater than 4 kWh/m^2. Additionally, distances from existing roads and transmission networks were considered for the analysis. Renewable energy project developers prefer sites that are closer to roads and transmission network since the longer distances incur higher construction and project development costs. For solar-PV farms, steep slopes are avoided wherever possible in order to cut down on construction costs and minimize the negative effect that development has on the local geomorphology.

Table 3.1 Restriction layers for the suitability analysis of hybrid renewable energy systems

Restriction Layer	Criteria	Reference
R01 - Distance from Active Fault Lines	Less than 100 m	[3-32], [3-33]
R02 - Distance from Protected Areas and Ancestral Domains	Less than 1 km	[3-34]–[3-36]
R03 - Distance from Urban Areas	Less than 2 km	[3-37], [3-38]
R04 - Distance from streams/rivers*	Greater than 2 km	[3-39], [3-40]

*This restriction layer is only applied for the suitability analysis of hydropower plants and hybrid hydro-solar energy systems

Table 3.2 Socio-environmental suitability objectives and criteria for construction of wind energy facilities

Socio-Environmental Objectives	Criteria	Reference
C01 - Distance from airports	Greater than 3 km	[3-14], [3-37], [3-41]
C02 - Distance from protected and conservation areas	Greater than 2 km	[3-37], [3-42], [3-43]
C03 - Distance from urban areas	Greater than 2 km	[3-13]–[3-15]
C04 - Distance from rural settlements	Greater than 1 km	[3-13], [3-37], [3-41]
C05 - Distance from coastlines	Greater than 400 m	[3-13]–[3-15]

Table 3.3 Socio-environmental suitability objectives and criteria for construction of solar energy facilities

Socio-Environmental Objectives	Criteria	Reference
C06 - Distance from coastline	Greater than 100 m	[3-44], [3-45]
C07 - Distance from airports	Greater than 3 km	[3-44], [3-45]
C08 - Distance from lakes and wetlands	Greater than 2.5 km	[3-10], [3-45], [3-46]
C09 - Distance from agricultural areas	Greater than 1 km	[3-8], [3-10], [3-12]

Table 3.4 Socio-environmental suitability objectives and criteria for construction of hydropower

facilities

Socio-Environmental Objectives	Criteria	Reference
C10 - Distance from protected and conservation areas	Greater than 1 km	[3-47]–[3-49]
C11 - Distance from urban areas	Greater than 3 km	[3-47]–[3-50]
C12 - Distance from agricultural areas	Greater than 1 km	[3-47], [3-49], [3-50]
C13 - Distance from residential areas	Greater than 1 km	[3-47]–[3-49], [3-51]

Table 3.5 Techno-economic suitability objectives and criteria for construction of wind farms

Techno-Economic Objectives	Criteria	Reference
C14 -Wind Speed	Greater than 4.5 m/s	[3-13]–[3-15]
C15 - Slope	Lesser than 30%	[3-13]–[3-15], [3-42]
C16 - Distance from transmission lines	Lesser than 10 km	[3-14], [3-15], [3-45]
C17 - Distance from main roads	Lesser than 10 km	[3-13]–[3-15], [3-45]

Table 3.6 Techno-economic suitability objectives and criteria for construction of solar energy facilities

Techno-Economic Objectives	Criteria	Reference
C18 - Solar energy generation	Greater than 4 kWh/m2 (yearly)	[3-8], [3-12], [3-45], [3-52]
C19 - Slope	Lesser than 3%	[3-9], [3-10], [3-52]
C20 - Distance from transmission lines	Lesser than 10 km	[3-8]–[3-10], [3-52]
C21 - Distance from main and minor roads	Lesser than 10 km	[3-9], [3-12], [3-52], [3-53]

Table 3.7 Techno-economic suitability objectives and criteria for construction of hydropower facilities

Techno-Economic Objectives	Criteria	Reference
C22 - Slope	Greater than 2°	[3-47], [3-48], [3-54]
C23 - Distance from transmission network	Lesser than 20 km	[3-47], [3-50], [3-54], [3-55]
C24 - Distance from main and minor roads	Lesser than 10 km	[3-50], [3-55], [3-56]
C25 - Distance from site with identified energy potential	Lesser than 3 km	[3-47], [3-50], [3-54], [3-55]

3.3. Fuzzification of Socio-Environmental and Techno-Economic Criteria and Calculation of Fuzzy-AHP Weights

Tables 2 to 7 show that socio-environmental and techno-economic suitability objectives involve fuzziness and ambiguity (criteria values in range instead of crisp discrete values), which are common features of many complex decision-making problems. By expressing previously socio-environmental and techno-economic objectives and criteria characteristics for wind, solar, and hydro energy systems as fuzzy sets, Fuzzy Set Theory is utilized to deal with complexity and ambiguity. The process of transforming raw data from identified socio-environmental and techno-economic suitability objectives into fuzzy membership values is referred to as "fuzzification." This conversion occurs on the basis of a decisively specified fuzzy membership function for each component. A fuzzy set can be described mathematically as follows [3-56]:

$$FS = \{X, \mu_{FS}\} \text{ for each } x \in X \tag{3-1}$$

where X is a group of objects represented by the symbol x. The membership function (MF) that specifies the degree of membership of X in a fuzzy set is represented by μ_A. The MF can take on any value between 1 and 0, inclusive of both of those values, for any given FS, where having an μ_{FS} value of 0 indicates that the value x does not belong to FS and having an μ_{FS} value of 1 indicates that it belongs totally to FS. Alternatively, a value of μ_{FS} that is greater than 0 but lesser than 1 suggests that x is related to A to some degree. In the event when $X = \{x_1, x_2, ..., x_n\}$, the previously stated equation can be rewritten as follows:

$$FS = \{[x_1, \mu_{FS}(x_1)] + [x_2, \mu_{FS}(x_2)] + \ldots + [x_n, \mu_{FS}(x_n)]\} \tag{3-2}$$

Figure 3.5 shows the different types of fuzzy membership (FM) functions used in fuzzification while the summary of the fuzzy membership functions for each criteria selected in this study is shown in Table 3.8. In simple terms, Eqs. (1) and (2) mean that for every x that belongs to the set X, there is a MF that describes the degree of ownership of x in FS. For socio-environmental and techno-economic suitability objectives and criteria with increasing values for wind, solar, and hydro energy systems the following Linear Ascending FM was used.

$$\mu_{FS}(x) = f(x) = \begin{Bmatrix} 0 & x \leq a \\ x - a/b - a & a < x < b \\ 1 & x \geq b \end{Bmatrix} \tag{3-3}$$

where x is the input data and a, b are the limit values.

For socio-environmental and techno-economic suitability objectives and criteria with decreasing values the following Linear-Descending MF was used:

$$\mu_{FS}(x) = f(x) = \begin{Bmatrix} 0 & x \leq a \\ b - x/b - a & a < x < b \\ 1 & x \geq b \end{Bmatrix} \quad (3\text{-}4)$$

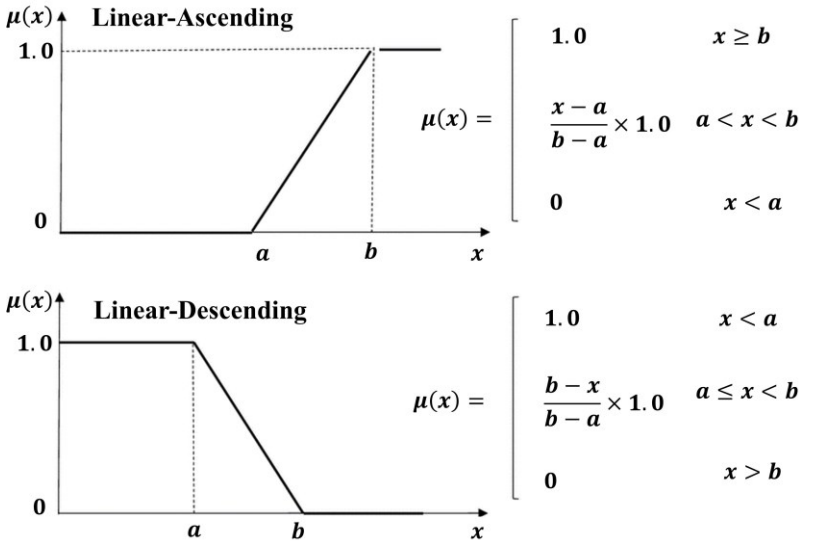

Figure 3.5 Types of Fuzzy Membership (FM) Functions

Table 3.8 Summary of FM function type for different socio-environmental and techno-economic suitability objectives and criteria

Suitability Criteria	FM Type	a-value	b-value
Wind (Socio-Environmental)			
C01 - Distance from airports	Linear-Ascending	3 km	6 km
C02 - Distance from protected and conservation areas	Linear-Ascending	2 km	8 km
C03 - Distance from urban areas	Linear-Ascending	2 km	6 km
C04 - Distance from rural settlements	Linear-Ascending	1 km	7 km
C05 - Distance from coastlines	Linear-Ascending	400 m	1 km
Solar (Socio-Environmental)			
C06 - Distance from coastline	Linear-Ascending	100 m	1 km
C07 - Distance from airports	Linear-Ascending	3 km	6 km
C08 - Distance from lakes and wetlands	Linear-Ascending	2.5 km	6 km
C09 - Distance from agricultural areas	Linear-Ascending	1 km	2 km
Hydropower (Socio-Environmental)			
C10 - Distance from protected and conservation areas	Linear-Ascending	1 km	6 km
C11 - Distance from urban areas	Linear-Ascending	3 km	8 km
C12 - Distance from agricultural areas	Linear-Ascending	1 km	5 km

C13 - Distance from residential areas	Linear-Ascending	1 km	5 km
Wind (Techno-Economic)			
C14 - Wind Speed	Linear-Ascending	4.5 m/s	8 m/s
C15 - Slope	Linear-Descending	10%	30%
C16 - Distance from transmission lines	Linear-Descending	5 km	10 km
C17 - Distance from main roads	Linear-Descending	2 km	10 km
Solar (Techno-Economic)			
C18 - Solar energy generation	Linear-Ascending	4 kWh/m^2	5 kWh/m^2
C19 - Slope	Linear-Descending	1%	3%
C20 - Distance from transmission lines	Linear-Descending	3 km	10 km
C21 - Distance from urban areas	Linear-Descending	3 km	10 km
Hydropower (Techno-Economic)			
C22 - Slope	Linear-Ascending	2 °	10 °
C23 - Distance from transmission network	Linear-Descending	3 km	10 km
C24 - Distance from major and minor roads	Linear-Descending	3 km	10 km
C25 - Distance from site with identified energy potential	Linear-Descending	500 m	3 km

3.5.1 Fuzzy-AHP

After the fuzzification of different socio-environmental and techno-economic suitability criteria, Fuzzy-AHP was used to determine the weights of each criterion, which are then used to calculate different suitability indices. Fuzzy-AHP, which was first proposed by van Laarhoven [3-57] and further developed by Chang [3-58] , is a technique for making decisions based on multiple criteria that combines Analytic Hierarchy Process (AHP) [3-59] with Fuzzy Sets. This approach is used to establish the relative importance of various criteria and alternatives. In contrast to AHP, fuzzy AHP replaces precise numbers with fuzzy numbers that reflect linguistic expressions. This tolerates ambiguous judgments by giving membership degrees to specific numbers in order to reflect the extent to which these numbers belong to an expression [3-60]. Table 3.9 shows the Saaty's Scale for Decision-making using Fuzzy-AHP [3-61].

Figure 3.6 shows the overall process of the calculation of criteria weights using Fuzzy-AHP. First, the problem is structured in a hierarchy. For example, to determine the socio-environmental suitability index of wind energy systems, criteria C01, C02, C03, C04, and C05 were considered in the decision-making process shown in Figure 3.7. These criteria were used to create comparison matrix.

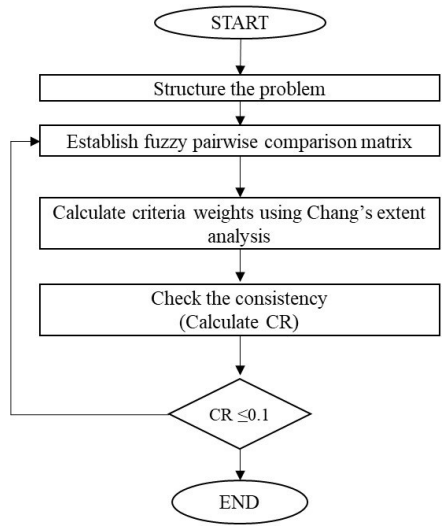

Figure 3.6 The calculation process of fuzzy AHP

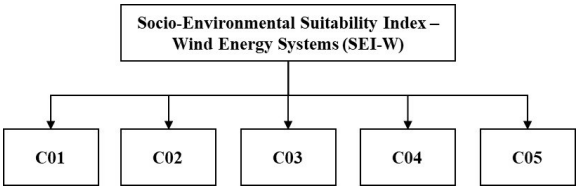

Figure 3.7 Sample hierarchical problem structure for determining the socio-environmental suitability of wind energy systems

Table 3.9 Saaty's Scale for Decision-making using Fuzzy-AHP

Linguistic Scalesfor Importance	**Triangular Fuzzy Number (TFN)**	**Triangular Fuzzy Reciprocal Numbers**
Equally Important (EI)	(1,1,1)	(1,1,1)
Intermediate 1 (IM1)	(1,2,3)	(1/3,1/2,1)
Moderately Important (MI)	(2,3,4)	(1/4,1/3,1/2)
Intermediate 2 (IM2)	(3,4,5)	(1/5, 1/4, 1/3)
Important (I)	(4,5,6)	(1/6,1/5,1/4)
Intermediate 3 (IM3)	(5,6,7)	(1/7,1/6/1/5)
Very Important (VI)	(6,7,8)	(1/8,1/7,1/6)
Intermediate 4 (IM4)	(7,8,9)	(1/9,1/8,1/7)
Absolutely Important (AI)	(9,9,9)	(1/9,1/9,1/9)

After creating the hierarchical structure of the problem, a fuzzy pairwise comparison matrix based on AHP is established. The decision-maker judges or decides the relative importance between each criterion based on the Triangular Fuzzy Numbers (TFNs) on Table 3.9. Mathematically, the decision-maker's quantified judgement is expressed in an *n* x *n* matrix as

follows:

$$A = (a_{ij})_{nxn} = \left\{ \begin{pmatrix} a_{11} & \cdots & a_{1n} \\ \vdots & \ddots & \vdots \\ a_{n1} & \cdots & a_{nn} \end{pmatrix} \right\} \tag{3-5}$$

$$a_{ij} = (l_{ij}, m_{ij}, u_{ij})_{nxn} = {a_{ji}}^{-1} = \left(\frac{1}{l_{ij}}, \frac{1}{m_{ij}}, \frac{1}{u_{ij}}\right) \tag{3-6}$$

where n is the number of criteria, $i,j = 1,\ldots, n$ and $i \neq j$.

After constructing the pairwise comparison matrix using TFNs, Chang's extent analysis [3-58] approach is utilized to eliminate uncertainty. Based on this approach, fuzzy synthetic extent $S\_\{i\}$ with respect to ith criterion is computed using the following formula:

$$\mathrm{S_i} = \left(\frac{\sum_{j=1}^{n} \mathrm{l_{ij}}}{\sum_{i=1}^{n} \sum_{j=1}^{n} \mathrm{u_{ij}}}, \frac{\sum_{j=1}^{n} \mathrm{m_{ij}}}{\sum_{i=1}^{n} \sum_{j=1}^{n} \mathrm{m_{ij}}}, \frac{\sum_{j=1}^{n} \mathrm{u_{ij}}}{\sum_{i=1}^{n} \sum_{j=1}^{n} \mathrm{l_{ij}}} \right) \tag{3-7}$$

After calculating the synthetic value, the degree of possibility is then determined for each convex TFNs. Suppose, $\mathrm{M_2} = (\mathrm{l_2}, \mathrm{m_2}, \mathrm{u_2})$ and $\mathrm{M_1} = (\mathrm{l_1}, \mathrm{m_1}, \mathrm{u_1})$ are two TFNs shown in Figure 3.8, the degree of possibility that $\mathrm{M_1}$ is greater than or equal to $\mathrm{M_1}$which is represented by $\mathrm{V}(\mathrm{M_1} \geq \mathrm{M_2})$ is defined as follows:

$$V(M_2 \geq M_1) = \sup\left[\min\left(\mu_{M1}(x), \mu_{M2}(y)\right)\right], \quad y \geq x \tag{3-8}$$

$$V(M_2 \geq M_1) = \begin{cases} 1 & if\ m_1 \geq m_2 \\ 0 & if\ l_2 \geq u_1 \\ \dfrac{l_2 - u_1}{(m_1 - u_2) - (m_2 - l_2)} & otherwise \end{cases} \tag{3-9}$$

where x and y are the x- and y-axis values of the membership function of each criterion, respectively, and d is the ordinate of D, which is the highest intersection between M_1 and M_2. The values for M_1 and M_2 are required for the comparison of the two TFNs. In addition, the following equations are used to calculate the degree of possibility for a convex fuzzy number to be greater than k convex fuzzy numbers:

$$V(M \geq M_1, M_2, M_3, \ldots, M_k)$$
$$= V[(M \geq M_1)\ and\ (M \geq M_2)\ and\ (M \geq M_3)\ and\ \ldots\ and (M \geq M_k) \tag{3-10}$$

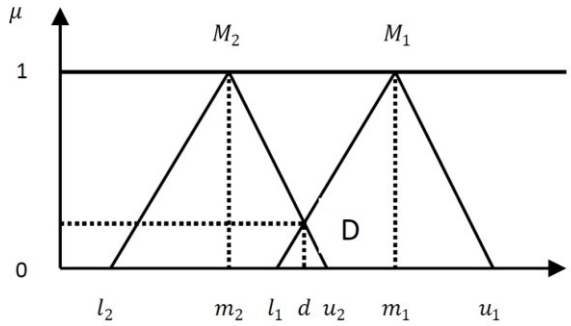

Figure 3.8 Sample intersection between two TFNs

With the assumption that $d'(a_i) = minV(M_i \geq M_k)$ or k = 1,2,3 ⋯ n; k ≠ i, the weight vector is obtained using the following equation:

$$W^{'} = \left(d^{'}(A_1), d^{'}(A_2), d^{'}(A_3), \dots, d^{'}(A_n)\right)^T \tag{3-13}$$

where $A_i(\mathrm{i} = 1,2,3 \dots n)$ are n elements. The weight vector is then normalized to obtain the non-fuzzy weight using the following equation:

$$W = \left(d(A_1), d(A_2), d(A_3), \dots, d(A_n)\right)^T \tag{3-14}$$

The Fuzzy AHP also includes mathematical measures that can be used to determine whether or not judgments are consistent. A consistency ratio (CR) can be calculated using the properties of reciprocal matrices. The largest eigenvalue, $\lambda_{\max}$, is always greater or equal to the number of rows or columns, n, in a reciprocal matrix. If there are no inconsistencies in a pairwise comparison, $\lambda_{\max} = \mathrm{n}$ is used. The computed $\lambda_{\max}$ value will be closer to n if the comparisons are more consistent.

$$(A - \lambda_{\max} I) \times W = 0 \tag{3-15}$$

The inconsistencies of pairwise comparisons are measured by a consistency index, CI, which is written as:

$$CR = \frac{CI}{RI} \tag{3-16}$$

where *RI* is the random consistency index, which is the average consistency index of the randomly produced comparisons. As a rule of thumb, a *CR* value of 10% or less is regarded acceptable.

Otherwise, a re-evaluation of the comparison matrix must be carried out [3-59].

3.4. Calculation of Environmental Suitability Index and Economic Feasibility Index for Individual Renewable Energy Systems

Several indices were developed to determine the socio-environmental and techno-economic suitability for single renewable energy systems. The socio-environmental suitability indices for wind, solar, and hydro energy systems are Socio-Environmental Suitability Index for Wind Energy (SEI-W), Socio-Environmental Suitability Index for Solar Energy (SEI-S), and Socio-Environmental Suitability Index for Hydro Energy (SEI-H) while the techno-economic suitability indices are Techno-Economic Suitability Index for Wind Energy (TEI-W), Techno-Economic Suitability Index for Solar Energy (TEI-S), and Techno-Economic Suitability Index for Hydro Energy (TEI-H)

The different socio-environmental and techno-economic suitability indices were calculated using Weighted Linear Combination (WLC) based on their corresponding fuzzified objectives and criteria from Table 3.8 and Fuzzy-AHP weights using the following equation:

$$SI = \sum w_i C_i \tag{3-17}$$

where w_i is the Fuzzy-AHP weight of *i*th fuzzified criterion C_i. For example, in the case shown in Figure 3.7, the SEI-W is calculated using the fuzzified criteria C01-C05 and their corresponding Fuzzy-AHP weights.

3.5. Identification of Suitable Sites for Individual Renewable Energy Systems

In a GIS environment, spatial analysis is used to find sites that are suitable for the construction and development of single renewable energy systems. In this study, ArcGIS was used to carry out the spatial analysis. Separate layers in the GIS environment were generated to reflect each criterion associated with socio-environmental and techno-economic suitability objectives, as previously discussed. After calculating the different socio-environmental and techno-economic

indices, the overall suitability indices were determined and mapped using the fuzzy AND operator, as shown in Figure 3.9. The overall suitability indices for wind, solar, and hydro energy systems are referred to as the Overall Suitability Index for Wind Energy (OSI-W), the Overall Suitability Index for Solar Energy (OSI-S), and the Overall Suitability Index for Hydro Energy (OSI-H), respectively.

The suitable sites for single renewable systems are then identified using the site selection rules shown in Table 3.10. The first and second columns in Table 3.10 reflect the two different suitability indices used to calculate the overall suitability index and determine the suitable site. For example, the first and second columns for wind energy systems are SEI-W and TEI-W, respectively. Suitable sites for wind energy systems are those with suitability indices that have values of at least 0.5 for both SEI-W and TEI-W. For solar and hydro energy systems, the same technique is used to establish the overall suitability index and the suitable site maps.

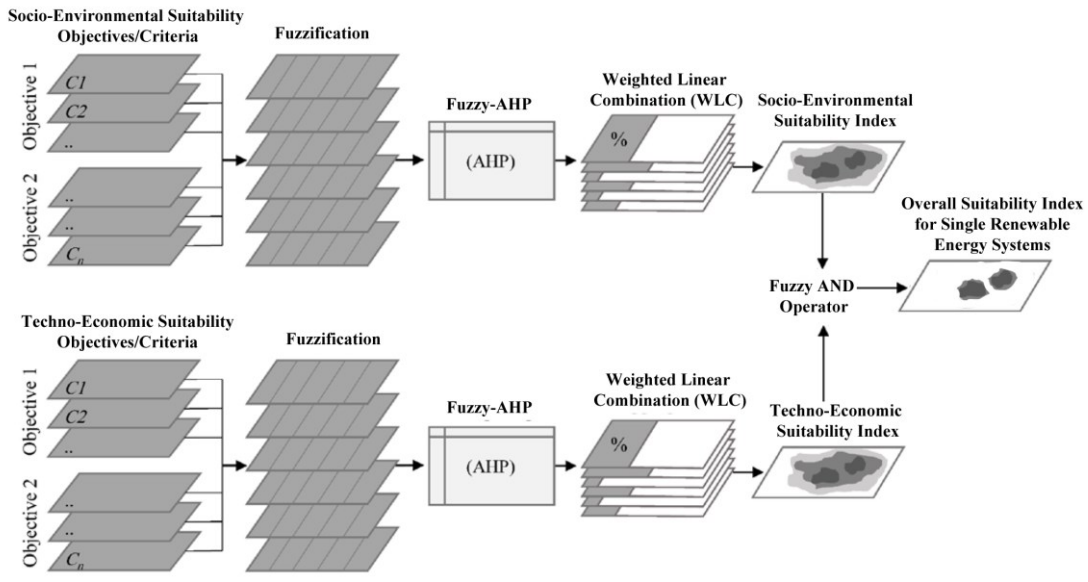

Figure 3.9 Spatial analysis for determining of suitable sites for individual renewable energy systems

Table 3.10 Site selection rules for single and hybrid renewable energy systems based on Fuzzy AND operator

Suitability Indices - component 1 (HPI or EIS or EIW)	Suitability Indices - component 2 (HPI or SPI or WPI)	Priority sites for individual energy (OH, OS, OW) and hybrid energy (OHHS, OHWS)	Decision
$0 \leq SI_1 < 0.5$	$0 \leq SI_2 < 0.5$	0	Reject (Unsuitable)
$0 \leq SI_1 < 0.5$	$0.5 \leq SI_1 \leq 0.5$	0	Reject (Unsuitable)
$0.5 \leq SI_1 \leq 1.0$	$0 \leq SI_2 < 0.5$	0	Reject (Unsuitable)
$0.5 \leq SI_1 \leq 1.0$	$0.5 \leq SI_2 \leq 1.0$	minimum[SI_1,SI_2]	Accept (Suitable)

3.6. Identification of Suitable Sites for Hybrid Renewable Energy Systems

To identify sites that are suitable for the construction and development of hybrid renewable energy systems, overall suitability indices for individual renewable energy systems are overlaid using the fuzzy AND operator, and the same site selection rules as in Table 3.10 are applied. As shown in Figure 3.9, the overall suitability indices for hybrid wind-solar and hybrid hydro-solar energy systems are OSI-WS and OSI-HS, respectively. The map for OSI-WS is created by using fuzzy AND on OSI-W and OSI-S. The same process is used in creating the map for OSI-HS using OSI-S and OSI-H.

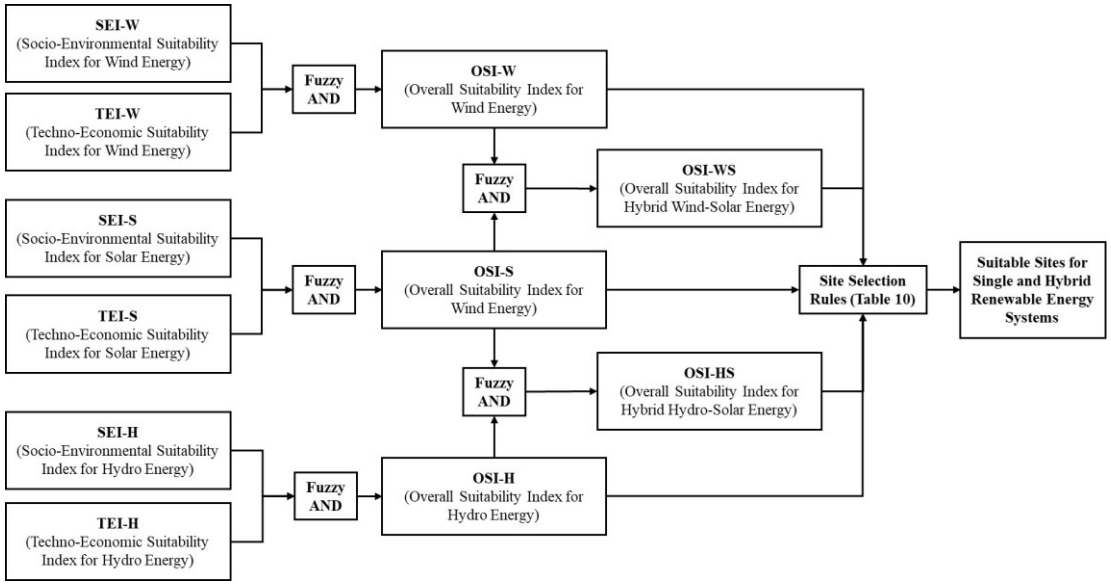

Figure 3.10 Flowchart for the determining suitable sites for individual and hybrid renewable energy systems using different indices

3.7. Results and Discussion

This section discusses the details of the results of the performed suitability analysis.

3.7.1. Fuzzy AHP Weights

The weights for each socio-environmental and techno-economic criteria which are calculated using Fuzzy-AHP are summarized in Table 3.11 and Table 3.12, respectively. Based on Table 3.11, criteria C02, C09, and C10 with weights of 37.83%, 46.96%, and 45.80%, the most important factors for considering the socio-environmental suitability of wind, solar, and hydro energy systems, respectively. Table 3.12 shows that for criteria that are considered the most important for determining techno-economic suitability of single renewable energy systems are the criteria associated with energy production. For solar energy systems, C18 which is the criterion associated with solar energy generation was given the most importance with a calculated weight of 51.17% while for wind and hydro energy systems the criteria C14 and C25 have the highest weights of 52.15% and 49.53%, respectively. In real-life practice, renewable energy project developers determine areas that have high energy potential first before considering other factors, which is a confirmation of the previous studies reviewed and discussed in the earlier section.

Table 3.11 Summary of calculated socio-environmental criteria weights using Fuzzy-AHP

Suitability Criteria	**Calculated Weight**
Wind (Socio-Environmental)	
C01 - Distance from airports	4.60%
C02 - Distance from protected and conservation areas	37.83%
C03 - Distance from urban areas	9.82%
C04 - Distance from rural settlements	13.14%
C05 - Distance from coastlines	34.61%
Solar (Socio-Environmental)	
C06 - Distance from coastline	10.31%
C07 - Distance from airports	18.75%
C08 - Distance from lakes and wetlands	23.98%
C09 - Distance from agricultural areas	46.96%
Hydro (Socio-Environmental)	
C10 - Distance from protected and conservation areas	45.80%
C11 - Distance from urban areas	8.83%
C12 - Distance from agricultural areas	28.31%
C13 - Distance from residential areas	17.06%

Table 3.12 Summary of calculated techno-economic criteria weights using Fuzzy-AHP

Suitability Criteria	Calculated Weight
Wind (Techno-Economic)	
C14 - Wind Speed	52.16%
C15 - Slope	20.91%
C16 - Distance from transmission lines	19.00%
C17 - Distance from main roads	7.93%
Solar (Techno-Economic)	
C18 - Solar Energy Generation	51.17%
C19 - Slope	25.91%
C20 - Distance from transmission lines	17.08%
C21 - Distance from urban areas	5.84%
Hydro (Techno-Economic)	
C22 - Slope	10.05%
C23 - Distance from transmission network	17.06%
C24 - Distance from major and minor roads	23.36%
C25 - Distance from site with identified energy potential	49.53%

3.7.2. Suitable Sites for Wind, Solar, and Hydro Energy Systems

Using the proposed framework shown in Figure 3.1, the overall suitability index and suitable site maps for wind, solar, and hydro energy systems in the study area, Lanao del Norte, were created as shown in Figure 3.11 and Figure 3.12, respectively. As shown in these figures, the areas that are considered suitable for the construction and development of renewable energy systems have an overall suitability index of at least 0.5, with 1 as the highest value. Sites that are considered unsuitable have overall suitability index value of lesser than 0.5, with 0 as the lowest value. These unsuitable areas These unsuitable sites include areas that are covered by the restriction layers and areas that have a high socio-environmental suitability index but with low techno-economic suitability index, and vice versa. The spatial analysis performed in ArcGIS for the site selection process is driven by the site selection rules shown in Table 3.10. For example, in determining sites that are suitable for solar energy systems, some areas that have a high socio-environmental suitability index are eliminated due to a low techno-economic suitability index or because they have inadequate energy potential.

The results of the site selection for single renewable energy systems are summarized in Table 3.13. The table shows the total area suitable for wind, solar, and hydro energy systems (in km^2) for each municipality in Lanao del Norte. Furthermore, based on the results, the province

has total areas of 155.93 km^2, 1230 km^2, and 1206 km^2 for wind, solar, and hydro energy systems, respectively. Most of the areas which have the highest potential for construction of solar power plant are located near the coastline. This is due to solar energy potential and suitability factors having the highest values in these areas. Municipalities nearby Iligan Bay also have the highest total number of potential areas with high suitability for solar plant construction. Out of the 23 municipalities, only 10 have areas suitable for wind farm. Since most of the areas in the province have wind speeds lower than 5 m/s only a few municipalities have areas that are suitable for construction of the facilities. Municipalities with the highest potential areas are either located nearby Ilana Bay or at the part of Iligan Bay where wind funneling effect occurs. For suitable hydro energy potential sites in the province, Iligan City has the highest number of suitable sites. This is because Mandulog River and Agus River, two of the major rivers in the province, flows through the city.

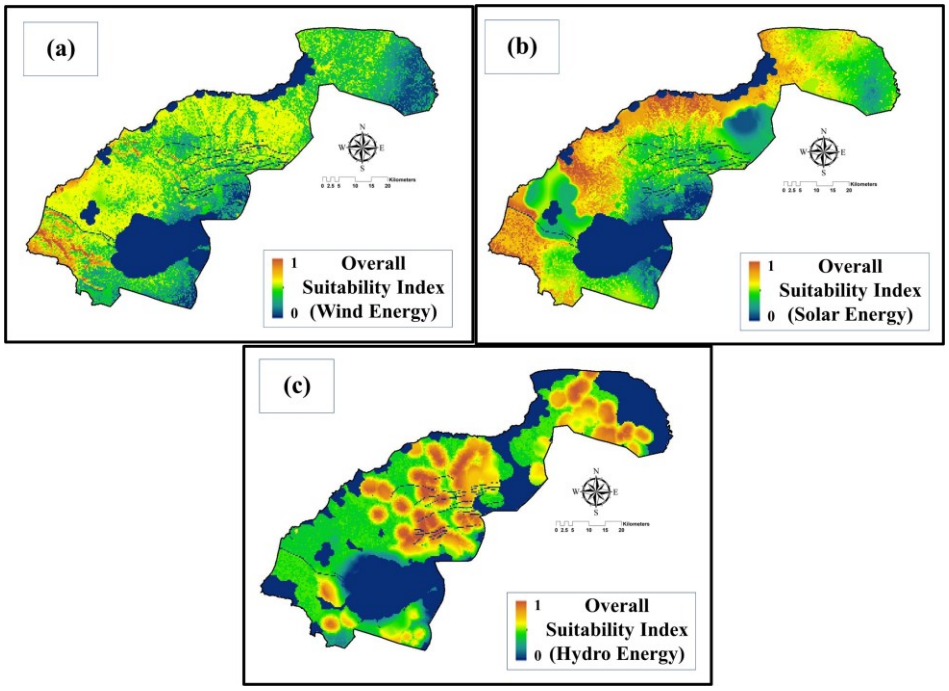

Figure 3.11 Overall suitability indices for (a) wind energy; (b) solar energy; and (c) hydro energy systems

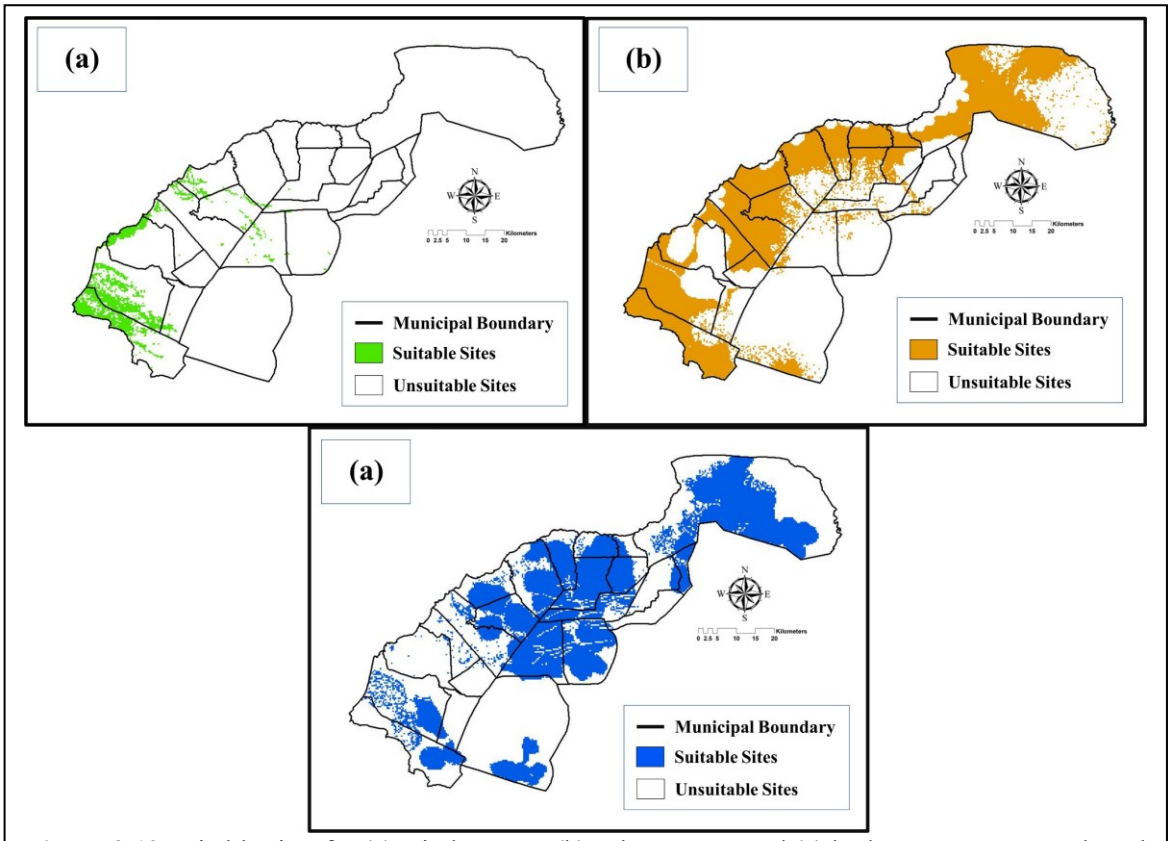

Figure 3.12 Suitable sites for (a) wind energy; (b) solar energy; and (c) hydro energy systems based on the calculated overall suitability indices

3.7.3. Suitable Sites for Hybrid Renewable Energy Systems

For hybrid wind-solar and hybrid hydro-solar energy systems, the overall suitability index and suitable site maps are shown in Figure 3.13. The suitable sites for hybrid renewable energy systems based on Overall Suitability Index for Hybrid Wind-Solar Energy (OSI-WS) and Overall Suitability Index for Hybrid Hydro-Solar Energy (OSI-HS) were then selected using same site selection rule shown Table 3.10. Hybrid wind-hydro energy systems was not considered in this study since only a small area of northwestern part of the province has an acceptable wind speed for wind farm and there are no suitable area for the combined suitable wind energy and hydro energy. Based on the results of the suitability analysis, suitable sites for hybrid wind-solar energy systems are the areas that has high overall suitability index for wind energy since these areas also have high overall suitability index for solar energy. Furthermore, as shown in Table 3.13 the total area that are suitable for hybrid wind-solar and hybrid hydro-solar are 126.60 km^2 and 629.02 km^2, respectively. The installation and development of hybrid renewable energy systems in these

identified sites can aid in increasing the rural electrification of the province while addressing the issue of single renewable energy systems' intermittency problems.

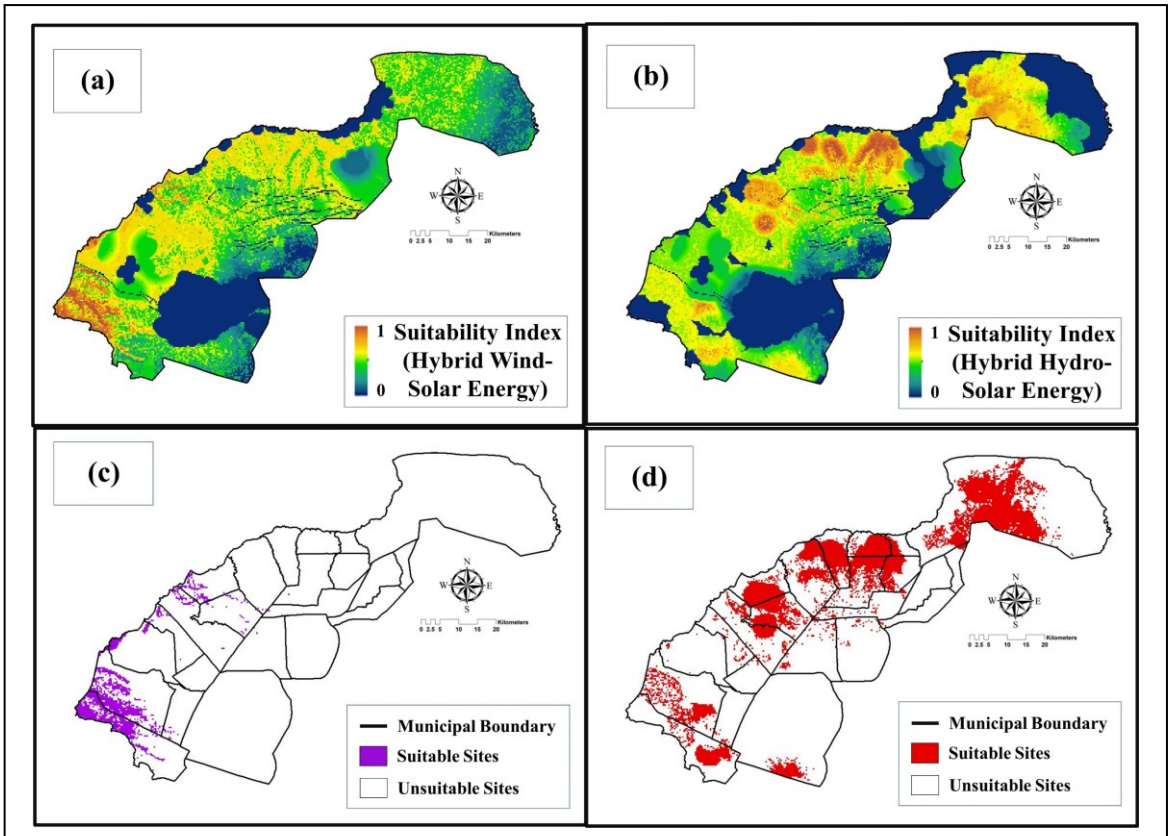

Figure 3.13 Suitability index for hybrid (a) wind-solar energy; and (b) hydro-solar energy systems and suitable sites for hybrid (c) wind-solar energy; and (d) hydro-solar energy systems

Table 3.13 Summary of total suitable areas for the construction renewable energy facilities for each municipality/city

Municipality /City	Area Suitable - Wind (km^2)	Area Suitable - Solar (km^2)	Area Suitable - Hydro (km^2)	Area Suitable - Wind-Solar (km^2)	Area Suitable- Hydro-Solar (km^2)
Bacolod	0	46.89	43.84	0	37.23
Baloi	0	2.48	10.74	0	0
Baroy	4.13	50.36	5.09	2.97	4.60
Iligan City	0	333.56	316.31	0	203.26
Kapatagan	58.25	119.62	68.71	50.35	50.27
Kauswagan	0	40.74	30.39	0	30.34
Kolambugan	8.00	63.87	35.30	8.00	35.26
Lala	17.05	29.13	2.79	8.13	1.40
Linamon	0	17.13	7.38	0	7.38
Magsaysay	4.97	59.59	66.45	3.17	46.28
Maigo	0	75.22	77.66	0	44.07
Matungao	0	26.52	38.69	0	24.50
Munai	1.06	8.01	97.87	0	3.38
Nunungan	0	31.23	61.28	0	18.76

Pantao Ragat	0	8.29	47.08	0	7.01
Pantar	0	5.50	2.07	0	0.61
Poona Piagapo	0	43.22	81.60	0	41.58
Salvador	0	19.94	0.90	0	0.90
Sapad	3.25	10.97	7.44	1.26	2.01
Sultan Naga Dimaporo	49.29	123.63	43.61	47.48	34.61
Tagoloan	0	1.90	21.62	0	1.90
Tangcal	4.46	9.35	104.38	0	6.40
Tubod	5.47	103.59	34.79	4.84	27.26
Total	155.93	1230.73	1206.00	126.20	629.02
Total	**155.93**	**1230.73**	**1206.00**	**126.20**	**629.02**

3.7.4. Sensitivity Analysis

A sensitivity analysis was performed to determine the difference between the results of suitability analysis with and without the calculated Fuzzy-AHP weights. For the suitability analysis of hybrid renewable energy systems (wind-solar and hydro-solar) without Fuzzy-AHP, the weights for the socio-environmental and techno-economic objectives and criteria. These equal weights are then used to calculate the different suitability indices (SEI-W, SEI-S, SEI-H, TEI-W,TEI-S, TEI-H). Using the same spatial analysis and site selection rule from the previous section, the different the suitable sites are single and hybrid renewable energy systems then selected. Figure 3.14 shows the results for hybrid hydro-solar systems and wind-solar systems, respectively. Based on the results, there is an increase of identified suitable sites when Fuzzy-AHP weights were not applied in the analysis. However, parts of these identified suitable areas, which have low energy production, are not preferred by the experts who made the judgement for weighting the different criteria. Table 3.14 shows the total areas that were identified using equal weights and Fuzzy-AHP weights.

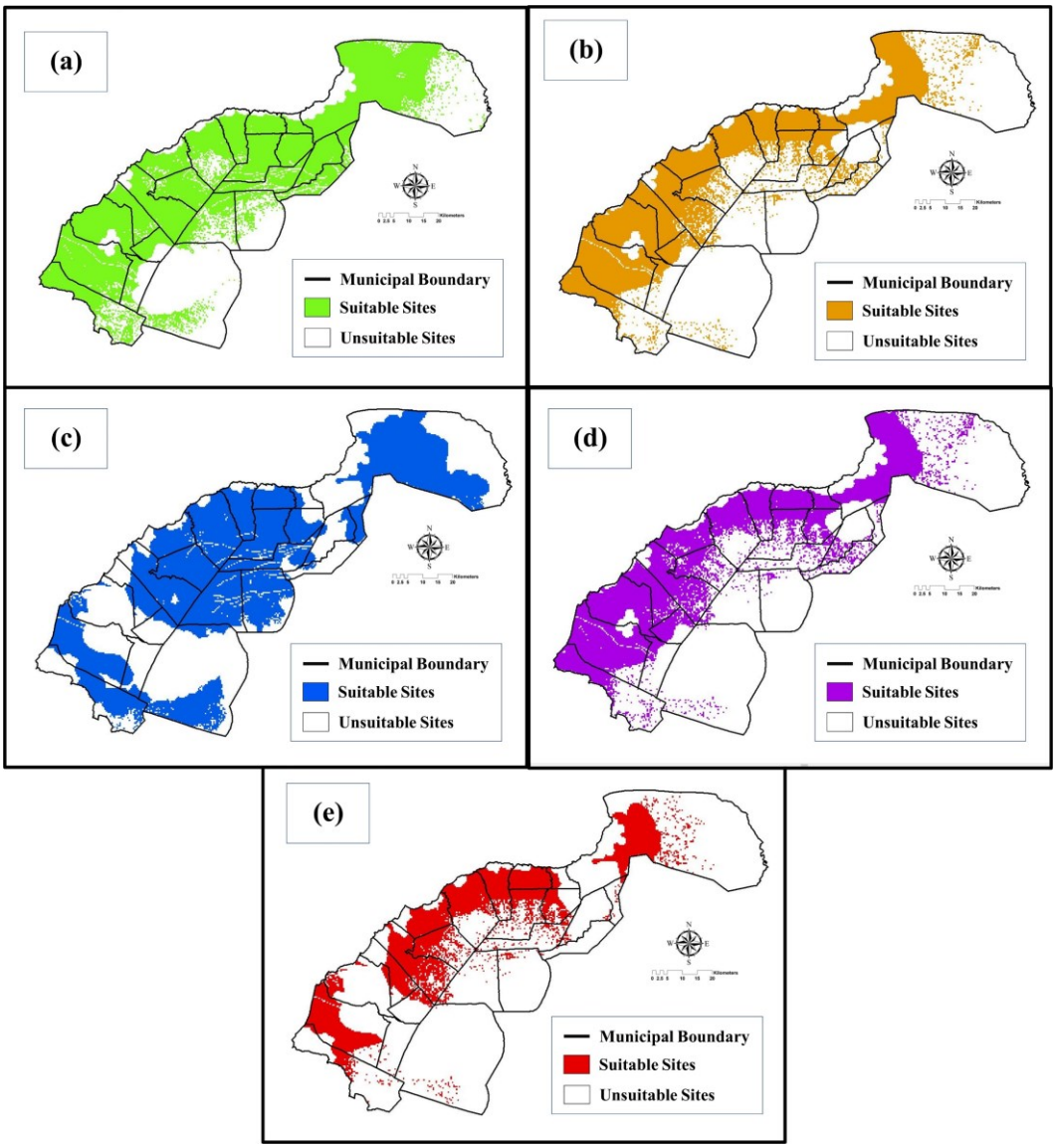

Figure 3.14 Identified suitable sites for single and hybrid renewable energy systems using equal weights for different criteria

Table 3.14 Total suitable areas using Fuzzy-AHP Weights and Equal Weights

Renewable Energy System Type	**Suitable Area - Fuzzy-AHP Weights (km^2)**	**Suitable Area - Equal Weights (km^2)**
Wind	155.93	1762.66
Solar	1230.73	1149.14
Hydro	1206.00	1610.22
Wind-Solar	126.20	1116.76
Hydro-Solar	629.02	750.12

3.8. Summary

It is now widely acknowledged that renewable energy systems have the ability to mitigate the environmental harm caused by energy use. Previous research has looked on the disadvantages of renewable energy technologies. Unpredictable power supply from stand-alone renewable energy systems as a result of fluctuating weather and climatic conditions is a significant issue. A more technical way of putting it is that wind turbines can only create electricity constantly provided the wind speed is maintained at a consistent level at all times. Unlike the last scenario, this one is not feasible. Several renewable energy technologies should be incorporated into a hybrid system in order to assure power generating dependability.

Among the many contributions and benefits of this research are the following:

1. A GIS-based technique for selecting appropriate sites for individual and hybrid renewable energy systems based on Fuzzy-AHP.
2. An MCDM technique is used to evaluate the environmental acceptability of hydropower, wind energy, and solar energy, as well as the economic feasibility of achieving these goals.
3. The approach and criteria developed in this research may be used to perform analogous suitability studies for many kinds of individual and hybrid renewable energy systems, especially in study locations with similar geographical and environmental characteristics and restrictions.
4. The findings provide a more thorough picture of present wind farm sites, as well as possible locations for hybrid hydro-solar and hybrid wind-solar energy systems in the future.
5. The suggested hybrid renewable energy systems site selection technique can assist decision-makers and investors in choosing places that are both economically and ecologically feasible.
6. 6. This site selection approach may be simply modified to other renewable energy instruments despite the fact that the present implementation only considers hydropower, wind, and solar–PV systems.

3.9. Chapter 3 References

[3-1] R. P. Tarife, A. P. Tahud, E. J. G. Gulben, H. A. R. C. P. Macalisang, and Ma. T. T. Ignacio, "Application of Geographic Information System (GIS) in Hydropower Resource Assessment: A Case Study in Misamis Occidental, Philippines," Int. J. Environ. Sci. Dev., vol. 8, no. 7, pp. 507–511, 2017, doi: 10.18178/ijesd.2017.8.7.1005.

[3-2] A. P.- Tahud, and N. R. Estoperez, "Evaluation of Potential Hydropower Sites in Iligan City Using Geographic Information System (GIS)," in 5th Annual International Conference on Sustainable Energy and Environmental Sciences (SEES 2016), Feb. 2016. doi: 10.5176/2251-189X_SEES16.11.

[3-3] F. M. Howari and H. Ghrefat, "Chapter 4 - Geographic information system: spatial data structures, models, and case studies," in Pollution Assessment for Sustainable Practices in Applied Sciences and Engineering, A.-M. O. Mohamed, E. K. Paleologos, and F. M. Howari, Eds. Butterworth-Heinemann, 2021, pp. 165–198. doi: 10.1016/B978-0-12-809582-9.00004-9.

[3-4] O. A. C. Hoes, L. J. J. Meijer, R. J. van der Ent, and N. C. van de Giesen, "Systematic high-resolution assessment of global hydropower potential," PLOS ONE, vol. 12, no. 2, p. e0171844, Feb. 2017, doi: 10.1371/journal.pone.0171844.

[3-5] V. Sammartano, L. Liuzzo, and G. Freni, "Identification of Potential Locations for Run-of-River Hydropower Plants Using a GIS-Based Procedure," Energies, vol. 12, no. 18, p. 3446, Sep. 2019, doi: 10.3390/en12183446.

[3-6] I. A. Guiamel and H. S. Lee, "Potential hydropower estimation for the Mindanao River Basin in the Philippines based on watershed modelling using the soil and water assessment tool," Energy Rep., 2020.

[3-7] G. Alcalá, L. F. Grisales-Noreña, Q. Hernandez-Escobedo, J. J. Muñoz-Criollo, and J. D. Revuelta-Acosta, "SHP Assessment for a Run-of-River (RoR) Scheme Using a Rectangular Mesh Sweeping Approach (MSA) Based on GIS," 2021.

[3-8] L. Albraheem and L. Alabdulkarim, "Geospatial Analysis of Solar Energy in Riyadh Using a GIS-AHP-Based Technique," ISPRS Int. J. Geo-Inf., vol. 10, no. 5, p. 291, May 2021, doi: 10.3390/ijgi10050291.

[3-9] A. Sunarso, K. Ibrahim-Bathis, S. A. Murti, I. Budiarto, and H. S. Ruiz, “GIS-Based Assessment of the Technical and Economic Feasibility of Utility-Scale Solar PV Plants: Case Study in West Kalimantan Province,” Sustainability, vol. 12, no. 15, p. 6283, Aug. 2020, doi: 10.3390/su12156283.

[3-10] H. Yousefi, H. Hafeznia, and A. Yousefi-Sahzabi, “Spatial Site Selection for Solar Power Plants Using a GIS-Based Boolean-Fuzzy Logic Model: A Case Study of Markazi Province, Iran,” Energies, vol. 11, no. 7, p. 1648, Jun. 2018, doi: 10.3390/en11071648.

[3-11] D. Palmer and R. Blanchard, “Evaluation of High-Resolution Satellite-Derived Solar Radiation Data for PV Performance Simulation in East Africa,” Sustainability, vol. 13, no. 21, p. 11852, Oct. 2021, doi: 10.3390/su132111852.

[3-12] E. Noorollahi, D. Fadai, M. Akbarpour Shirazi, and S. Ghodsipour, “Land Suitability Analysis for Solar Farms Exploitation Using GIS and Fuzzy Analytic Hierarchy Process (FAHP)—A Case Study of Iran,” Energies, vol. 9, no. 8, p. 643, Aug. 2016, doi: 10.3390/en9080643.

[3-13] P. Díaz-Cuevas, “GIS-Based Methodology for Evaluating the Wind-Energy Potential of Territories: A Case Study from Andalusia (Spain),” Energies, vol. 11, no. 10, p. 2789, Oct. 2018, doi: 10.3390/en11102789.

[3-14] A. S. Zalhaf et al., “A High-Resolution Wind Farms Suitability Mapping Using GIS and Fuzzy AHP Approach: A National-Level Case Study in Sudan,” Sustainability, vol. 14, no. 1, p. 358, Dec. 2021, doi: 10.3390/su14010358.

[3-15] D. G. Vagiona and M. Kamilakis, “Sustainable Site Selection for Offshore Wind Farms in the South Aegean—Greece,” 2018.

[3-16] P. D. Rigo et al., “Renewable Energy Problems: Exploring the Methods to Support the Decision-Making Process,” 2020.

[3-17] M. Ramezanzade et al., “Implementing MCDM Techniques for Ranking Renewable Energy Projects under Fuzzy Environment: A Case Study,” Sustainability, vol. 13, no. 22, p. 12858, Nov. 2021, doi: 10.3390/su132212858.

[3-18] F. Ali, A. Bennui, S. Chowdhury, and K. Techato, “Suitable Site Selection for Solar-Based Green Hydrogen in Southern Thailand Using GIS-MCDM Approach,” Sustainability, vol.

14, no. 11, p. 6597, May 2022, doi: 10.3390/su14116597.

[3-19] A. Mardani, A. Jusoh, E. K. Zavadskas, F. Cavallaro, and Z. Khalifah, “Sustainable and Renewable Energy: An Overview of the Application of Multiple Criteria Decision Making Techniques and Approaches,” 2015.

[3-20] M. S. Genc and F. Karipoglu, “Wind-Solar Site Selection using a GIS-MCDM-based Approach with an Application in Kayseri Province/Turkey,” in 7th Iran Wind Energy Conference (IWEC2021), Shahrood, Iran, May 2021, pp. 1–4. doi: 10.1109/IWEC52400.2021.9467003.

[3-21] M. R. Elkadeem, “Sustainable siting and design optimization of hybrid renewable energy system: A geospatial multi-criteria analysis,” Appl. Energy, 2021.

[3-22] P. Díaz-Cuevas, “Integrating MCDM and GIS for renewable energy spatial models: assessing the individual and combined potential for wind, solar and biomass energy in Southern Spain”.

[3-23] DOE, “Distribution Utility Profile - Lanao del Norte Electric Cooperative (LANECO).” https://www.doe.gov.ph/ducsp/laneco (accessed Sep. 21, 2021).

[3-24] ASTER, “ASTER Global Digital Elevation Map.” https://asterweb.jpl.nasa.gov/gdem.asp (accessed Sep. 30, 2021).

[3-25] Solargis, “Global Solar Atlas 2.0.” https://solargis.com/maps-and-gis-data/download/philippines (accessed Aug. 25, 2021).

[3-26] Global Wind Atlas, “Philippines - Wind Speed.” https://globalwindatlas.info/api/gis/country/PHL/wind-speed/50 (accessed Aug. 25, 2021).

[3-27] Phil LiDAR 2 Program, “PHIL LIDAR 2: Nationwide Detailed Resources Assessment using LiDAR.” https://dream.upd.edu.ph/ about/phil-lidar-2/ (accessed Aug. 14, 2021).

[3-28] PhilGIS, “Philippines-Lanao del Norte Data.” http://philgis.org/province-page/lanao-del-norte (accessed Aug. 01, 2021).

[3-29] PHIVOLCS, “Hazard Maps for Lanao Del Norte, Region X (Northern Mindanao).” https://gisweb.phivolcs.dost.gov.ph/gisweb/ earthquake-volcano-related-hazard-gis-information (accessed Oct. 25, 2021).

[3-30] OpenStreetMap, “OpenStreetMap Data for Philippines.”

https://download.geofabrik.de/asia/philippines.html (accessed Aug. 01, 2021).

[3-31] DOE, “Transmission Development Plan 2014-2015 Final Report.” https://www.doe.gov.ph/energy-information-resources?q= transmission-development-plan&withshield=1 (accessed Sep. 21, 2021).

[3-32] T. Nakata and T. Kumamoto, “Land use issues against potential danger of active faults, and‘Active Fault Zones Act,” Act. Fault Res., vol. 2003, no. 23, pp. 13–18, 2003, doi: 10.11462/afr1985.2003.23_13.

[3-33] B. M. Pacheco, “Safety of PH structures during quakes,” Apr. 09, 2011. https://mmda.gov.ph/en/20-faq/297-safety-of-ph-structures-during-quakes.html (accessed Aug. 10, 2021).

[3-34] D. Latinopoulos and K. Kechagia, “A GIS-based multi-criteria evaluation for wind farm site selection. A regional scale application in Greece,” Renew. Energy, vol. 78, pp. 550–560, Jun. 2015, doi: 10.1016/j.renene.2015.01.041.

[3-35] Biodiversity Management Bureau, “Guidebook to Protected Areas of the Philippines; Biodiversity Management Bureau – Department of Environment and Natural Resources, 2015.” . https://www.denr.gov.ph/images/DENR_Publications/PA_Guidebook_Complete.pdf (accessed Mar. 07, 2022).

[3-36] Congress of the Philippines, “Republic Act No. 7586 - National Integrated Protected Areas System Act of 1992,” Jun. 01, 1992. https://www.officialgazette.gov.ph/1992/06/01/republic-act-no-7586/

[3-37] Y. Noorollahi, “Multi-criteria decision support system for wind farm site selection using GIS,” Sustain. Energy Technol. Assess., 2016.

[3-38] D. Voivontas, D. Assimacopoulos, and A. Mourelatos, “EVALUATION OF RENEWABLE ENERGY POTENTIAL USING A GIS DECISION SUPPORT SYSTEM”.

[3-39] N. Ghorbani, H. Makian, and C. Breyer, “A GIS-based method to identify potential sites for pumped hydro energy storage - Case of Iran,” Energy, vol. 169, pp. 854–867, Feb. 2019, doi: 10.1016/j.energy.2018.12.073.

[3-40] J. Görtz, M. Aouad, S. Wieprecht, and K. Terheiden, “Assessment of pumped hydropower energy storage potential along rivers and shorelines,” Renew. Sustain. Energy Rev., vol.

165, p. 112027, Sep. 2022, doi: 10.1016/j.rser.2021.112027.

[3-41] L. Gigović, D. Pamučar, D. Božanić, and S. Ljubojević, “Application of the GIS-DANP-MABAC multi-criteria model for selecting the location of wind farms: A case study of Vojvodina, Serbia,” Renew. Energy, vol. 103, pp. 501–521, Apr. 2017, doi: 10.1016/j.renene.2016.11.057.

[3-42] M. Szurek, J. Blachowski, and A. Nowacka, “GIS-based method for wind farm location multi-criteria analysis,” Min. Sci., 2014, doi: 10.5277/MS142106.

[3-43] J. Huang, X. Huang, N. Song, Y. Ma, and D. Wei, “Evaluation of the Spatial Suitability of Offshore Wind Farm—A Case Study of the Sea Area of Liaoning Province,” 2022.

[3-44] C.-D. Yue and S.-S. Wang, “GIS-based evaluation of multifarious local renewable energy sources: a case study of the Chigu area of southwestern Taiwan,” Energy Policy, vol. 34, no. 6, pp. 730–742, Apr. 2006, doi: 10.1016/j.enpol.2004.07.003.

[3-45] N. Y. Aydin, E. Kentel, and H. Sebnem Duzgun, “GIS-based site selection methodology for hybrid renewable energy systems: A case study from western Turkey,” Energy Convers. Manag., vol. 70, pp. 90–106, Jun. 2013, doi: 10.1016/j.enconman.2013.02.004.

[3-46] A. Vrînceanu et al., “Impacts of Photovoltaic Farms on the Environment in the Romanian Plain,” Energies, vol. 12, no. 13, p. 2533, Jul. 2019, doi: 10.3390/en12132533.

[3-47] M. Jafari, R. Fazloula, M. Effati, and A. Jamali, “Providing a GIS-based framework for Run-Of-River hydropower site selection: a model based on sustain,” Civ. Eng. Environ. Syst..

[3-48] P. Rojanamon, T. Chaisomphob, and T. Bureekul, “Application of geographical information system to site selection of small run-of-river hydropower project by considering engineering/economic/ environmental criteria and social impact,” Renew. Sustain. Energy Rev., 2009.

[3-49] C.-S. Yi, J.-H. Lee, and M.-P. Shim, “Site location analysis for small hydropower using geo-spatial information system,” Renew. Energy, 2010.

[3-50] S. C. Rana, “Selection of best location for small hydro power project using AHP, WPM and TOPSIS methods”.

[3-51] R. P. Singh, “Analytical hierarchy process (AHP) application for reinforcement of

hydropower strategy in Nepal," Renew. Sustain. Energy Rev., 2016.

[3-52] A. H. Nebey, B. Z. Taye, and T. G. Workineh, "Site Suitability Analysis of Solar PV Power Generation in South Gondar, Amhara Region," J. Energy, vol. 2020, pp. 1–15, May 2020, doi: 10.1155/2020/3519257.

[3-53] B. Halder et al., "Land Suitability Investigation for Solar Power Plant Using GIS, AHP and Multi-Criteria Decision Approach: A Case of Megacity Kolkata, West Bengal, India," 2022.

[3-54] T. Supriyasilp, K. Pongput, and T. Boonyasirikul, "Hydropower development priority using MCDM method," Energy Policy, vol. 37, no. 5, pp. 1866–1875, May 2009, doi: 10.1016/j.enpol.2009.01.023.

[3-55] C. Bolli, "A GIS-based Multi-Criteria Analysis for Suitability Assessment of Micro Hydropower Stations A Case Study from Suriname," University of Salzburg, Salzburg, Austria, 2017. [Online]. Available: http://unigis.sbg.ac.at/files_en/Mastertheses/Full/104199.pdf

[3-56] Alex. B. McBratney and I. O. A. Odeh, "Application of fuzzy sets in soil science: fuzzy logic, fuzzy measurements and fuzzy decisions," Geoderma, vol. 77, no. 2–4, pp. 85–113, Jun. 1997, doi: 10.1016/S0016-7061(97)00017-7.

[3-57] P. J. M. van Laarhoven and W. Pedrycz, "A fuzzy extension of Saaty's priority theory," Fuzzy Sets Syst., vol. 11, no. 1, pp. 229–241, Jan. 1983, doi: 10.1016/S0165-0114(83)80082-7.

[3-58] D.-Y. Chang, "Applications of the extent analysis method on fuzzy AHP," Eur. J. Oper. Res., vol. 95, no. 3, pp. 649–655, Dec. 1996, doi: 10.1016/0377-2217(95)00300-2.

[3-59] T. L. Saaty, "Analytic Hierarchy Process," in Encyclopedia of Biostatistics, 2005. doi: 10.1002/0470011815.b2a4a002.

[3-60] Y. Liu, C. M. Eckert, and C. Earl, "A review of fuzzy AHP methods for decision-making with subjective judgements," Expert Syst. Appl., vol. 161, p. 113738, Dec. 2020, doi: 10.1016/j.eswa.2020.113738.

[3-61] R. Aliyev, H. Temizkan, and R. Aliyev, "Fuzzy Analytic Hierarchy Process-Based Multi-Criteria Decision Making for Universities Ranking," 2020.

Chapter 4 Optimization of Electric Transmission Line (ETL) Routing for a Renewable Energy-Based Microgrid using LCP Analysis and GIS-MCDA

4.1. Introduction

Classical electric transmission line siting spends a lot of time huddling paper maps, sketching various possible paths, and then weighing and assessing their feasibility to obtain a single preferred route. This approach needs an expert's interpretation and judgment and is often criticized because it lacks a defendable procedure and fails in engaging alternative perspectives when tracing a preferred route [4-1] . Additionally, the conventional way of transmission line routing is costly, laborious, and tedious. Since most potential sites are found in mountainous, ungauged and remote portions of stream networks and transmission lines start in every potential site to deliver power from renewable energy sources to the load centers, problems such as area inaccessibility, security and safety arise. Through GIS, the optimal goal in transmission line siting for a renewable energy-based microgrid system is to effectively minimize negative impacts on people and the environment while cost savings, reliability, and safety are guaranteed [4-2]. These challenges are addressed in this study which provides transmission line routing for a planned renewable energy-based micro-grid system for the study area, Brgy. Rogongon, Iligan City, Philippines, using remotely sensed data and GIS technology.

4.2. Overall Methodology for the ETL Routing

Figure 4.1 shows the overall methodology for an alternative electric transmission line (ETL) routing method for a renewable energy microgrid. The cost surface was created using a weighted ranking system and a geographic suitability index. The overall methodology is a modification of the Electric Power Research Institute-Georgia Transmission Corporation (EPRI-GTC) method for overhead electric transmission line siting based on the available data and review of the study area. Analytic Hierarch Process (AHP) was used to determine the weights of the

criteria for routing. GIS-MCDA and Least Cost Path (LCP) algorithm (Dijkstra's algorithm) produced three alternative routes based on three perspectives: built, natural, and engineering. The final route is created by combining the alternative routes in a simple perspective.

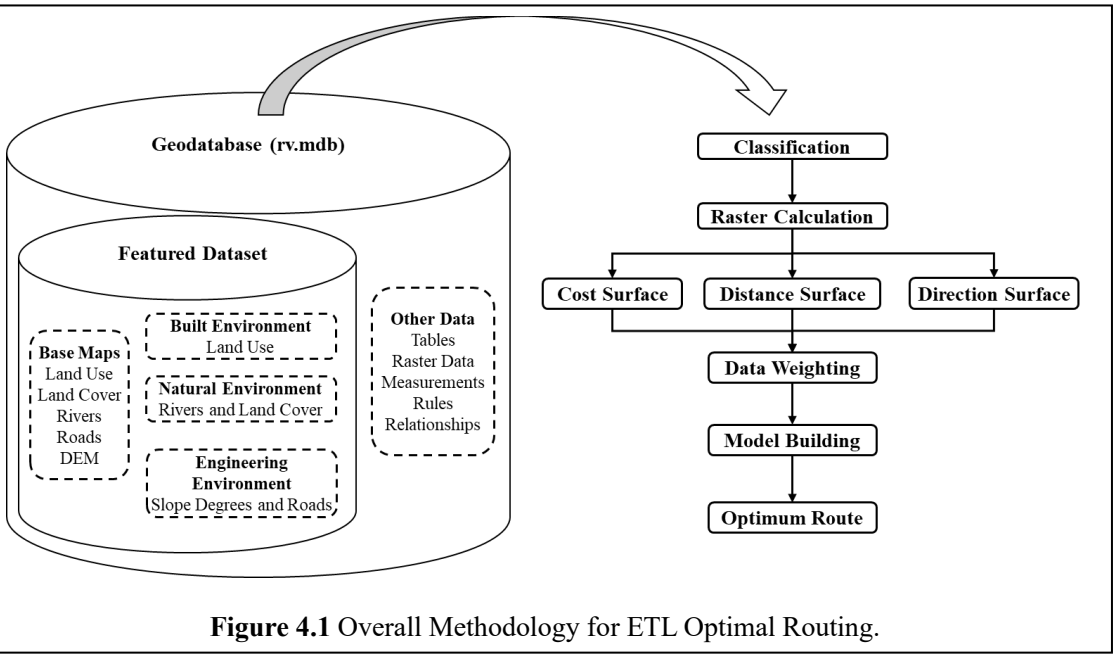

Figure 4.1 Overall Methodology for ETL Optimal Routing.

4.3. GIS Datasets, Data Preparation, Software and Tools

Datasets used in this study are obtained from different sources which include Iligan City Planning and Development Office (ICPDO) and Philippine DREAM Program and internet-based mapping service providers Google Maps, Google Earth, ESRI/ArcGIS® Online and Philippine GIS (PhilGIS). Table 4.1 shows the datasets gathered.

Dataset preparations were performed which include organization of datasets in a geodatabase, georeferencing and necessary coordinate definitions and projections, creation of new shapefiles, reconditioning of the DEM and preparation of spatial models. PCS-WGS 1984 UTM Zone 51N was used as the base coordinate system for this study. ArcMap™ for Desktop 10.2.2 and ArcCatalog™ of ESRI ArcGIS® product and required extensions were used. Extensions like 3D Analyst, Spatial Analyst, Data Interoperability and other free tools for ArcGIS®.

Table 4.1 Datasets with Source and Format

Layer	Source	Format
DEM, Rogongon	ICPDO	Raster, 10-m resolution
Landuse	DREAM	Shapefile (polygon)
River Networks	ICPDO	Shapefile (line)
Municities	PhilGIS	Shapefile (polygon)
Country Region	PhilGIS	Shapefile (polygon)
Land Cover	PhilGIS	Shapefile (polygon)
Rogongon Roads	OpenstreetMap	Shapefile (polyline)

4.4. Determination of Path Selection Criteria and Factors

The path selection criteria and factors were selected and given with features with its corresponding suitability value. Data values were calibrated to the suitability scale using a Delphi Process of transmission sitting experts performed. The data layers weights used were based on the EPRI-GTC (2006) model which used an Analytical Hierarchy Process (AHP) to set the percent influence weighting for each layer group.

The path selection criteria and factors were selected and given with features with its corresponding suitability value. Data values were calibrated to the suitability scale using a Delphi Process of transmission sitting experts performed. The data layers weights used were based on the EPRI-GTC (2006) model which used an Analytical Hierarchy Process (AHP) to set the percent influence weighting for each layer group.

The siting model breaks analysis into three environments with related criteria. The engineering perspective considers factors like terrain slope, intensive agricultural development, and opportunities to site transmission lines in parallel to existing infrastructure. The natural perspective considers environmental features such as wetlands, waterways, public lands, and wildlife habitat. The built perspective considers land use, proximity to buildings, building density, and proposed developments.

Features of a certain data layer can be classified to several classes depending on the new values required. Weights are then assigned to the classes based on the influence or importance in relation with the suitability for electric transmission line routing. As an example, low slopes are assigned with lower weights while steep slopes are assigned with higher weights. Influence of the data

layers individual features used a numeric system in ranking. This clearly identifies each feature influence order. Number one shows lower weight and nine shows a higher weight. The Weighted Overlay then scales the input on a defined scale shown in Figure 4.2.

Number 1 was considered to be the most favorable for electric transmission line routing while the rest was schemed for the next suitability levels up to the least suitable. These values are assigned as attributes to each feature class based on the importance.

Missing factors of the study area with respect to the Delphi calibrations and analytical hierarchy weightings were practically adjusted. Adjustments were based on the actual criteria and factors identified in the study area and the correlation of the factors. Table 4.2 shows the calibrations and weightings for the path selection criteria and factors while Table 4.3 shows the scale used for the weighting.

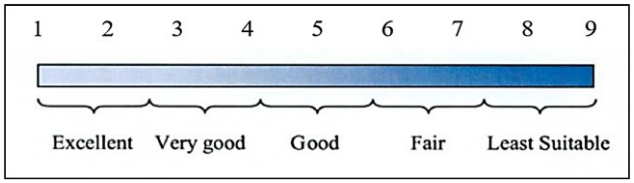

Figure 4.2 Weighted overlay ranking system.

Table 4.2 Delphi-based Calibration and Analytical Hierarchy Weightings.

Built Environment		**Natural Environment**		**Engineering Environment**	
Land Use	100%	Wetlands	44%	Infrastructure	54%
Undeveloped	2	Background	1	Roads	1
		Rivers	3	Backgrounds	3
		Land Cover	56%	Slope (°)	46%
Non-Residential	3	Open/Barren	1	0-10	2
		Grassland	1		
		Shrubs	2	10-20	4
Agricultural	5	Wooded Grassland	4		
		Open Forest	5	20-30	6
		Perennial Crop	6		
Residential	9	Closed Forest	7	30-40	8
		Annual Crop	7		
		Built-up	8	Over 40	9
		Inland Water	9		

4.5. Points for Path Identification

The source (generation points) and destination (load center) points for path identification were determined from actual reconnaissance activities and previous research done by [4-3]. Table 4.3 shows the selected locations of the micro-hydro power and solar-photovoltaic sites in the study area with their corresponding generating capacity while Table 4.4 shows details of the identified load centers with corresponding load demand. Figure 4.3 shows the generation and load sites for path identification

Table 4.3 Hydro and Solar-PV Sites for Path Identification

Site Name	Latitude	Longitude	Capacity
Hydro Site 1	8° 12' 48.00"	124° 26' 44.67"	15.14 kW
Hydro Site 2	8° 12' 40.17"	124° 26' 41.39"	96.85 kW
Hydro Site 3	8° 12' 35.92"	124° 26' 42.28"	94.70 kW
Hydro Site 4	8° 14' 8.00"	124° 28' 7.60"	29.38 kW
Hydro Site 5	8° 14' 5.80"	124° 28' 13.20"	20.76 kW
Hydro Site 6	8° 14' 6.10"	124° 28' 12.40"	17.53 kW
Solar Site 1 (773)	8° 13' 57.04"	124° 27' 5.79"	30kW
Solar Site 2 (858)	8° 13' 49.87"	124° 27' 8.60"	30kW
Solar Site 3 (943)	8° 13' 41.56"	124° 27' 29.42"	30kW
Solar Site 4 (1133)	8° 13' 22.52"	124° 26' 28.15"	30kW

Table 4.4 Load Centers for Path Identification

Site Name	Latitude	Longitude	Load
Salingsing	8° 13' 7.71"	124° 28' 32.65"	25 kW
Languisan	8° 13' 0.97"	124° 28' 4.98"	20 kW
Libandayan	8° 13' 22.25"	124° 27' 24.35"	18 kW
Gabunan	8° 13' 42.87"	124° 27' 23.60"	15 kW
Malagsum	8° 13' 23.76"	124° 26' 26.41"	25 kW

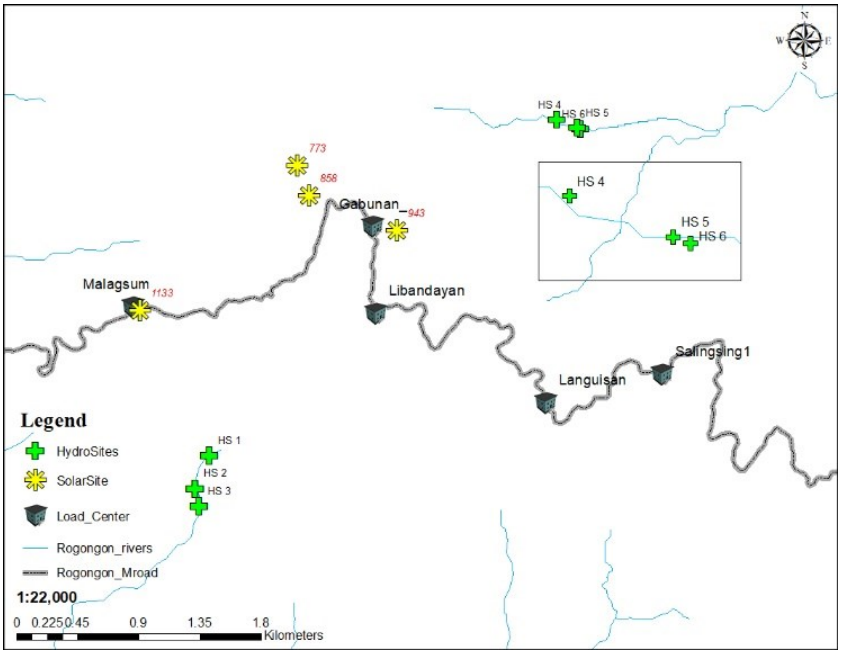

Figure 4.3 Hydro, Solar-PV and Load Center Sites for Path Identification

4.6. Overlay Analysis

Overlay analysis is a group of methodologies applied in optimal site selection or suitability modeling. It is a technique for applying a common scale of values to diverse and dissimilar inputs to create an integrated analysis [4-4]. Overlay analysis overlays several layers together wherein layers must be classified into common preference scale and weights each according to its importance. Figure 4.4 shows the illustration of the weighted overlay analysis technique.

For this study, each input raster was weighted based on its percent influence or importance. The weight is a relative percentage, and the sum of the percent influence must be equal to 100. Changing the percentage influences or the evaluation scales can change the results of the weighted overlay analysis. Equation (1) was used to calculate output raster by the weighted overlay analysis is presented by the equation:

$$Raster_{out} = \sum_{i=1}^{n} Raster_n \cdot Influence_n \quad (4\text{-}1)$$

where $Raster_{out}$ is the output cell value, $Raster_n$ is the input raster cell value and $Influence_n$ is the

input raster cell influence.

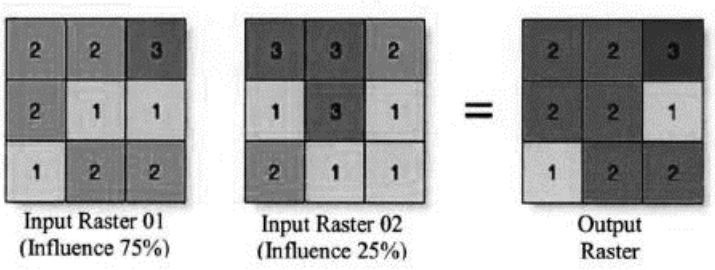

Figure 4.4 Sample overlay analysis

4.7. Analytic Hierarchy Process (AHP)

Saaty developed the analytical hierarchy process (AHP) in 1970, and it is a technique for doing pairwise comparisons. This approach is well recognized as a powerful tool for doing Multiple-Criteria Decision Analysis (MCDA) in the context of complicated decision-making situations. It is composed of all components in a hierarchical arrangement and consists of three steps: first, describing the complicated decision-making issue; second, comparing the selection factors pairwise; and third, creating the choice result using a hierarchical structure, as described above. The criteria are ranked by the expert or decision-maker in order of their relative relevance to the situation [4-5].

The ideal route of transmission lines is often determined by a combination of diverse and sometimes contradictory factors. The use of MCDA became necessary in order to simplify the route selection for the transmission lines of the proposed renewable energy-based micro-grid system, which was previously complicated. It is easier to make judgments for complicated situations when qualities are compared in pairs, since the decision-maker only has to consider two characteristics and assess their relevance at the same time, rather than all four traits at the same time. A total of five specialists in the fields of microgrid development and renewable energy were selected for this research, and they were asked to score the link between each criteria according to their point of view using the Saaty scale displayed in Table 4.5.

Table 4.5 Saaty's Scale of Preference

Intensity of Importance	Definition	Explanation
1	Equal Importance	Two indicators contribute equal to the

		objective
2	Weak or slightly importance	Experience and judgment slightly favour one over another
3	Moderate importance	
4	Moderate plus	Experience and judgment strongly favour one over another
5	Strong importance	
6	Strong plus	Experience and judgment strongly favour one over another; its dominance demonstrated in practice
7	Very strong or demonstrated importance	
8	Very, very strong	The evidence favouring one over another is of the highest possible order of affirmation

4.8. Least Cost Path Analysis

The least-cost path tool derives a discrete preference surface and calculating an accumulated preference surface and determining the optimal path concerning the spatial distribution of the relative preferences for locating an electric transmission line. Using Dijkstra's algorithm in ArcGIS, the LCP procedure calculates the most suitable route for each perspective. As a result, accumulated preference surfaces that simulate routing for an electric transmission line from a starting point to all the other locations in the project area. The LCP identifies the path with the least resistance along the accumulated cost surface that minimizes the less preferred areas that are crossed along the route connecting the starting point to the destination point.

4.9. Results and Discussion

This section discusses the results of the optimal ETL routing process.

4.9.1 Cost Surfaces for Different Perspectives

To generate the cost surface for different perspectives, different data layers were converted to raster format and each data layer is reclassified into a common preference or scale before overlaying the data layer. Figure 4.5 shows the cost surface for the alternate routes (built environment, natural environment, engineering environment) and optimal route (simple combined perspective).

For the built environment perspective, there is only one data layer available for the study area which is land use. After the reclassification, the classified map is obtained based on Delphi Ranks for overlaying. In this case, there's only one data layer to be considered, the final cost surface is the reclassified land use data layer. This means that land use has a 100% influence on the cost surface. As shown in Figure 4.5, there are only four cost values for the built environment cost surface. The lowest value which is 2 is for the undeveloped areas while the highest, 9, is for the residential areas. Most of the areas surrounding the identified renewable energy sites and load centers are agricultural which has a cost value of 5.

For the natural environment perspective, two layers were merged. These data layers are required to be merged based on each data layer influences. One of the layers, wetlands has an influence of 44% while the other layer, land cover, has an influence of 56%. The generated cost surface has six different values with 1 as the lowest and 6 as the highest.

To create the cost surface of the engineering environment perspective, the two layers, infrastructure and slope in degrees were merged. The infrastructure layer has an influence of 54% while the slope layer has an influence of 46%. The resulting cost surface has six different cost values with 2 as the lowest and 7 as the highest.

After calculating the cost surfaces for the built, natural and engineering environment perspectives, the cost surface for the simple combined perspective by combining these three layers. The built environment, natural environment, and engineering environment have influence values of 33%, 33%, and 34%, respectively. The resulting cost surface has 6 different values with 2 as the lowest and 7 as the highest.

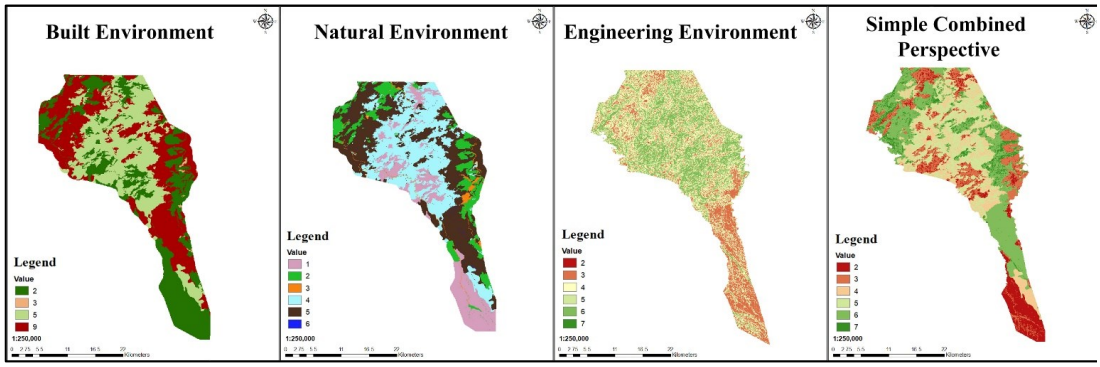

Figure 4.5 Cost Surface for different environments/perspective

4.9.2 LCP Alternative Routes and Optimal Routes

After creating the cost surface for different perspectives, the alternative and routes were obtained using the least cost path tool. Table 4.6 summarizes the distances of the routes generated. As shown in the table, nine different routes connect the renewable energy generating sites to the load centers. Hydro Site 1, Hydro Site 2, Hydro Site 3, and Solar Site 4 are connected to the Malagsum Load Center while Hydro Site 4, Hydro Site 5, Hydro Site 6, Solar Site 1, Solar Site 2, and Solar Site 3 are connected to Gabunan Load Center. These two load centers were selected by the LCP since they are closer to the renewable energy sites geographically as compared to other load centers.

The routes generated on the built environment perspective have the lowest value of distances while the natural environment perspective has the routes with the highest distances. Although not the lowest distance values, the LCP routes generated on the simple combined perspective are considered the optimal routes since it considers all the criteria from the three different perspectives. Figure 4.6 shows the optimal routes.

As also observed from the results, the distances of the routes generated between load centers and solar sites are shorter compared to those distances between hydro sites and load centers. In reality, these power line distances are not considered the transmission line level. Hence, the design for the interconnection between solar sites and load centers should be modified to distribution levels.

Table 4.6 Distance from renewable energy generation sites to the corresponding load center

Route Name	**Source**	**Load Center**	**Distance (m)**			
			Alternative Routes			***Optimal Route***
			Built Environment	***Natural Environment***	***Engineering Environment***	***Simple Combined Perspective***
LCP-HS1	Hydro Site 1	Malagsum	1316.70	1907.70	1475.31	1323.69
LCP-HS2	Hydro Site 2	Malagsum	1807.21	1817.86	1681.41	1522.76
LCP-HS3	Hydro Site 3	Malagsum	1919.80	2004.02	1798.39	1848.91
LCP-HS4	Hydro Site 4	Gabunan	1640.66	1666.76	1701.08	1648.14
LCP-HS5	Hydro Site 5	Gabunan	1787.81	1788.11	1860.80	1760.04
LCP-HS6	Hydro Site 6	Gabunan	1814.77	1806.59	1898.17	1786.06
LCP-SS773	Solar Site 1	Gabunan	724.96	729.05	777.02	724.43
LCP-SS858	Solar Site 2	Gabunan	551.00	551.54	598.54	547.20
LCP-SS943	Solar Site 3 (943)	Gabunan	204.63	199.57	198.64	207.90
LCP-SS1133	Solar Site 4 (1133)	Malagsum	65.51	66.59	63.14	65.52

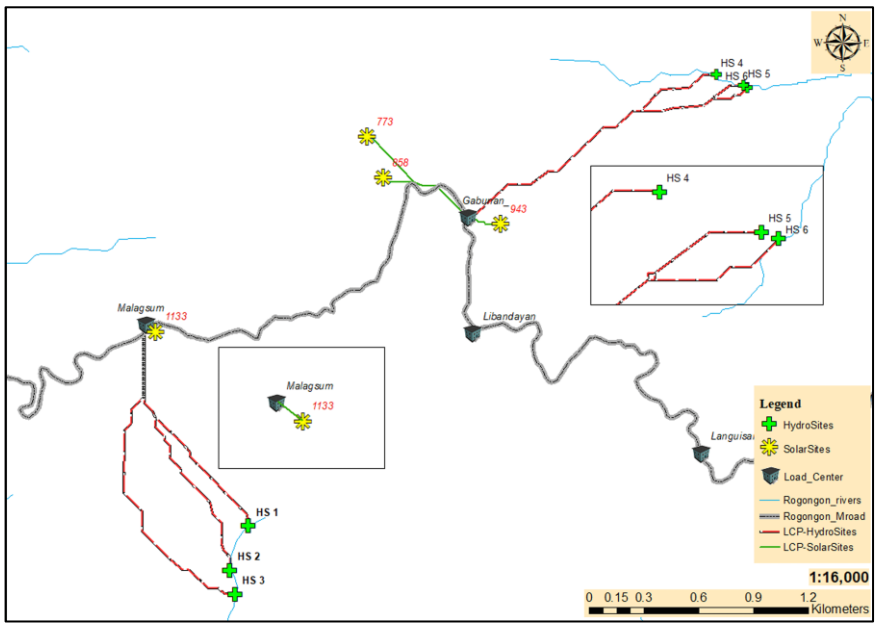

Figure 4.6 The optimal routes for the whole study area

4.9.3 Secondary Route Selection and Evaluation based on Alternatives Routes

Among the three generated alternative routes, the engineering environment perspective routes were selected as the preferred secondary alternative routes for the study area. During reconnaissance activities, the area was identified to have high and rugged terrain which means that it is very difficult and not preferable to plant transmission poles without accounting the stepped slopes. Regarding this, the other alternative route perspectives do not include this feature. Additionally, the majority of the study area is undeveloped, hence, the different land categories can be safely set aside in the process. Thereby, terrains must be a high priority for the secondary route selection. Also, the least-cost path routes generated in the engineering environment perspective are much closer to the trail created by the local guides after surveying the identified potential hydropower sites. Figure 4.7 shows the preferred secondary alternative route

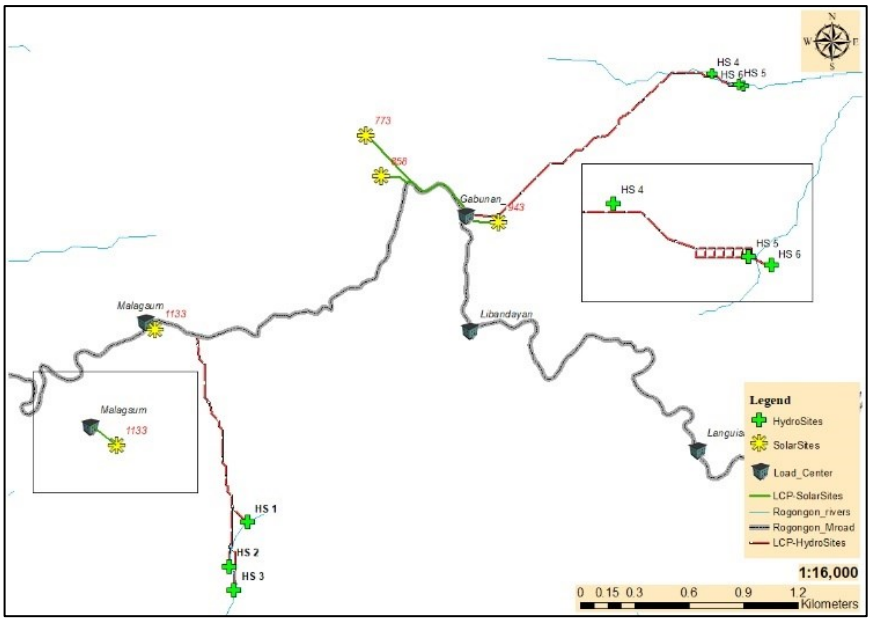

Figure 4.7 The optimal routes for the whole study area

4.10. Summary

The use of GIS spatial analysis in this study provided a framework for finding LCP routes of ETL for renewable energy-based microgrid by selecting, categorizing, and weighting the criteria and subcriteria with AHP with ArcGIS; and finding the optimal and alternative LCP routes considering different perspectives. The spatial models produced a standardized, defendable, and transparent siting process for the electric transmission line route decision-making process.

The use of remotely sensed data and Geographic Information System technology in this study provided an efficient, scalable, and risk-free electric transmission line routing. This study also presents a framework for optimal transmission line routing and route selection using the ArcGIS Spatial Analyst tool to assist the design and development of renewable energy-based microgrid system in the study area. Moreover, the automation of routing develops a geographic model of the problem to reduce the time consumed and the gap between planning.

Plausible problems of using the developed framework primarily include that the models' results are only nearly as good because of the data used. Important data types employed in the analysis

might be nonexistent or incomplete. Outputs will also be erroneous if errors are introduced into the analysis. For future studies, new algorithms can be used and explored with numerous criteria and maps to increase the reliability of the best routes.

4.11. Chapter 4 References

[4-1] J. Berry, "Beyond Mapping III Topic 19: Routing and Optimal Paths," Innovative GIS, Jul. 2003. http://www.innovativegis.com/basis/MapAnalysis/Topic19/Topic19.htm (accessed Feb. 10, 2020).

[4-2] A. Schmidt, "Implementing a GIS Methodology for Siting High Voltage Electric Transmission Lines".

[4-3] D. A. Q. Badang, C. F. Sarip, and A. P. Tahud, "Geographic Information System (GIS) and Multicriteria Decision Making (MCDM) for Optimal Selection of Hydropower Location in Rogongon, Iligan City," in 2018 IEEE 10th International Conference on Humanoid, Nanotechnology, Information Technology,Communication and Control, Environment and Management (HNICEM), Baguio City, Philippines, Nov. 2018, pp. 1–5. doi: 10.1109/HNICEM.2018.8666266.

[4-4] ESRI, "Understanding overlay analysis," ArcGIS for Desktop, 2016. https://desktop.arcgis.com/en/arcmap/10.3/tools/spatial-analyst-toolbox/understanding-overlay-analysis.htm (accessed Jan. 06, 2020).

[4-5] T. L. Saaty, "Decision making with the analytic hierarchy process," Int. J. Serv. Sci., vol. 1, no. 1, p. 83, 2008, doi: 10.1504/IJSSCI.2008.017590.

Chapter 5 Integrated Optimal Sizing and Operation of Hybrid Renewable Energy Microgrid using Multi-Objective Particle Swarm Optimization (MOPSO)

5.1. Introduction

Global energy consumption is outpacing global population growth, which is cause for concern since it means that more sustainable energy sources are required [5-1]. Developing countries, where over 759 million people do not have access to electricity, are expected to have the highest increase in demand in the coming years [5-2]. To combat this issue, several countries around the world have considered the development of renewable-energy-based microgrids for rural electrification, and mechanisms to encourage the establishment of local energy communities have been developed and implemented. As an example, Poland decided to establish an energy cooperative that aims to bridge the gap in the growth of the civil dimension of energy on a local scale, while improving the efficiency of using renewable energy sources in rural regions and reducing the electrification issue to match the European Union's energy development direction [5-3]. A developing country in Southeast Asia, the Philippines, is attempting to address a lack of energy access and security to unviable regions, including all off-grid areas, by enacting policies and programs such as the Total Electrification Program (TEP), which stimulates the development of renewable energy technologies [5-4].

A microgrid is a decentralized group of electricity sources and loads that normally operate in conjunction with and in synchronization with the traditional wide area synchronous grid (macrogrid) but is also capable of disconnecting from the interconnected grid and operating autonomously in "island mode" or "off-grid" when technical or economic conditions require it [5-5]. With the increasing popularity of microgrids, traditional energy systems are being modified to incorporate renewable energy sources as renewable energy technologies, such as solar photovoltaics, wind power, and hydropower, become more widely used [5-6], [5-7].

The use of optimization tools in the design and operation of a hybrid renewable energy microgrid (HREM) is a way to make decisions that are easier to make when there is a lot of variability in renewable energy sources, different energy demand profiles, and equipment with

different performance and cost characteristics, among other things. HREMs have been evaluated using a variety of performance models, optimization software tools, and techniques, with the findings reported in a number of publications. Using a dynamic programming model, the approach described in by authors in [5-8] is used to find the optimum operating strategy for a wind–diesel–battery system over the course of a day with a 1 h time step; meanwhile, in [5-9], with heat and electrical constraints, it is implemented to optimize the microgrid operation. To overcome the dimensionality issue of a microgrid, the authors in [5-10] used approximation dynamic programming (ADP) and constructed an ADP-based energy management system that included a wind turbine, a chiller plant, thermal storage, and a cooling load. In [5-11], a component sizing technique was developed that determines the optimal hybrid system design by minimizing the size of the battery and the use of the diesel generator, and the model was built using yearly wind and solar data.

Optimizing microgrids by using different methods and developing power management strategies (PMS) or energy management systems (EMS) has also been a trend in the past years. The authors in [5-12] proposed an energy EMS that reduces daily operating expenses, battery degradation, energy purchased from the main grid, diesel generator fuel costs, and pollution costs for the real-time operation of a prototype stochastic and dynamic microgrid, made up of a diesel generator, solar panels, and batteries. The authors in [5-13] proposed a model predictive control (MPC)-based supervisory PMS for a stand-alone direct current (DC) microgrid with distributed generation and energy storage that solves an optimization problem with operational constraints utilizing the whole mathematical model of the system; meanwhile, in [5-14], a PMS was developed for a microgrid that includes plug-in hybrid electric vehicles (PHEVs) that maximizes the utilization of renewable energy generation.

Several authors have employed simulation tools to aid in the optimization of HREM [5-15]–[5-20]. The most common software that was used by these authors is the hybrid optimization model for electric renewables (HOMER), which is a simulation tool that is frequently used in the area of renewable energy. Using HOMER, most of these studies performed the techno-economic feasibility of their proposed HREM design. Although this tool optimizes system design, it does not necessarily do it automatically. This is owing to the fact that, before the optimization process

can begin, the sizes of the individual components must be specified and determined by the user. Other recent research has focused on mixed-integer linear programming (MILP) based methods for optimizing microgrids, such as those that used the distributed energy resources customer adoption model (DER-CAM) developed by the Microgrid group at the Lawrence Berkeley National Laboratory (LBNL), University of California at Berkeley [5-21]–[5-23]. In [5-24], using two-stage stochastic mixed-integer linear programming (MILP) models that factored in generation uncertainty, net present cost, installed capacity, and flexibility, the optimal system design consisting of photovoltaics, wind turbines, micro-hydropower, and BESS was selected.

Microgrid optimization employing nature-inspired metaheuristic algorithms such as the genetic algorithm (GA) and particle swarm optimization (PSO) are also used to optimize the design, control, and operation of HREM [5-25]–[5-29]. Other nature-inspired metaheuristic algorithms, such as the strength Pareto evolutionary algorithm (SPEA), the firefly algorithm (FA), ant colony optimization (ACO), and grey wolf optimization (GWO) have also been used in recent studies [5-30]–[5-33]. In microgrid energy management, new algorithms such as Harris Hawks optimization (HHO) and the water cycle algorithm (WCA) have been used, and they have been shown to be more efficient than the traditional ones [5-34], [5-35]. These algorithms have the benefit of being able to effectively optimize a number of different objectives at the same time. Furthermore, despite the drawback of coding complexity, evolutionary algorithms offer the advantage of being able to deal with a vast number of different factors and operating strategies in an efficient manner compared with other methods. HREM optimization based evolutionary algorithms, as a whole, deliver higher performance, with much a lower response time and improved convergence compared with other methods.

In most of the above-mentioned published studies, a single objective or two objectives were examined and separately optimized, with a single or two renewable energy components included in their HREM design. In addition to this, some of the optimization methods that were used do not take into account the simultaneous optimization of multiple objectives; as a result, sizing, analysis, and selection of the optimal HREM configuration are dependent on a time-consuming process of selecting various alternatives based on various constraints and tradeoffs.

Thus, this study presents an optimization of a proposed off-grid HREM, which includes a solar

photovoltaic (PV) system, a run-of-the-river (ROR) hydropower system, a battery energy storage system (BESS), and a diesel generator, to meet the load demand of a rural agricultural area in the Southern Philippines. Although there are several existing published works on microgrid optimization, as previously mentioned, the innovative aspect of this work lies in the comprehensive modeling and integrated methodology of optimal sizing and operation of HREM by utilizing a modified multi-objective particle swarm optimization (MOPSO) algorithm that is capable of simultaneous optimization of multiple conflicting objectives with several constraints and a proposed multi-case power management strategy. The datasets that were used for the optimization are actual datasets from a rural agricultural area, which include meteorological data and multiple types of load data from household surveys. The proposed HREM design and research methodology, which utilizes optimization through MOPSO, is based on a cost-effective approach that aims to find the best microgrid configuration while also considering increased system reliability, minimization of the operational cost, and environmental impact through emission reduction.

5.2. Description of the Study Area

The proposed HREM is planned to be constructed for rural agricultural communities in Rogongon, Iligan City, Philippines. Rogongon is a barangay, a native Filipino term for a village or district, in Iligan City that covers 35,555 hectares (355.55 km^2), accounting for nearly 44% of the city's total land area. It is one of Iligan City's 44 barangays and is situated in the province of Lanao del Norte in the Southern Philippines, between 8°12′ and 8°17′ latitude and 124°22′20″ and 124°33′30″ longitude. The area's climate is classified as Type III, which means no very pronounced maximum rain period and a very short dry season that lasts from one to three months during the period from March to May [5-36]. However, despite the fact that it has considerable hydropower and solar energy potential, it is one of the city's most isolated rural districts, with steep terrain, and the majority of its residents are without access to electricity. The study area in Rogongon is further narrowed down to five unelectrified sites. Table 5.1 lists the sites without electricity and the number of households in each site, with their locations depicted on the map of the study area shown in Figure 5.1. The available meteorological data in the study area which

were used in the optimization of the HREM are shown in Figure 5.2 and Figure 5.3. Figure 5.4 shows the daily average of the Malikongkong River, on which the run-of-the-river hydropower system will be installed.

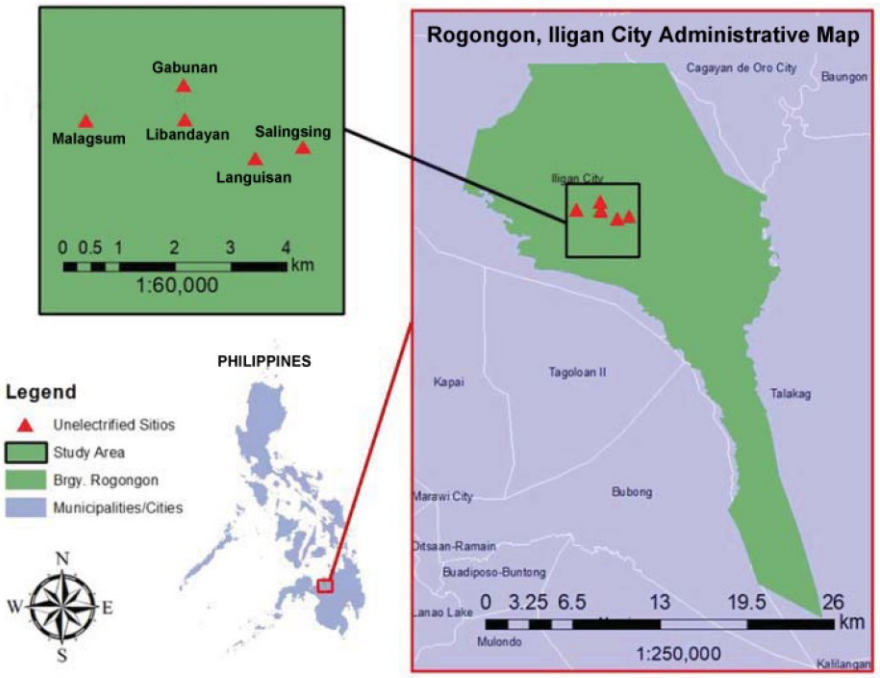

Figure 5.1 Study area—rural agricultural area composed of five unelectrified sitios, or sites, in Rogongon, Iligan City, Lanao del Norte, Philippines.

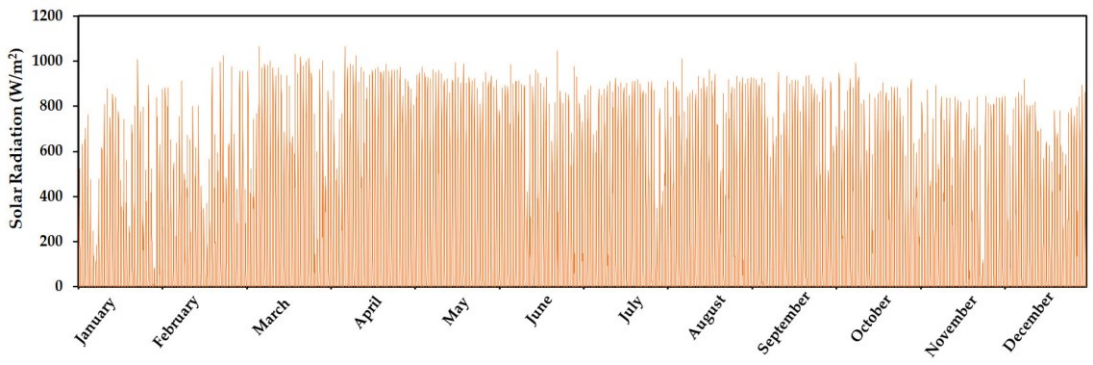

Figure 5.2 Hourly solar radiation in Rogongon, Iligan City.

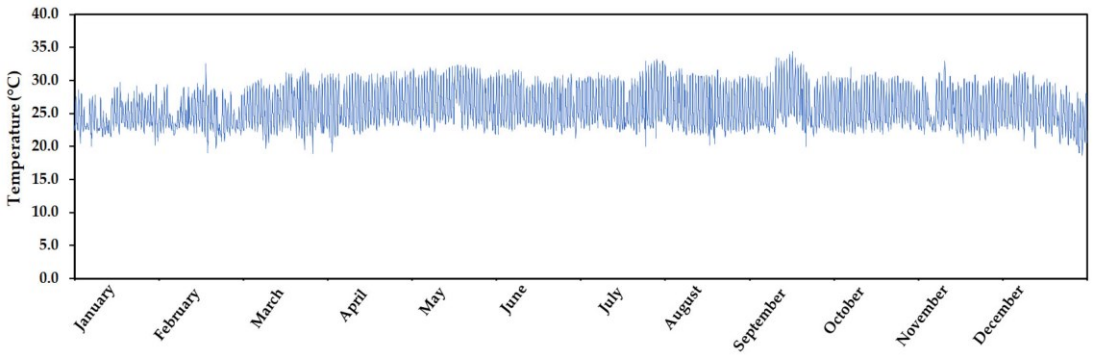

Figure 5.3 Hourly ambient temperature in Rogongon, Iligan City.

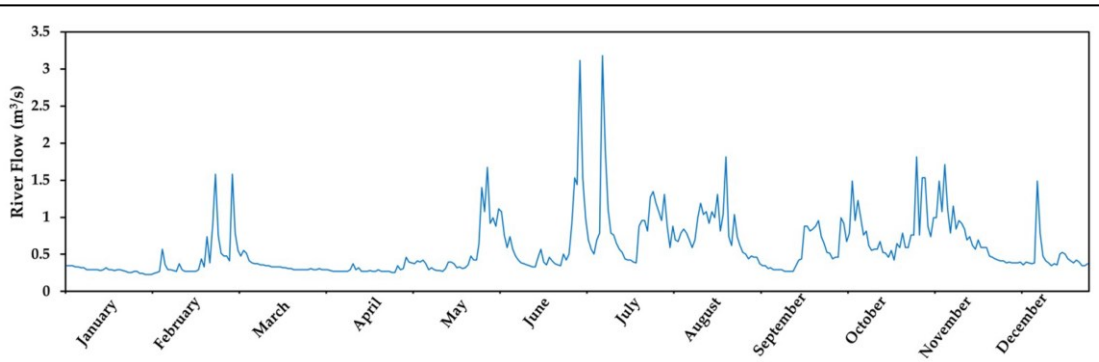

Figure 5.4 Daily average flow rate of the Malikongkong River.

Table 5.1 Selected unelectrified sites with corresponding number of households.

Site	Number of Households
Sitio Gabunan	20
Sitio Languisan	15
Sitio Libandayan	18
Sitio Malagsum	25
Sitio Salingsing	25

The area is also the ancestral home to an indigenous people group called Higauonon, and their main sources of income are from farming and remittances from family members working in nearby cities. Their main agricultural product is abaca (Musa textilis), which is harvested for its fiber and sold as a raw material for making tea bags, filter paper, and banknotes, etc. Currently, the fibers are extracted manually due to a lack of access to electricity and agricultural machinery. As part of the sustainability plan for the installation of the HREM in the area, a processing facility will also be constructed which will contain a decorticating machine, which is an electric

agricultural machinery for extracting the fibers from abaca. Using the machine will improve agricultural activities by increasing the efficiency and production of the fibers. As a result, it will boost the farmers' earnings and enable the residents to sustain the operation and maintenance of the HREM.

5.3. Hybrid Renewable Energy Microgrid System Modeling

Based on the available resources in the study area, the HREM system proposed in this study includes solar PV, ROR hydropower, BESS, and a diesel generator, which are modeled mathematically. These components have a big impact on the microgrid system's cost, reliability, and environmental impact. These multiple renewable energy sources improve system efficiency and reduce the need for energy storage. Figure 5.5depicts the HREM's schematic structure. For simplicity, most components are represented by a certain number of units, with one comparable battery representing the BESS capacity. Due to the fact that auxiliary equipment (such as inverters and charge controllers) is included in the main equipment's efficiency and capital cost, their size and number are not defined. The units for power and energy are set to kilowatts (kW) and kilowatt-hours (kWh), respectively, and the timestep for the optimization process and analysis is set to one hour.

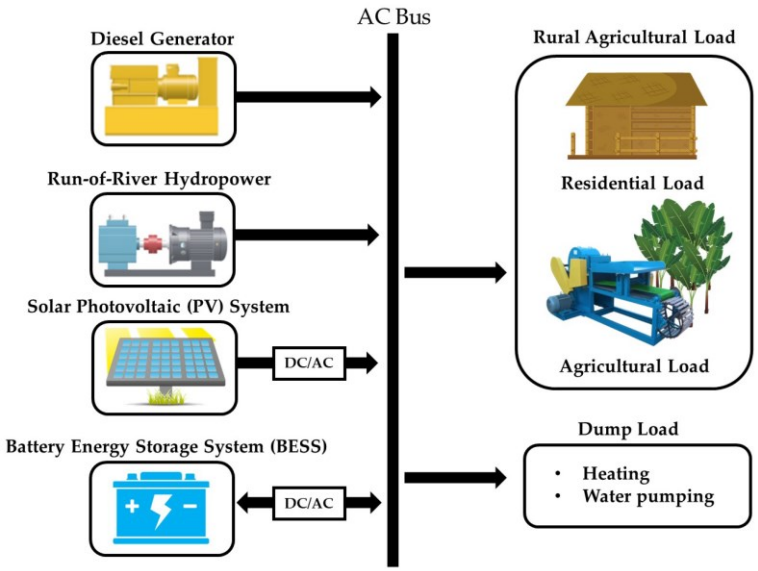

Figure 5.5 Proposed HREM model schematic structure.

5.3.1. Solar PV Model

The Philippines' geographical position, just above the equator, receives a high amount of sunlight each year, with an average of 12 daylight hours every day. Hence, it would be preferable to incorporate a PV system into the HREM structure.

Solar cells, also known as PV cells, are electrical devices that convert solar energy from the sun into electrical energy for use in various applications. In a PV system, the total power created by each PV panel constitutes the power generated by the system as a whole, while the power generated by each panel at each hour is calculated using solar radiation and cell temperature. The following equation gives the output power of a PV system in kilowatts (kW) [5-37]:

$$P_{PV}(t) = \frac{N_{PV} \times P_{PV,panel}(t)}{1000} \tag{5-1}$$

$$P_{PV,panel}(t) = P_{PV,rating} \times \frac{I(t)}{I_{REF}}\left[1 + \gamma_{pv} \times (T_{CELL}(t) - T_{REF})\right] \times \eta_R \tag{5-2}$$

$$T_{CELL}(t) = T_{AMB}(t) + \frac{NOCT - 20^{\circ}\mathrm{C}}{800\sim \mathrm{W/m^2}} \times I(t) \tag{5-3}$$

where N_{PV} is the number of PV panels; $P_{PV,panel}(t)$ is the hourly power generated by each panel; $P_{PV,panel}(t)$ is the PV panel rating (kW), $I(t)$ is the hourly solar radiation (W/m^2); I_{REF} is the solar radiation at standard temperature (W/m^2); $NOCT$ is the nominal operation cell temperature (°C); T_{REF} is the standard temperature (°C); T_{AMB} is the ambient temperature (°C); η_R is PV regulator efficiency; and γ_{pv} is the temperature power coefficient.

5.3.2. Battery Energy Storage System

A BESS is required in a microgrid to prevent power imbalances. The type of power required and the power supplied by the battery energy storage unit determine the type of battery energy storage unit to be used. Lithium-ion batteries were chosen for this study due to their high energy density, long life cycle, and high efficiency. BESS should not be discharged below 20% of its capacity and should not be charged over 90% of its capacity in order to maximize battery life [5-38]. The state of charge (SOC) of BESS, which is a percentage of its total capacity at time, t, with a one-hour time step, is calculated using the following equation [5-39]:

$$SOC_{BESS}(t) = \frac{E_{BESS}(t)}{N_{BESS}} \times 100\% \quad (5\text{-}4)$$

where $E_{BESS}(t)$ is the amount of energy stored in the BESS (kWh) and N_{BESS} is the size capacity of the BESS in (kWh).

When the BESS is charging, the SOC at time, *t*, is given by the following equation:

$$SOC_{BESS}(t) = SOC_{BESS}(t-1) + \frac{P_{BESS,CH}(t) \times \Delta t \times \eta_{BESS,CH}}{N_{BESS}} \times 100\% \quad (5\text{-}5)$$

where $P_{BESS,CH}(t)$ is the power charging the BESS (kW), Δt is the time step, and $\eta_{BESS,CH}$ is the charging efficiency of the BESS.

The SOC of BESS when discharging is given by the following equation:

$$SSOC_{BESS}(t) = SOC_{BESS}(t-1) - \frac{P_{BESS,DCH}(t) \times \Delta t}{N_{BESS} \times \eta_{BESS,DCH}} \times 100\% \quad (5\text{-}6)$$

where $P_{BESS,CH}(t)$ is the power being discharged by the BESS (kW), and $\eta_{BESS,DCH}$ is the discharging efficiency of the BESS.

5.3.3. Run-of-the-River Hydropower Model

ROR, or run-of-the-river hydropower, is the most appropriate kind of hydropower for streams or rivers that can sustain a minimum level of flow. ROR hydropower can supplement the lack of generation from PV after daytime and during days with very low solar radiation.

Despite seasonal changes in the flow of the Malikongkong river where ROR will be installed, the channel model for the ROR system utilized in this study assumes a constant upper water level independent of these fluctuations. Through the spillway gates, river flow that exceeds the turbine discharge and reaches the nominal water level is directed away from ROR installations. The turbine type used in this study is crossflow. The constant power produced by run-of-the-river hydropower in kW at time, *t*, considering the efficiency of the generator and turbine, can be

determined using the following equation [5-40]:

$$P_{ROR}(t) = 9.8 \times Q_D \times (H_G - H_L) \times \eta_t \times \eta_g \quad (5\text{-}7)$$

$$H_L = \frac{10.64L}{C^{1.852}D^{4.87}} Q_D^{1.852} \quad (5\text{-}8)$$

where Q_D is the design flow of ROR (m^3/s); HG is the gross head or elevation difference between intake and discharge of ROR (m); H_L is the total head loss in the pipe; η_t is the turbine efficiency of ROR; η_g is the generator efficiency; L is penstock or pipe length; C is the Hazen–Williams coefficient of pipe roughness; and D is pipe diameter (m).

5.3.4. Run-of-the-River Hydropower Model

Diesel generators are a more traditional form of energy that is utilized as a backup to compensate for power shortages in HREM. Typically, it serves as the primary mover, compensating for the imbalance between renewable energy sources and load, especially in remote microgrids. The following equation is used to determine the diesel generator's fuel consumption in liters/hour [5-41]:

$$FC_{disgen}(t) = \alpha_{DSG} P_{disgen}(t) + \beta_{DSG} N_{disgen} \quad (5\text{-}9)$$

where $P_{disgen}(t)$ is the hourly power output of the diesel generator (kW); N_{disgen} is the rated power or size capacity of diesel generator (kW); and α_{DSG} and β_{DSG} are the fixed and variable coefficients of the fuel consumption curve (liters/kWh), respectively.

5.3.5. Demand Estimation and Load Profile

Two different daily load profiles have been considered, as shown in Figure 5.6. The agricultural load from the processing facility, which is mainly composed of decorticating machines (162 kWh in a day), has a maximum load of 15 kW and a daily energy demand of 162 kWh. This is based on the projected operation of the facility from 7:00 a.m. until 6:00 p.m. Throughout the span of one year, the facility is projected to be operating six times a week (Monday–Saturday); additionally, based on the planting, harvesting, and processing seasons of the abaca, which occur a maximum of four times a year, the facility is also estimated to operate on the months of March, June, September, and December. For January, February, April, May, July, August, October, and November, the load being served is only residential. The residential load for 105 households is estimated to have a maximum load of 29.6 kW with a daily energy demand of

211 kWh. The residential load was calculated based on the household surveys performed during the course of this research.

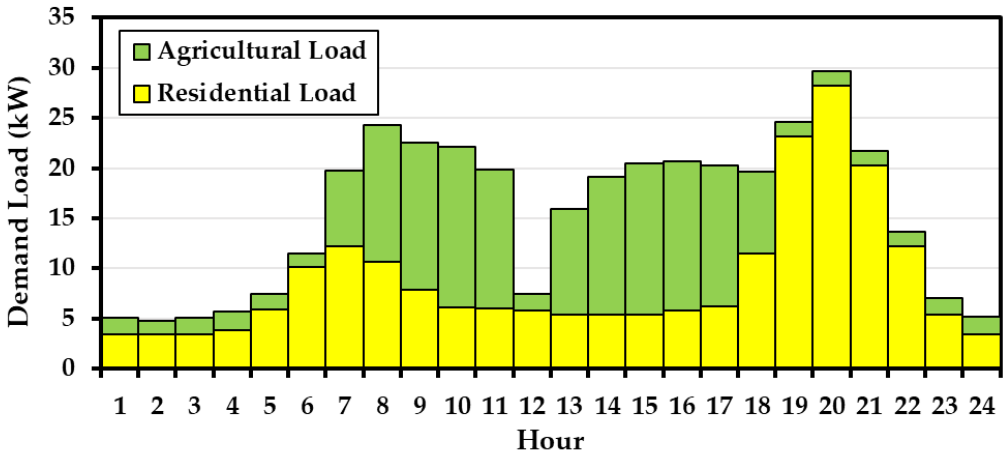

Figure 5.6 Estimated hourly combined residential and agricultural load demand of the study area based on household surveys.

5.3.6 Dump Load

For grid-tied microgrids, the excess generation is usually sold to the main grid. However, for off-grid systems, it is dealt with differently by using a dump load. A dump load is a secondary electrical load that takes over when the BESS is at maximum SOC. Thus, the excess power being generated is diverted to the dump load. The charge controller will switch from battery charging to sending power to the dump load to balance the generation and load demand [5-42]. In our proposed HREM, the dump load considered is heating and water pumping. These loads are also excluded from the cost calculation.

5.3.6. Power Management Strategy

With renewable energy resources being intermittent, a sophisticated power management approach must be devised for HREM, which is particularly important when a dependable supply of energy is required to meet the temporal distribution of load demand. Because the quantity of electricity that can be produced from renewable resources is limited, the capacity of these power

generating units cannot be quickly expanded to meet the increasing demand for electricity. As a result, having a power management plan in place would be one of the most important considerations when designing such systems. In order to implement power management strategy in the optimization process, the following cases will be taken into consideration:

Case 1: Energy produced in sufficient quantities is sourced from renewable sources, with any excess energy being utilized to charge a battery bank.

Case 2: This case is similar to Case 1, except that the excess energy produced by renewable resources, PV and ROR hydropower, exceeds the amount of energy required to power the load and the BESS. This means that the excess electricity is used to supply the dump load in this instance.

Case 3: The total power generated by PV and ROR hydropower is just barely sufficient to supply the load demand.

Case 4: The total power generated by PV and ROR hydropower is not enough to meet the load demand of HREM. The utilization of the stored energy in the BESS takes precedence over the operation. The BESS is used to make up for the lack of available power.

Case 5: This case is similar to Case 4, except the SOC of the BESS is at the minimum limit. In this instance, a diesel generator is used to make up for the lack of available power generation.

Figure 5.7 depicts the primary flowchart for the various modes of operation. In Figure 5.8 and Figure 5.9, the algorithms for charging and discharging are shown.

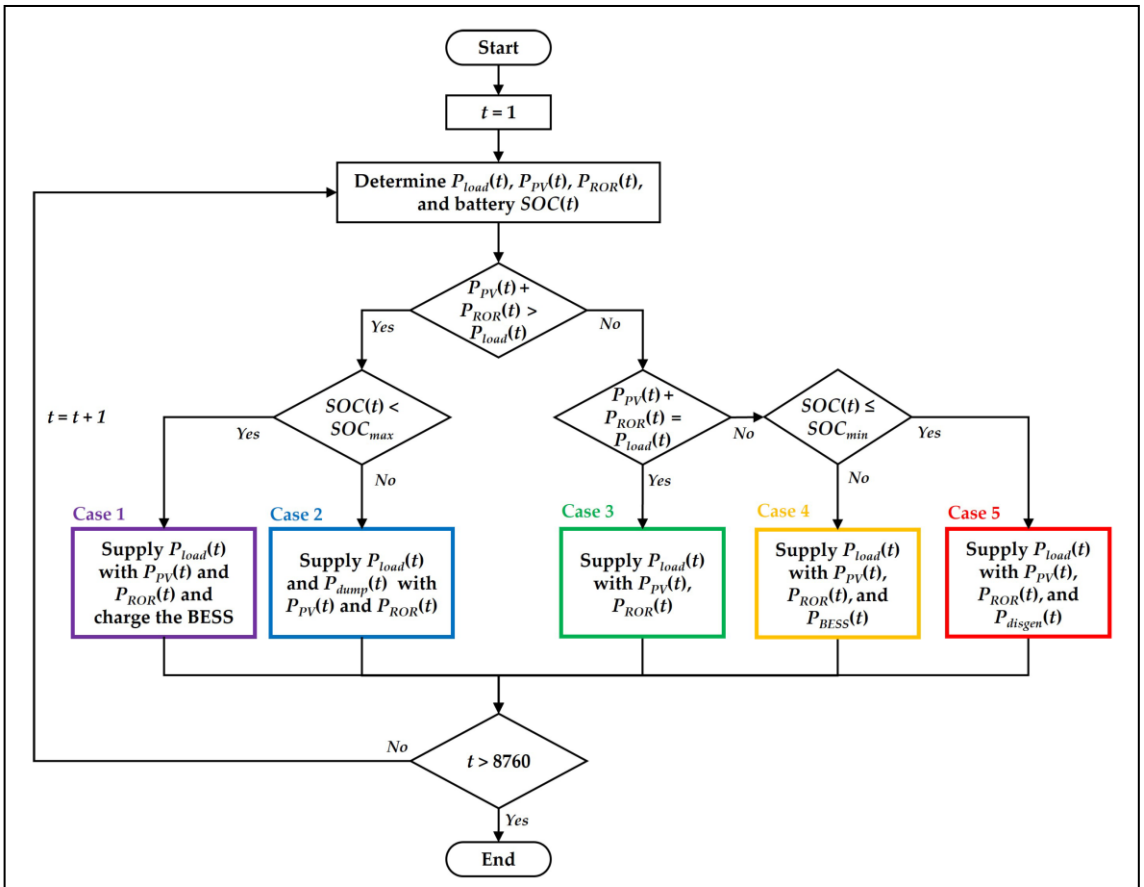

Figure 5.7 Primary flowchart of the HREM operation with power management strategy.

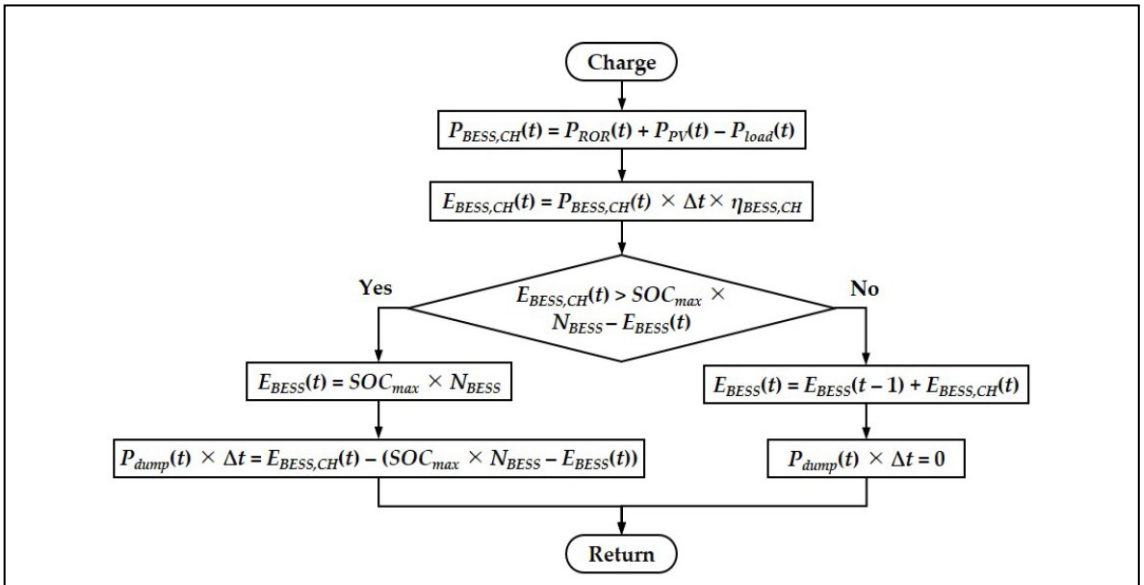

Figure 5.8 Flowchart of HREM charging algorithm.

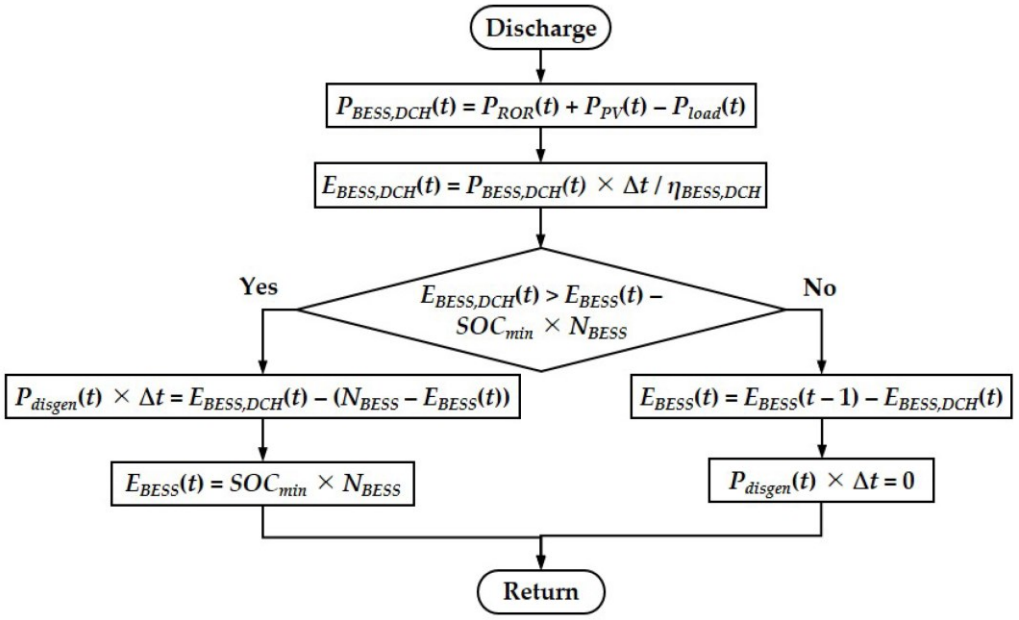

Figure 5.9 Flowchart of HREM discharging algorithm.

5.4. Optimization Setup

This section introduces the proposed approach for the optimal sizing and operation of HREM and discusses the details about the objectives considered for the optimization of HREM, constraints of the optimization, decision variables, PSO, and MOPSO.

5.4.1. Optimization Objectives

The optimization problem is based on minimizing the levelized cost of electricity (LCOE), loss of power supply probability (LPSP), and greenhouse gas (GHG) emissions, simultaneously.

5.4.1.1 Levelized Cost of Electricity

The levelized cost of electricity (LCOE) is a well-known and often used metric of a microgrid's economic feasibility. LCOE is the total cost of installing, operating, and maintaining an HREM in its entirety over the annual energy produced and it also depicts the cost of energy

per kWh throughout the system's lifetime. The annual energy generated and the annual costs are considered to remain constant throughout the lifetime of HREM in this study. A low, levelized cost of energy correlates to a low power cost. The LCOE (USD/kWh) is calculated using the following equation [5-43], [5-44]:

$$LCOE = \frac{TLCC_{HREM}}{E_{ALD}} \tag{5-10}$$

$$TLCC_{HREM} = TLCC_{ROR} + TLCC_{PV} + TLCC_{BESS} + TLCC_{disgen} \tag{5-11}$$

$$E_{ALD} = \sum_{t=1}^{8760} P_{load}(t) \times \Delta t \tag{5-12}$$

where $TLCC_{HREM}$ is the total life cycle cost (TLCC) of HREM (USD); EALD is annual energy demand of the system (kWh); and $TLCC_{ROR}$, $TLCC_{PV}$, $TLCC_{BESS}$, and $TLCC_{disgen}$ are the TLCC of ROR hydropower, PV system, BESS, and diesel generator, respectively.

The TLCC of each component of the HREM is determined based on the component's capital cost. The $TLCC_{ROR}$ and $TLCC_{PV}$ are calculated using the following equations [5-45]–[5-47]:

$$TLCC_{ROR} = P_{ROR} \times C_{cc,ROR} \times \left(1 + \frac{C_{om,ROR}}{CRF}\right) \tag{5-13}$$

$$TLCC_{PV} = N_{PV} \times P_{PV,panel} \times C_{cc,PV} \times \left(1 + \frac{C_{om,PV}}{CRF}\right) \tag{5-14}$$

$$CRF = \frac{IR \cdot (1+IR)^{LT}}{(1+IR)^{LT} - 1} \tag{5-15}$$

where $C_{cc,ROR}$ is the capital cost of ROR (USD/kW); $C_{om,ROR}$ is the operation and maintenance cost of ROR (%/year); $C_{cc,PV}$ is the capital cost of PV (USD/kW); $C_{om,PV}$ is the operation and maintenance cost of PV (%/year); CRF is the capital recovery factor; IR is the interest rate (%); and LT is the lifetime of the system (years).

For BESS, the TLCC is computed using the following equations:

$$TLCC_{BESS} = N_{BESS} \times C_{cc,BESS} + \frac{TE_{CH,DCH} \times C_{o,BESS} + N_{BESS} \times C_{m,BESS}}{CRF} \tag{5-16}$$

$$TE_{CH,DCH} = \sum_{t=1}^{8760} \left(P_{BESS,CH}(t) + P_{BESS,DCH}(t)\right) \Delta t \tag{5-17}$$

where $C_{cc,BESS}$ is the capital cost of BESS (USD/kWh); $TE_{CH,DCH}$ is the total annual energy charged and discharged by the BESS (kWh); $C_{o,BESS}$ is the operation cost (USD/kWh); and $C_{m,BESS}$ is the maintenance cost (USD/kWh).

The TLCC of the diesel generator is determined using the following equations

$$TLCC_{disgen} = N_{disgen} \times C_{cc,dsg} + \frac{n_{dsgh} \times C_{m,dsg} + AFG_{disgen} \times C_{o,dsg}}{CRF} \quad (5\text{-}18)$$

$$AFC_{disgen} = \sum_{t=1}^{8760} FC_{disgen}(t) \quad (5\text{-}19)$$

where $C_{cc,dsg}$ is the capital cost of diesel generator (USD/kW); n_{dsgh} is the total number of operating hours of the diesel generator (h); $C_{m,dsg}$ is the maintenance cost (USD/h); AFC_{disgen} is the total annual fuel consumption; and $C_{o,dsg}$ is the operation cost (USD/L).

5.4.1.2 Loss of Power Supply Probability

Loss of power supply probability (LPSP) is a statistical measure that shows the likelihood of a power supply failure owing to a lack of power generated by renewable energy sources and other power generating components or a breakdown in technical infrastructure to satisfy load demand. It is determined by the following equations:

$$LPSP = \frac{\sum_{t=1}^{8760}\left(P_{load}(t) + P_{BESS,CH}(t) - P_{supply}(t) - P_{BESS,CH}(t)\right)}{\sum_{t=1}^{8760} P_{load}(t)} \quad (5\text{-}20)$$

$$P_{supply}(t) = P_{ROR}(t) + P_{PV}(t) + P_{disgen}(t) + P_{BESS,DCH}(t) \quad (5\text{-}21)$$

The reliability assessment is carried out under the most adverse situations possible, such as when

$$P_{load}(t) > P_{supply}(t) \quad (5\text{-}22)$$

5.4.1.3 Greenhouse Gas Emissions

One of the measures for determining the environmental impact of an HREM is the amount of the greenhouse gases (GHG) emitted by its power generating components. HREMs are capable of exploiting the advantages of renewable energy sources and energy storage equipment flexibly and efficiently, and thus having less environmental impact by meeting energy conservation and emission reduction targets. In this study, the amount of GHG produced (kg) by the diesel generator component of HREM is computed using the following equation:

$$GHG_{em} = \sum_{t=1}^{8760} FC_{disgen}(t) \times EF_{GHG} \quad (5\text{-}23)$$

$$EF_{GHG} = EF_{CO_2} + EF_{CH_4} + EF_{N_2O} + +EF_{NOx} + EF_{CO} \quad (5\text{-}24)$$

where EF_{GHG} is the total emission factor of diesel generator for greenhouse gasses (kg/L) and EF_{CO2}, EF_{CH4}, EF_{N2O}, EFNOx, and EFCO are the carbon dioxide, methane, nitrous oxide, nitrogen

oxides, and carbon monoxide emission factors (kg/L), respectively.

5.4.2. Decision Variables

The HREM's decision variables may be classified as design variables or operational variables. The independent choice factors for sizing the essential components are as follows: number of the PV panels (N_{PV}) which directly determines the size of PV system, diesel generator size (N_{disgen}), and size of the BESS (N_{BESS}). All these component sizes influence fuel consumption and greenhouse gas emission, influencing the environmental impact and cost of the system. Getting the optimal size of BESS and diesel generator is beneficial as it improves the flexibility and reliability of the HREM. These decisions variables are continuous variables that are constrained to be real numbers.

The decision variables involved in the HREM are as follows:

$$\vec{X} = \left[N_{PV}, N_{BESS}, N_{disgen}\right]^T \tag{5-25}$$

5.4.3. Optimization Constraints

In microgrid optimization research, the constraints on different optimization options are varied. A microgrid's design and operation should be flexible in order to increase the reliability of a distribution system. Microgrid optimization research is often intimately related to cost optimization, either economically or environmentally. Microgrid power balance, generating capacity, and energy storage are just a few things to consider when determining how well a microgrid should work at all times.

The load–generation balance constraint is defined by the following equation:

$$\begin{aligned} P_{load}(t) + P_{BESS,CH}(t) + P_{dump}(t) \\ = P_{ROR}(t) + P_{PV}(t) + P_{disgen}(t) + P_{BESS,DCH}(t) \end{aligned} \tag{5-26}$$

Each unit, including power producing and energy storage units, has a lower and higher limit on the amount of power or energy it can generate. The following equations describe these constraints:

$$P_{ROR,min} \leq P_{ROR}(t) \leq P_{ROR,max} \quad (5\text{-}27)$$
$$P_{PV,min} \leq P_{PV}(t) \leq P_{PV,max} \quad (5\text{-}28)$$
$$P_{disgen,min} \leq P_{disgen}(t) \leq P_{disgen,max} \quad (5\text{-}29)$$
$$E_{BESS,min} \leq E_{BESS}(t) \leq E_{BESS,max} \quad (5\text{-}30)$$

Limitations on the charging and discharging rates of the storage unit are shown as follows [5-46], [5-47]:

$$u_{CH}(t) + u_{DCH}(t) \leq 1 \quad (5\text{-}31)$$
$$SOC_{min} \leq SOC(t) \leq SOC_{max} \quad (5\text{-}32)$$
$$SOC(t) = SOC(t-1) + \frac{E_{BESS,CH}(t) \times u_{CH}(t) - E_{BESS,DCH}(t) \times u_{DCH}(t)}{N_{BESS}} \quad (5\text{-}33)$$

where $u_{CH}(t)$ and $u_{DCH}(t)$ are the charging and discharging states, respectively, with values either 0 or 1, and $SOC(t)$ and $SOC(t-1)$ are the state of charge of the BESS at the current and previous times, respectively.

5.4.4. Multi-Objective Optimization

Many real-world problems require simultaneous optimization of multiple objective functions, which are frequently non-proportional and in conflict. This optimization technique produces a collection of solutions rather than an ideal solution, since no one solution can be identified by evaluating all of the objectives at the same time. As a result, the multi-objective optimization (MOO) problem necessitates the simultaneous maximization or minimization of many objective functions while simultaneously satisfying a range of equality and inequality constraints. When a MOO problem has conflicting objectives, it is critical to develop a Pareto front of feasible solutions. Figure 5.10 shows a sample Pareto front solution set. Non-dominated solutions to optimization problems, such as a Pareto front, disclose actual tradeoffs between various objectives. A non-dominated solution is one in which no other solution performs better on any objective than the non-dominated solution. Due to PSO's capacity to create a large number of solutions, it excels in multi-objective optimization problems.

Mathematically, multi-objective optimization can be expressed as follows:

$$\text{Minimize } F(\vec{X}) = \left[F_1(\vec{X}), F_2(\vec{X}), \dots, F_N(\vec{X})\right]^T \quad (5\text{-}34)$$

Subject to the following:

$$G_i(\vec{X}) < 0 \quad i = 1,2, \dots, N_{\text{INEQ}} \quad (5\text{-}35)$$

$$H_i(\vec{X}) = 0 \quad i = 1,2,\dots,N_{\mathrm{EQ}} \tag{5-36}$$

where F is a vector comprising the MOO functions; $\vec{X}$ is a vector containing the decision variables of $F_i(\vec{X})$, representing the ith objective function; $G_i(\vec{X})$ is the inequality constraints; $H_i(\vec{X})$ is the equality constraints; and N is the number of objective functions defined in the problem.

Two conditions must be satisfied in order to decide if one solution dominates the other. First, the solution must be no worse than the others in all of the objective functions. Second, the solution is objectively superior than the alternative in all respects. It can be described as follows:

$$F_j(X_1) \leq F_k(X_2) \;\; \exists k \in \{1,2,\dots,N\} \tag{5-37}$$

$$F_k(X_1) \leq F_j(X_2) \;\; \forall j \in \{1,2,\dots,N\} \tag{5-38}$$

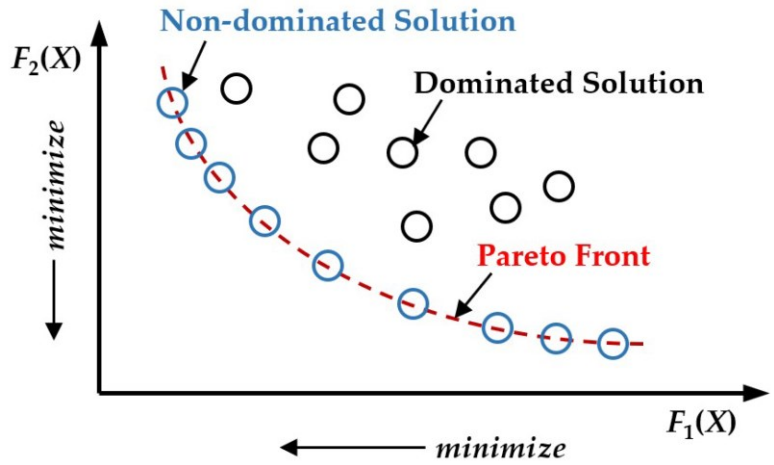

Figure 5.10 Sample Pareto front solution set for MOO.

5.4.5. Particle Swarm Optimization

Particle swarm optimization (PSO), which Kennedy and Eberhart initially defined in 1995, is driven by two distinct concepts: swarm intelligence, which is based on the social interaction of swarms, and evolutionary computing [5-48]. In the PSO algorithm, the best two values determine the position of every particle. The first value is the particle's current maximum value, which has been kept and is also known as the particle's "personal best". The second value is termed the "global best", which is generated by the algorithm from the population's current state. Additionally, every particle has a position, which indicates the values of the variables, and

a velocity that drives it toward personal and global bests. The fitness function is an objective function that determines the optimal solution from among all feasible solutions. Constraints may also be applied to the fitness function of PSO. The PSO method is shown in Figure 5.11.

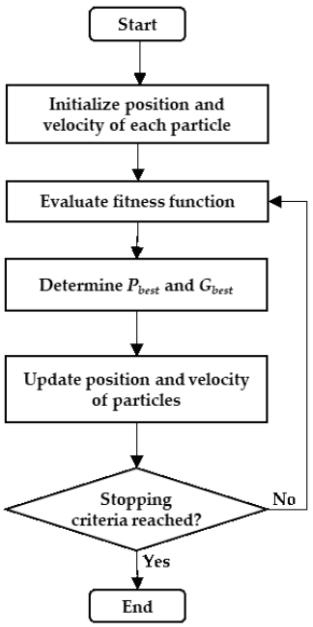

Figure 5.11 PSO algorithm flowchart.

While the algorithm is being executed, each particle retains the best fitness value that it obtained throughout the course of the process. Furthermore, the particle with the best fitness value in contrast to the rest of the particles is determined and updated during the iteration process. When certain stopping criteria are met, such as the maximum number of iterations or the defined objective fitness values, the algorithm terminates. When a particle in the swarm moves, the position of that particle is updated using the following equation:

$$x_i(k+1) = x_i(k) + v_i(k+1) \tag{5-39}$$

where x is particle position and v is particle velocity in the iteration k. The velocity is calculated as follows:

$$v_i(k+1) = K \times v_i(k) + C_1 R_1 \left(P_{i,best}(k) - x_i(k)\right) + C_2 R_2 \left(G_{best}(k) - x_i(k)\right) \tag{5-40}$$

$$K = \frac{2}{2 - \varphi - \sqrt{\varphi^2 - 4\varphi}} \tag{5-41}$$

$$\varphi = C_1 - C_2 \quad \varphi > 4 \tag{5-42}$$

where $P_{i,best}$ is *i*th particle's personal best position; G_{best} is the global best position of the entire population; C_1 is the cognitive acceleration coefficient; C_2 is the social acceleration coefficient; and R_1 and R_2 are randomly generated numbers ranging from 0 to 1.

The equation for calculating the velocity of the particle contains two components. The first component, known as the cognitive component $C_1R_1\left(P_{i,best}(k) - x_i(k)\right)$ influences the particle to return to a previous position where it had a higher personal fitness value, whereas the second component, known as the social component $C_2R_2\left(G_{best}(k) - x_i(k)\right)$, directs it to the best area that the swarm or population has located thus far and to follow the direction of the best neighbor.

5.4.6. Application of MOPSO to HREM Optimization

The multiple objective functions (LCOE, LPSP, and GHGem) are solved in this work using the MOPSO algorithm, which is based on the PSO algorithm. PSO is recognized for having fast convergence, and although this is desirable in the optimization process, it may result in a false Pareto solution in MOPSO. As a result, MOPSO introduces a mutation operator, which is used after the particle's position is changed and thereby alters the position vector [5-49].

Compared with other existing algorithms that are also capable of solving MOO problems, MOPSO has relatively fewer parameters that need to be tuned, and it uses a fast convergent search operator to achieve its speed. The algorithm can also be easily modified to improve its performance, and it can achieve sub-optimal and optimal solutions in a relatively shorter amount of computational time than most other algorithms [5-50], [5-51]. The MOPSO algorithm shown in Figure 5.12 can be readily applied to our problem according to the following steps.

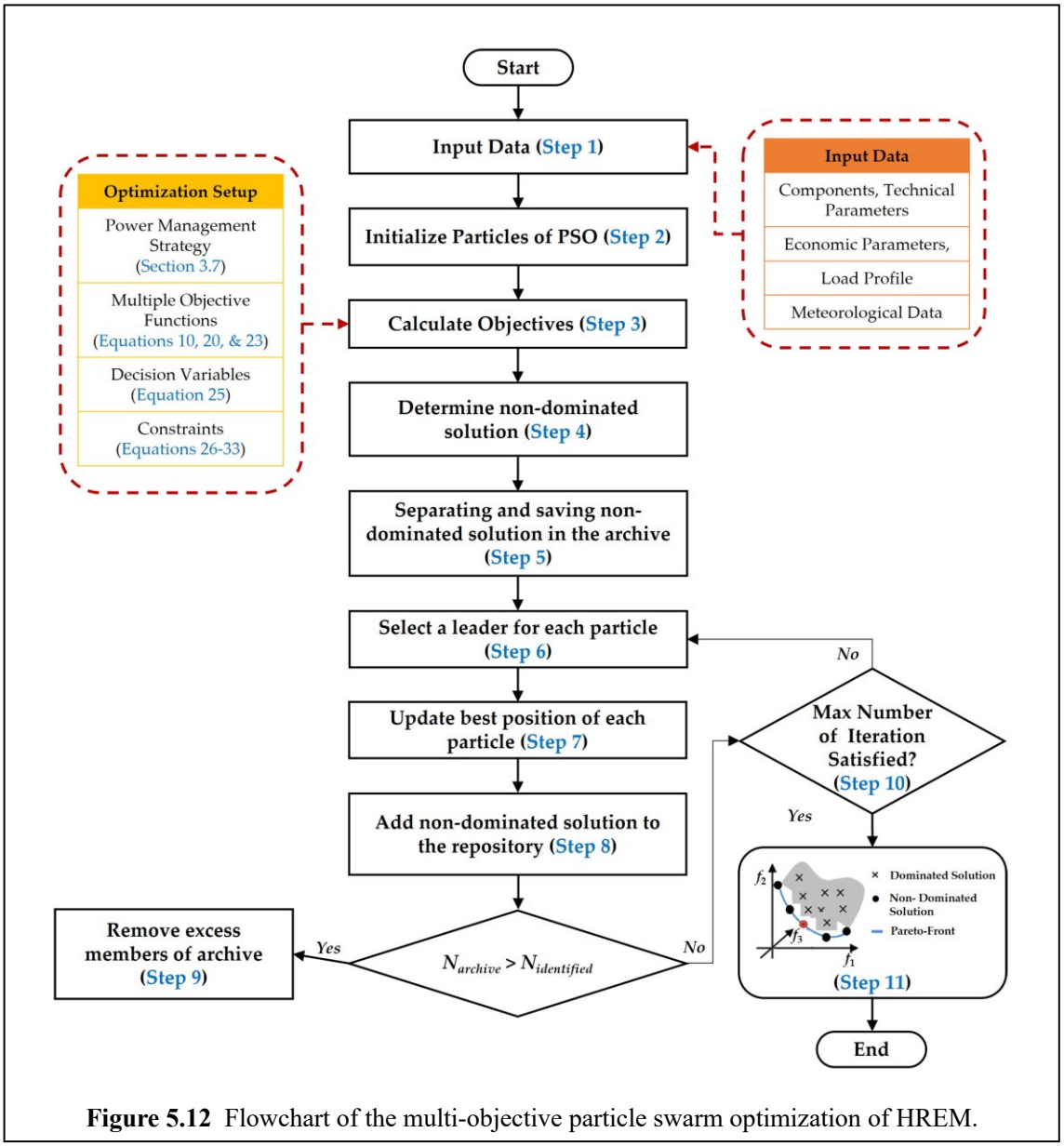

Figure 5.12 Flowchart of the multi-objective particle swarm optimization of HREM.

Step 1 The first step is to gather input data for the optimization. To begin, primary data includes information on the structure of the sample HREM, the technical and functional characteristics of the inverter, BESS, diesel generator, run-of-river hydropower, and solar power estimates for the next 24 hours, climatic conditions, and the daily load curve.

Step 2 Initialize the optimization process by generating the initial population, while taking into account the constraints of the problem, including the minimum and maximum values of decision variables.

Step 3 The created initial population is subjected to the load–generation balance, the proposed power management strategy, and other constraints.

All of these constraints are applied to each population formed, and the corresponding fitness function values are determined.

Step 4 Based on the generated solutions, determine non-dominated solutions.

Step 5 After identifying the solutions that are non-dominated, separate them from the dominated solutions and store them in an archive.

Step 6 The best particle is picked as a leader after storing the non-dominated solutions.

Step 7 Using Equations (39) and (40), calculate the updated position and velocity of each particle.

Step 8 Update each particle's best position after calculating their updated velocity and position.

Step 9 Remove non-dominated members from the archive after updating each particle's best position.

Step 10 Examine the terminating conditions; if favorable optimal conditions for the optimization process are attained, the algorithm is halted; otherwise, the procedure is resumed from Step 6.

Step 11 After finding the best Pareto solution from the non-dominated solutions, selecting a better option from the ideal solution is deemed required and critical for microgrid design and operation.

5.5. Results and Discussions

This section discusses the results of the optimization.

5.5.1. Initialization

To set up the optimization of HREM, several parameters were set and initialized. Table 5.2 shows the HREM's overall financial parameters while Table 5.3 shows the component model and manufacturer. Table 5.4 shows the technical and financial parameters used for each components. For the optimization process, Table 5.5 shows the values of the parameters used. The

minimum and maximum values of the decision variables are also shown in Table 5.6. The values of technical and economic parameters were either calculated and estimated based on the geographical conditions of the study area or taken from several sources which include product data sheet, previously published studies, reports, and manuals on diesel generators, PV, BESS, and ROR hydropower design [5-43], [5-45], [5-52][44,46,53,54,55,56,57,58,59,60].

Table 5.2 HREM financial parameters.

Parameter	Variable	Value	Unit
Interest rate	IR	6	%
System lifetime	LT	20	years

Table 5.3 HREM component model and manufacturer.

Component	Manufacturer	Unit
PV	YL250P-29b Solar Panels	352V1200AH
ROR Hydropower	Barrel Turbine Generating Unit	Hangzhou Regional Center (HRC)
Diesel Generator	DE33 GC Genset	CAT
BESS	352V1200AH	Jingsun Battery

Table 5.4 HREM component financial and technical parameters.

Component	Parameter	Variable	Value	Unit
ROR Hydropower	Design Flow	Q_D	0.12	m^3/s
	Gross Head	H_G	12	meters
	Penstock Length	H	100	meters
	Pipe Diameter	D	0.25	Meters
	Hazen-Williams Coefficient	C	200	
	Turbine Efficiency	η_t	85	%
	Generator Efficiency	η_g	93	%
	Captial Cost	$C_{cc,ROR}$	3400	USD/kW
	Operation and Maintenace Cost	$C_{om,ROR}$	4	% initial inv./year
PV System	Panel Rating	$P_{PV,rating}$	0.25	Kilowatts
	Temperature Coefficient of PV	γ_{pv}	-0.3	% / °C
	PV Regulator Efficiency	η_R	95	%
	Nominal Operation Cell Temperature	$NOCT$	41.5	°C
	Reference Temperature	T_{REF}	25	°C
	Capital Cost	$C_{cc,PV}$	1722.3	USD/kW
	Operation and Maintenance Cost	$C_{om,PV}$	1	% initial inv./year
BESS	Minimum State of Charge	SOC_{min}	20	%
	Maximum State of Charge	SOC_{max}	90	%
	Charging Efficiency	$\eta_{BESS,CH}$	80	%
	Discharging Efficiency	$\eta_{BESS,DCH}$	100	%
	Capital Cost	$C_{cc,BESS}$	241.31	USD/kW
	Operation Cost	$C_{o,BESS}$	0.00045	USD/kWh
	Maintenance Cost	$C_{m,BESS}$	11.10	USD/kWh-year
Diesel Generator	Carbon Dioxide Emission Factor	EF_{CO_2}	2.7	kg/L
	Methane Emission Factor	EF_{CH_4}	5.1×10^{-5}	kg/L
	Nitrous Oxide Emission Factor	EF_{N_2O}	1.7×10^{-4}	kg/L
	Nitrogen Oxide Emission Factor	EF_{NOx}	1.36×10^{-2}	kg/L
	Carbon Monoxide Emission Factor	EF_{CO}	1.53×10^{-2}	kg/L
	Fixed Consumption Coefficient	α_{DSG}	0.3058	L/kWh
	Variable Consumption Coefficient	β_{DSG}	0.0206	L/kWh
	Capital Cost	$C_{cc,dsg}$	377.26	USD/kW

	Operation Cost	$C_{o,dsg}$	1.61	USD/L
	Maintenance Cost	$C_{m,dsg}$	1.13	USD/L

Table 5.5 MOPSO parameters.

Parameter	Value	Parameter	Value
Population Size	100	w	0.4
Maximum Iteration	100	C_1	2
$N_{archive}$	200	C_2	2
Mutation percentage	0.5	N_{grid}	20
v_{max}	5		

Table 5.6 Minimum and maximum values of decision variables.

Decision Variable	Minimum Value	Maximum Value	Unit
N_{disgen}	0	30	kW
N_{BESS}	0	100	kWh
N_{PV}	0	100	panels

5.5.2. HREM Optimization Results

The Pareto optimal solution set was acquired by running the multi-objective optimization algorithm program. Figure 5.13 and Figure 5.14 show the 3D and 2D Pareto front results of the optimization, respectively. As shown in Figure 5.13, the value of each coordinate axis represents the objective functions while the non-dominated solutions obtained from the optimization form the Pareto front. In Figure 5.14, it can be seen that the lower the LPSP of a solution, the higher its LCOE and GHG emissions. Solutions with diesel generator components have lower LPSP values and higher LCOE and GHG emission values. The optimization generated values of LCOE, LPSP, and GHG emissions, varying in the ranges 0.0446–0.2556 USD/kWh, 0.0001–0.3201, and 0–16,598 kg, respectively. To simplify the analysis of the Pareto front formed by the non-dominated solutions, A, B, C, and D are located and chosen as solutions of interest. The solutions enclosed in the blue dashed line, which include solutions A and B, are the non-dominated solutions generated by the algorithm without a diesel generator component, while the non-dominated solutions that are enclosed by the purple dashed line, which include solutions C and D, are non-dominated solutions with a diesel generator component. Solutions A and B showed least value of LCOE and LPSP, respectively, while D contains the least LPSP overall. Solution C, which is midway between B and D, has the tradeoff of increasing the GHG emissions and LCOE. However,

this tradeoff also decreased the LPSP, which ensures greater reliability for the HREM. Thus, C was chosen for further analysis of the operation of HREM. Table 5.7 shows the values of the objective functions and decision variables for solutions of interest. On an AMD Ryzen 7 3700U @ 2.30 GHz, 8 GB RAM system, the developed programs are run using MATLAB software.

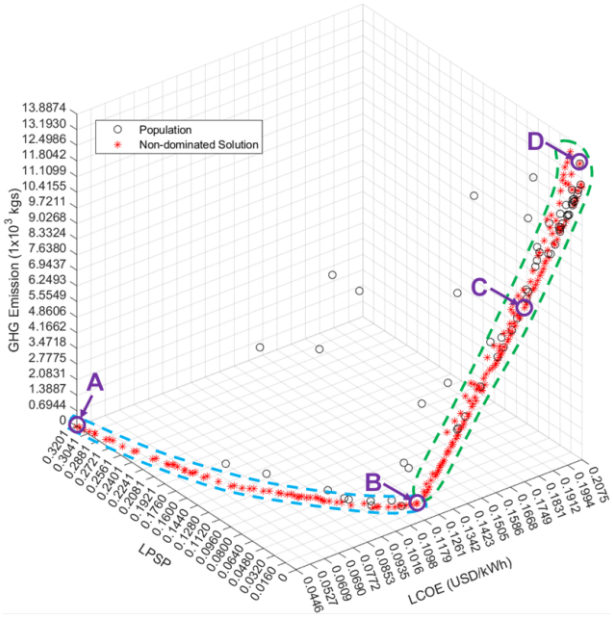

Figure 5.13 Multi-objective optimization frontier solution set of MOPSO.

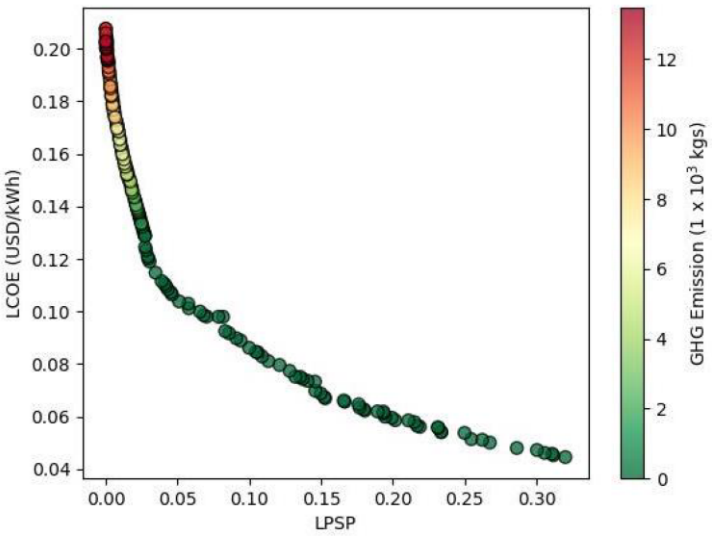

Figure 5.14 Two-dimensional scatter plot of frontier solution set of MOPSO.

Table 5.7 Solutions of interest – sizes of HREM Components

Solution	N_{disgen} (kW)	N_{BESS} (kWh)	N_{PV} (panels)	$LCOE$ (USD/kWh)	$LPSP$ (%)	GHG_{em} (kg)
A	0	0	0	0.0446	32	0
B	0	100	100	0.1245	2.74	0
C	13	100	100	0.1795	0.51	7874
D	20	100	100	0.2027	0	12,748

5.5.3. Monthly Energy Output

The monthly electricity generation by the system for four different solutions, A–D, is shown in Figure 5.15, Figure 5.16, Figure 5.17 and Figure 5.18, respectively. As shown in Figure 15, Solution A, with decision variable values of N_{disgen} = 0, N_{batt} = 0, and N_{PV} = 0, only has the hydropower as generation component producing varied monthly energy from 6720 kWh (lowest) to 7440 kWh (highest). The energy produced by hydropower alone is not enough to supply the monthly energy demand. Thus, this solution is not feasible for the reliable operation of HREM. Although Solution A has the lowest LCOE of 0.0446 USD/kWh and zero GHG emissions due to the absence of a diesel generator component, it has the highest LPSP of 32%, which means the system's operation is highly unreliable. On the other hand, Solution B, with decision variable values of N_{disgen} = 0, N_{batt} = 100 kWh, and N_{PV} = 100 panels, has an LCOE of 0.1245 USD/kWh with an LPSP of 2.74% and zero GHG emissions. It is the solution with the lowest LPSP within the Pareto front that has zero GHG emissions. As shown in Figure 5.16, the energy produced by hydropower is the same in Solution A with a monthly PV energy output varying from 2450 kWh (lowest) to 4111 kWh (highest), while the monthly BESS energy discharge varies from 1379 kWh (lowest) to 2264 kWH (highest).

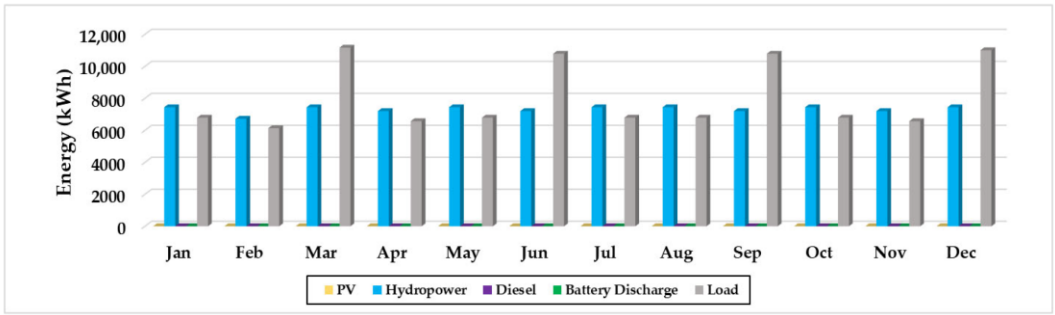

Figure 5.15 Energy generated by HREM components—Solution A.

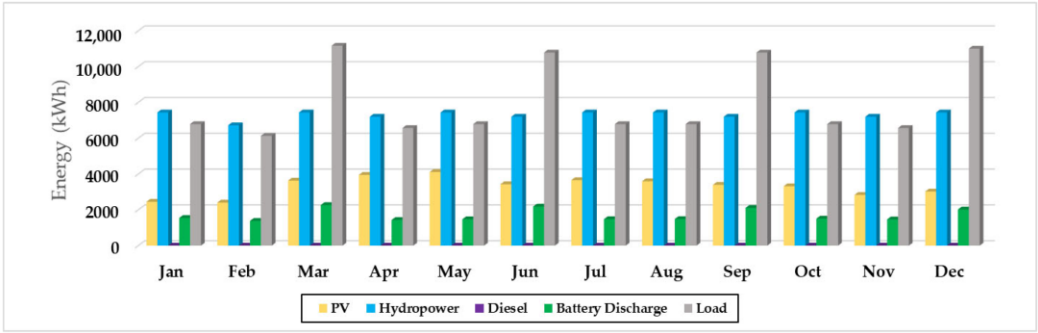

Figure 5.16 Energy generated by HREM components—Solution B.

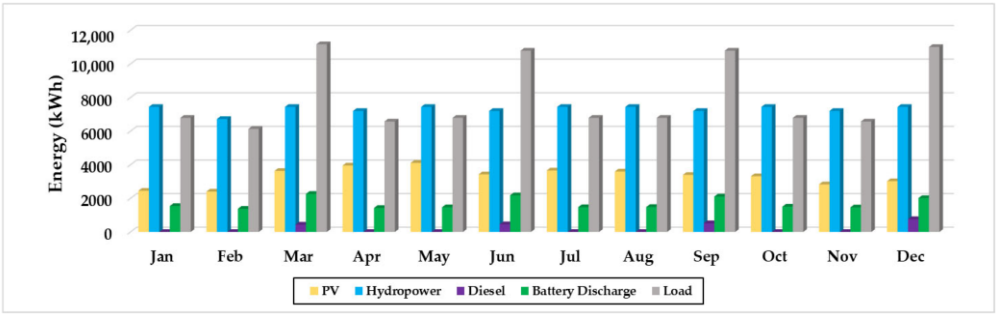

Figure 5.17 Energy generated by HREM components—Solution C.

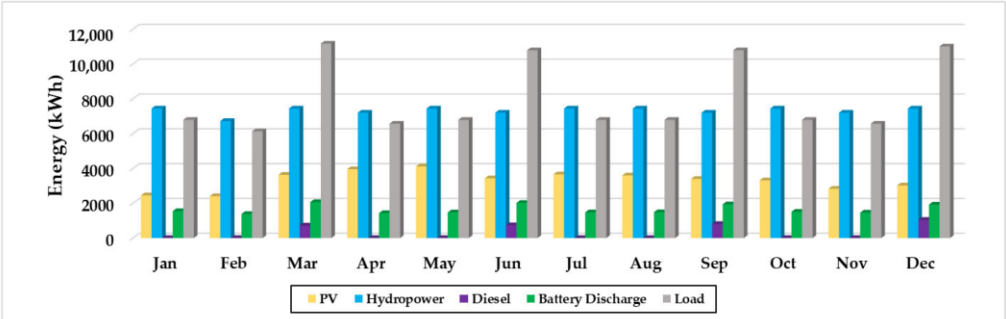

Figure 5.18 Energy generated by HREM components—Solution D.

Solutions C and D have the same monthly hydropower energy output as Solution A. However, both of these solutions have diesel generator components. Solution C, with Ndisgen = 13 kW, Nbatt = 100 kWh, and NPV = 100 panels, has an LCOE of 0.1795 USD/kWh, LPSP of 0.51%, and GHG emission of 7874 kg; meanwhile, Solution D, with Ndisgen = 20 kW, Nbatt =

100 kWh, and NPV = 100 panels, has an LCOE of 0.2027 USD/kWh, LPSP of 0%, and GHG emission of 12,748 kg. The monthly energy output from the diesel generator varies from 435 kWH to 759 kWh for Solution C and from 717 kWh to 1045 kWh for Solution D. As shown in Figure 5.17 and Figure 5.18, the diesel generator only has a monthly energy output in the months of May, June, September, and December. In these months, the diesel generator operates due to increased load from agricultural activities.

5.5.4. Energy Scheduling Analysis

To determine the performance of the system, four scenarios were considered for the scheduling analysis using component sizes from Solution C, shown in Table 5.8. The scenarios determine how the HREM performs under varying meteorological and load conditions. Figure 5.19, Figure 5.20, Figure 5.21 and Figure 5.23 show the results of the energy scheduling based on different conditions.

Table 5.8 Four scenarios for HREM scheduling analysis.

Scenario	Condition
1	No Agricultural Load and Low Solar Radiation
2	No Agricultural Load and High Solar Radiation
3	With Agricultural Load and Low Solar Radiation
4	With Agricultural Load and High Solar Radiation

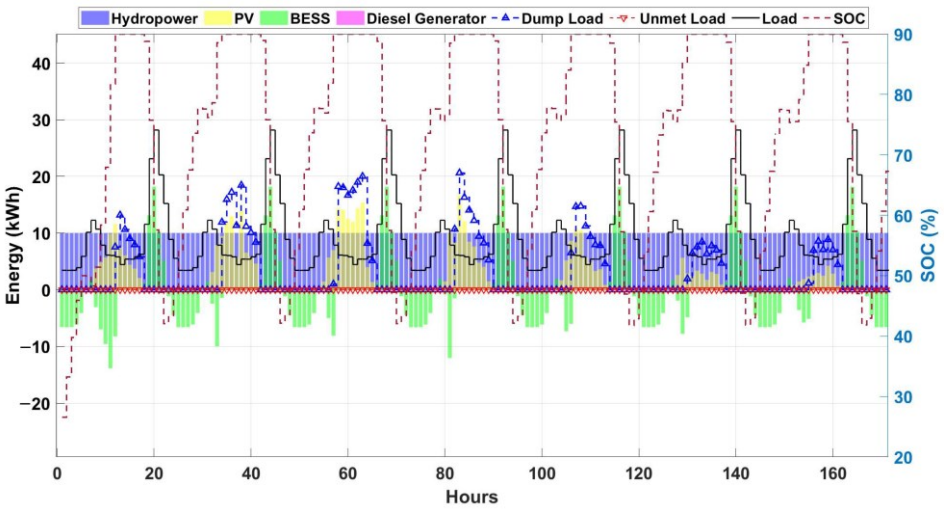

Figure 5.19 Energy scheduling—Scenario 1—no agricultural load and low solar radiation.

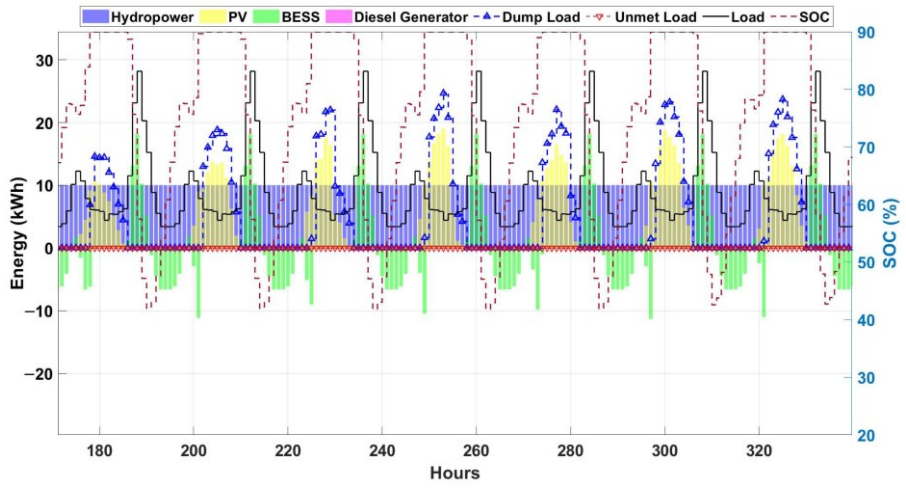

Figure 5.20 Energy scheduling—Scenario 2—no agricultural load and high solar radiation.

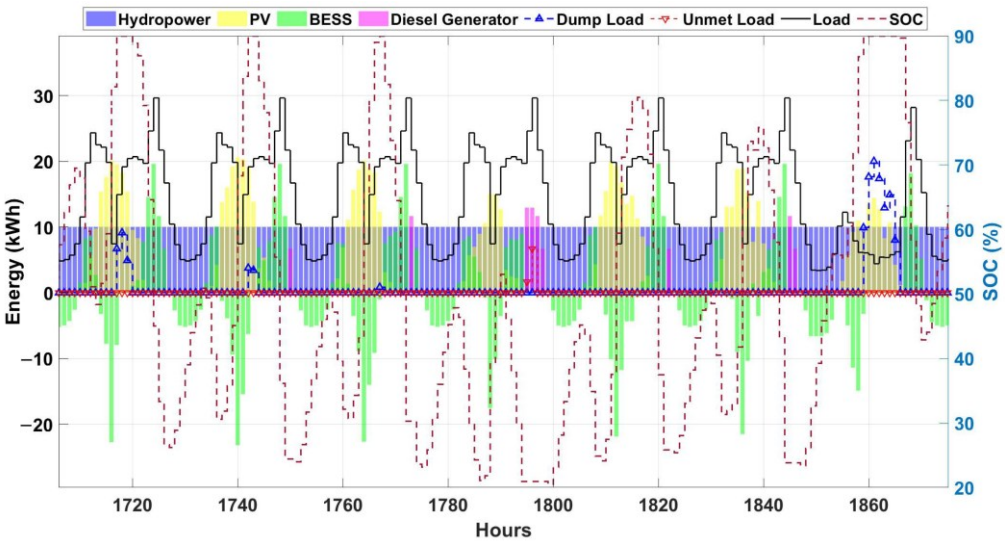

Figure 5.21 Energy scheduling—Scenario 3—with agricultural load and low solar radiation.

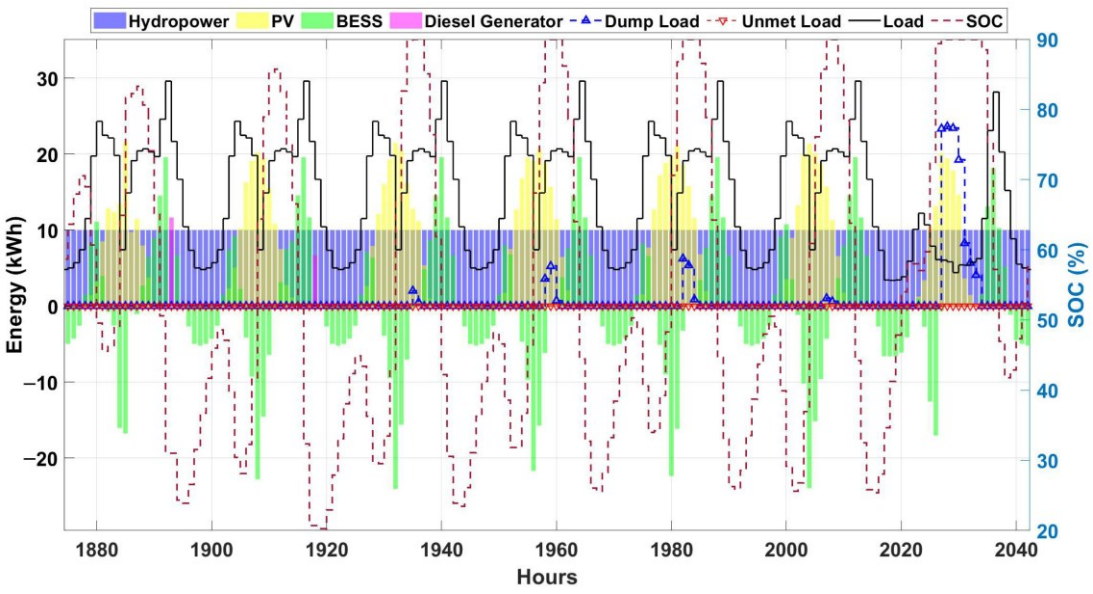

Figure 5.22 Energy scheduling—Scenario 4—with agricultural load and high solar radiation.

For Scenarios 1 and 2, shown in Figure 5.19 and Figure 5.20, respectively, the HREM operates with surplus power and the diesel generator is not being dispatched. This is due to the power generated by renewable energies being more than enough for the load from morning to afternoon. In the evening, when the load peaks, the battery dispatches the energy stored in the BESS from the charged excess energy. It can also be seen that, in both scenarios, the SOC of the battery varies from 20% to 90%. Thus, the constraints imposed on the battery's SOC are not violated.

In Scenario 3, there is an agricultural load from Monday to Saturday, and there are certain days with low solar radiation. As shown in Figure 5.21, the power generated by PV and hydropower is not enough to supply the combined residential and agricultural load and charge the battery with a surplus. The BESS discharges in both the morning and evening, unlike in Scenario 1 and 2. This is due to high load demand from 7 a.m. to 10 a.m. and from 7 p.m. to 10 p.m. It can also be seen in the figure that the diesel generator is being dispatched in the evening, when the load is at its peak, to compensate for the insufficient power generated by the hydropower and battery. There are days in this scenario where the SOC does not reach its maximum value of 90% and often dips below 30%.

As shown in Figure 5.23, in the scenario where there is high solar radiation, the power generated by each component of HREM is just enough for the combined residential and agricultural load and charging BESS. Thus, there is a small to zero surplus of power for the dump load except on Sunday when the load is only residential. The diesel generator operates sometimes for an hour when the load is at its peak. In the evening, the load peaks and the power generated by hydropower alone is insufficient, so the BESS starts discharging power to compensate. Except for Sunday, the SOC of the battery in this scenario often dips below 30% due to increased load and less excess energy from renewables for charging, as compared with Scenarios 1 and 2.

5.5.5. Sensitivity Analysis

The sensitivity analysis was expanded to qualify and quantify the influence of parametric variation on the levelized cost of electricity for HREM, as computed using the MOPSO algorithm. As sensitivity coefficients, four input parameters were chosen, and the results were determined with regard to Solution C, which is one of the solutions of interest and the nominal point in Table 5.7. Due to variations in the number of PV panels, size of diesel generator, size of BESS, and rural agricultural load of the study area, the influence on LCOE, as one of the main objectives, was investigated. Parameter variations from 50% to 150% were evaluated for sensitivity analysis and the sensitivity curve is shown in Figure 5.23. The LCOE is affected by the rural agriculture load, PV, and BESS in a nonlinear way. Because the total annual energy demand for the system is lower when the load is reduced, the LCOE values are higher. The LCOE is also influenced by a variation in the size of the diesel generator due to capital cost and fuel consumption, as seen in the graph. It can be seen that, with a lower rural agricultural load, number of PV panels, and BESS size, the LCOE values are higher and more sensitive. The LCOE is least affected by the number of PV panels. The reason for this is that the PV system has a lower overall cost (capital, operating, and maintenance) as compared with other components of the system.

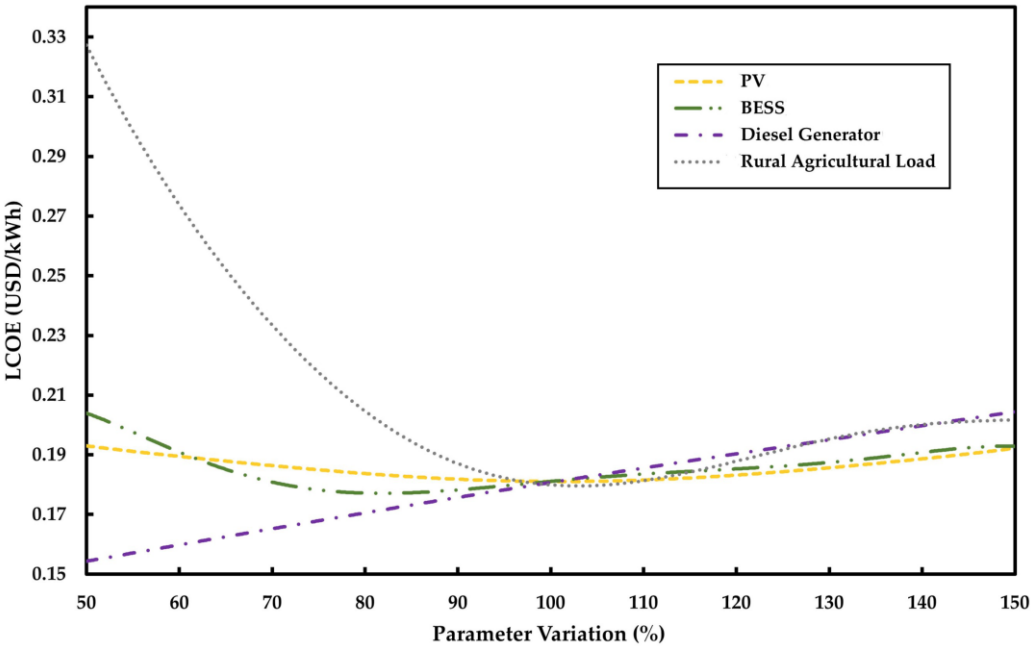

Figure 5.23 Sensitivity of LCOE to variation of different parameters.

5.6. Summary

This study presents the optimal design of an off-grid hybrid renewable energy microgrid system that can be used in order to meet the electrical load requirements in selected rural agricultural communities in the Southern Philippines. The multi-objective particle swarm optimization (MOPSO) algorithm is used to find the optimal system design and component sizes. The levelized cost of electricity (COE), the probability of loss of power supply (LPSP), and greenhouse gas emissions are all objective functions. A sensitivity analysis was also carried out to find out how much a change in the input values for a certain variable affects the results of the mathematical models that were used.

The algorithm generated 200 non-dominated solutions, of which 4 were selected as solutions of interest. Based on the results, the optimal size of the main components for the reliable operation of the system was estimated for the PV as 200 panels with a rating of 0.25 kW, for BESS as 100 kWh, and for the diesel generator as 13 kW, with an estimated system LCOE, LPSP, and GHG emission of 0.197 USD/kWh, 0.05%, and 7874 kg, respectively, for 1 year. The amount of energy generated by each component in a month using the HREM configuration that has been

chosen is more than adequate to meet the rural agriculture load and the dump load. The sensitivity analysis showed that decreased rural agricultural demand, PV panel count, and BESS size result in higher LCOE values, and that LCOE is least impacted by PV panel count, respectively. Furthermore, the main achievements and conclusions are listed below:

1. An optimized design of a hybrid renewable energy microgrid (HREM) composed of ROR hydropower, PV, BESS, and a diesel generator to supply electricity considering cost, reliability, and environmental impact.
2. A framework for simultaneous optimization of multiple generating units considering renewable energy's intermittent nature using MOPSO with three conflicting objectives, which are LCOE, LPSP, and GHG emissions, several constraints, and real meteorological data.
3. The proposed method also determines the capacity of each component of the system while considering the availability of renewable energy sources, load size, and several cost functions in order to obtain the configuration, while considering different tradeoffs for the lifetime of the microgrid in order to minimize costs and maximize reliability.
4. A power management strategy for optimal operation of the various components of the system and to ensure effective charging and discharging of the battery.
5. Energy demand estimation for an unelectrified rural agricultural area and load profiles for residential and agricultural loads were used for the optimization of the HREM.
6. Investigation and evaluation of the performance of the optimal design of HREM considering several scenarios within the study area.

5.7. Chapter 5 References

[5-1] IEA, "IEA—World Energy Outlook 2019." Available online: https://www.iea.org/reports/world-energy-outlook-2019 (accessed Aug. 15, 2021).

[5-2] The World Bank, "World Bank—Report: Universal Access to Sustainable Energy Will Remain Elusive without Addressing Inequalities." https://www.worldbank.org/en/news/press-release/2021/06/07/report-universal-access-tosustainable-energy-will-remain-elusive-without-addressing-inequalities (accessed Aug.

07, 2021).

[5-3] J. Jasiński, M. Kozakiewicz, and M. Sołtysik, “Determinants of Energy Cooperatives’ Development in Rural Areas—Evidence from Poland,” Energies, vol. 14, no. 2, p. 319, Jan. 2021, doi: 10.3390/en14020319.

[5-4] M. A. Quirapas-Franco, “Sustainable Energy Transition of the Poor Rural Communities in the Philippines,” 2021. : https://www.stratforumph.com/post/sustainable-energy-transition-of-the-poor-rural-communities-in-the-philippines (accessed Aug. 22, 2021).

[5-5] D. T. Ton and M. A. Smith, “The U.S. Department of Energy’s Microgrid Initiative,” Electr. J., vol. 25, no. 8, pp. 84–94, Oct. 2012, doi: 10.1016/j.tej.2012.09.013.

[5-6] M. H. Rehmani, M. Reisslein, A. Rachedi, M. Erol-Kantarci, and M. Radenkovic, “Integrating Renewable Energy Resources Into the Smart Grid: Recent Developments in Information and Communication Technologies,” IEEE Trans. Ind. Inform., vol. 14, no. 7, pp. 2814–2825, Jul. 2018, doi: 10.1109/TII.2018.2819169.

[5-7] P. Swain, S. Jagadish, and K. N. S. Uma Mahesh, “Integration of renewable sources of energy into power grid,” in 2017 IEEE Region 10 Symposium (TENSYMP), Cochin, Jul. 2017, pp. 1–5. doi: 10.1109/TENCONSpring.2017.8070012.

[5-8] L. An and T. Tuan, “Dynamic Programming for Optimal Energy Management of Hybrid Wind–PV–Diesel–Battery,” Energies, vol. 11, no. 11, p. 3039, Nov. 2018, doi: 10.3390/en11113039.

[5-9] M. Y. Nguyen, Y. T. Yoon, and N. H. Choi, “Dynamic programming formulation of Micro-Grid operation with heat and electricity constraints,” in 2009 Transmission & Distribution Conference & Exposition: Asia and Pacific, Seoul, South Korea, Oct. 2009, pp. 1–4. doi: 10.1109/TD-ASIA.2009.5356870.

[5-10] M. Strelec and J. Berka, “Microgrid energy management based on approximate dynamic programming,” in IEEE PES ISGT Europe 2013, Lyngby, Oct. 2013, pp. 1–5. doi: 10.1109/ISGTEurope.2013.6695439.

[5-11] L. K. Gan, J. K. H. Shek, and M. A. Mueller, “Hybrid wind–photovoltaic–diesel–battery system sizing tool development using empirical approach, life-cycle cost and performance analysis: A case study in Scotland,” Energy Convers. Manag., vol. 106, pp. 479–494, Dec.

2015, doi: 10.1016/j.enconman.2015.09.029.

[5-12] Y. Yoldas, S. Goren, and A. Onen, “Optimal Control of Microgrids with Multi-stage Mixed-integer Nonlinear Programming Guided Q-learning Algorithm,” J. Mod. Power Syst. Clean Energy, vol. 8, no. 6, pp. 1151–1159, 2020, doi: 10.35833/MPCE.2020.000506.

[5-13] S. Batiyah, R. Sharma, S. Abdelwahed, and N. Zohrabi, “An MPC-based power management of standalone DC microgrid with energy storage,” Int. J. Electr. Power Energy Syst., vol. 120, p. 105949, Sep. 2020, doi: 10.1016/j.ijepes.2020.105949.

[5-14] E. Fouladi, H. R. Baghaee, M. Bagheri, and G. B. Gharehpetian, “Power Management of Microgrids Including PHEVs Based on Maximum Employment of Renewable Energy Resources,” IEEE Trans. Ind. Appl., vol. 56, no. 5, pp. 5299–5307, Sep. 2020, doi: 10.1109/TIA.2020.3010713.

[5-15] A. Oulis Rousis, D. Tzelepis, I. Konstantelos, C. Booth, and G. Strbac, “Design of a Hybrid AC/DC Microgrid Using HOMER Pro: Case Study on an Islanded Residential Application,” Inventions, vol. 3, no. 3, p. 55, Aug. 2018, doi: 10.3390/inventions3030055.

[5-16] A. Aziz, M. Tajuddin, M. Adzman, M. Ramli, and S. Mekhilef, “Energy Management and Optimization of a PV/Diesel/Battery Hybrid Energy System Using a Combined Dispatch Strategy,” Sustainability, vol. 11, no. 3, p. 683, Jan. 2019, doi: 10.3390/su11030683.

[5-17] J. Lu, W. Wang, Y. Zhang, and S. Cheng, “Multi-Objective Optimal Design of Stand-Alone Hybrid Energy System Using Entropy Weight Method Based on HOMER,” Energies, vol. 10, no. 10, p. 1664, Oct. 2017, doi: 10.3390/en10101664.

[5-18] J. O. Oladigbolu, M. A. M. Ramli, and Y. A. Al-Turki, “Optimal Design of a Hybrid PV Solar/Micro-Hydro/Diesel/Battery Energy System for a Remote Rural Village under Tropical Climate Conditions,” Electronics, vol. 9, no. 9, p. 1491, Sep. 2020, doi: 10.3390/electronics9091491.

[5-19] Y. E. García-Vera, R. Dufo-López, and J. L. Bernal-Agustín, “Techno-Economic Feasibility Analysis through Optimization Strategies and Load Shifting in Isolated Hybrid Microgrids with Renewable Energy for the Non-Interconnected Zone (NIZ) of Colombia,” Energies, vol. 13, no. 22, p. 6146, Nov. 2020, doi: 10.3390/en13226146.

[5-20] W.-K. Chae, H.-J. Lee, J.-N. Won, J.-S. Park, and J.-E. Kim, “Design and Field Tests of

an Inverted Based Remote MicroGrid on a Korean Island," Energies, vol. 8, no. 8, pp. 8193–8210, Aug. 2015, doi: 10.3390/en8088193.

[5-21] G. Cardoso, T. Brouhard, N. DeForest, D. Wang, M. Heleno, and L. Kotzur, "Battery aging in multi-energy microgrid design using mixed integer linear programming," Appl. Energy, vol. 231, pp. 1059–1069, Dec. 2018, doi: 10.1016/j.apenergy.2018.09.185.

[5-22] W.-H. Park, H. Abunima, M. B. Glick, and Y.-S. Kim, "Energy Curtailment Scheduling MILP Formulation for an Islanded Microgrid with High Penetration of Renewable Energy," Energies, vol. 14, no. 19, p. 6038, Sep. 2021, doi: 10.3390/en14196038.

[5-23] A. Krishnan Prakash et al., "Solar+ Optimizer: A Model Predictive Control Optimization Platform for Grid Responsive Building Microgrids," Energies, vol. 13, no. 12, p. 3093, Jun. 2020, doi: 10.3390/en13123093.

[5-24] S. Balderrama, F. Lombardi, F. Riva, W. Canedo, E. Colombo, and S. Quoilin, "A two-stage linear programming optimization framework for isolated hybrid microgrids in a rural context: The case study of the 'El Espino' community," Energy, vol. 188, p. 116073, Dec. 2019, doi: 10.1016/j.energy.2019.116073.

[5-25] M. Yousif, Q. Ai, Y. Gao, W. A. Wattoo, Z. Jiang, and R. Hao, "Application of Particle Swarm Optimization to a Scheduling Strategy for Microgrids Coupled with Natural Gas Networks," Energies, vol. 11, no. 12, p. 3499, Dec. 2018, doi: 10.3390/en11123499.

[5-26] Y. Sun, Z. Cai, Z. Zhang, C. Guo, G. Ma, and Y. Han, "Coordinated Energy Scheduling of a Distributed Multi-Microgrid System Based on Multi-Agent Decisions," Energies, vol. 13, no. 16, p. 4077, Aug. 2020, doi: 10.3390/en13164077.

[5-27] J. L. Torres-Madroñero, C. Nieto-Londoño, and J. Sierra-Pérez, "Hybrid Energy Systems Sizing for the Colombian Context: A Genetic Algorithm and Particle Swarm Optimization Approach," Energies, vol. 13, no. 21, p. 5648, Oct. 2020, doi: 10.3390/en13215648.

[5-28] X. Wu, W. Cao, D. Wang, and M. Ding, "A Multi-Objective Optimization Dispatch Method for Microgrid Energy Management Considering the Power Loss of Converters," Energies, vol. 12, no. 11, p. 2160, Jun. 2019, doi: 10.3390/en12112160.

[5-29] F. Khlifi, H. Cherif, and J. Belhadj, "Environmental and Economic Optimization and Sizing of a Micro-Grid with Battery Storage for an Industrial Application," Energies, vol.

14, no. 18, p. 5913, Sep. 2021, doi: 10.3390/en14185913.

[5-30] R. Dufo-López et al., “Multi-objective optimization minimizing cost and life cycle emissions of stand-alone PV–wind–diesel systems with batteries storage,” Appl. Energy, vol. 88, no. 11, pp. 4033–4041, Nov. 2011, doi: 10.1016/j.apenergy.2011.04.019.

[5-31] J. D. Vasanth, N. Kumarappan, R. Arulraj, and T. Vigneysh, “Minimization of operation cost of a microgrid using firefly algorithm,” in 2017 IEEE International Conference on Intelligent Techniques in Control, Optimization and Signal Processing (INCOS), Srivilliputhur, Mar. 2017, pp. 1–6. doi: 10.1109/ITCOSP.2017.8303149.

[5-32] C. M. Colson, M. H. Nehrir, and C. Wang, “Ant colony optimization for microgrid multi-objective power management,” in 2009 IEEE/PES Power Systems Conference and Exposition, Seattle, WA, USA, Mar. 2009, pp. 1–7. doi: 10.1109/PSCE.2009.4840070.

[5-33] K. Nimma, M. Al-Falahi, H. D. Nguyen, S. D. G. Jayasinghe, T. Mahmoud, and M. Negnevitsky, “Grey Wolf Optimization-Based Optimum Energy-Management and Battery-Sizing Method for Grid-Connected Microgrids,” Energies, vol. 11, no. 4, p. 847, Apr. 2018, doi: 10.3390/en11040847.

[5-34] A. M. Helmi, R. Carli, M. Dotoli, and H. S. Ramadan, “Efficient and Sustainable Reconfiguration of Distribution Networks via Metaheuristic Optimization,” IEEE Trans. Autom. Sci. Eng., vol. 19, no. 1, pp. 82–98, Jan. 2022, doi: 10.1109/TASE.2021.3072862.

[5-35] M. Azam Muhammad, H. Mokhlis, K. Naidu, A. Amin, J. Fredy Franco, and M. Othman, “Distribution Network Planning Enhancementvia Network Reconfiguration and DGIntegration Using Dataset Approachand Water Cycle Algorithm,” J. Mod. Power Syst. Clean Energy, vol. 8, no. 1, pp. 86–93, 2020, doi: 10.35833/MPCE.2018.000503.

[5-36] PAGASA, “PAGASA—Climate of the Philippines.” https://www.pagasa.dost.gov.ph/information/climatephilippines (accessed Aug. 15, 2021).

[5-37] E. Lorenzo, “Energy collected and delivered by PV modules,” in Handbook of Photovoltaic Science an Engineering, Hoboken, NJ, USA: John Wiley & Sons, 2011.

[5-38] P. Vedel, “Modeling and Real Time Optimization of a Smart Microgrid,” Master’s Thesis, Technical University of Liberec, Liberec, Czech Republic, 2019.

[5-39] X. Jiang, G. Nan, H. Liu, Z. Guo, Q. Zeng, and Y. Jin, “Optimization of Battery Energy

Storage System Capacity for Wind Farm with Considering Auxiliary Services Compensation," Appl. Sci., vol. 8, no. 10, p. 1957, Oct. 2018, doi: 10.3390/app8101957.

[5-40] JICA, "Guideline and Manual for Hydropower Development," JICA, Tokyo, Japan, Technical Report Volume 2, 2011.

[5-41] M. S. Ismail, M. Moghavvemi, and T. M. I. Mahlia, "Techno-economic analysis of an optimized photovoltaic and diesel generator hybrid power system for remote houses in a tropical climate," Energy Convers. Manag., vol. 69, pp. 163–173, May 2013, doi: 10.1016/j.enconman.2013.02.005.

[5-42] S. Kewat, B. Singh, and I. Hussain, "Power management in PV-battery-hydro based standalone microgrid," IET Renew. Power Gener., vol. 12, no. 4, pp. 391–398, Mar. 2018, doi: 10.1049/iet-rpg.2017.0566.

[5-43] W. Short, D. J. Packey, and T. Holt, "A manual for the economic evaluation of energy efficiency and renewable energy technologies," NREL/TP--462-5173, 35391, Mar. 1995. doi: 10.2172/35391.

[5-44] S. Phommixay, M. L. Doumbia, and D. Lupien St-Pierre, "Review on the cost optimization of microgrids via particle swarm optimization," Int. J. Energy Environ. Eng., vol. 11, no. 1, pp. 73–89, Mar. 2020, doi: 10.1007/s40095-019-00332-1.

[5-45] A. Malheiro, P. M. Castro, R. M. Lima, and A. Estanqueiro, "Integrated sizing and scheduling of wind/PV/diesel/battery isolated systems," Renew. Energy, vol. 83, pp. 646–657, Nov. 2015, doi: 10.1016/j.renene.2015.04.066.

[5-46] I. Sperstad and M. Korpås, "Energy Storage Scheduling in Distribution Systems Considering Wind and Photovoltaic Generation Uncertainties," Energies, vol. 12, no. 7, p. 1231, Mar. 2019, doi: 10.3390/en12071231.

[5-47] H. Akter, H. O. R. Howlader, A. Y. Saber, A. M. Hemeida, H. Takahashi, and T. Senjyu, "Optimal Sizing and Operation of Microgrid in a Small Island Considering Advanced Direct Load Control and Low Carbon Emission," in 2021 International Conference on Science & Contemporary Technologies (ICSCT), Dhaka, Bangladesh, Aug. 2021, pp. 1–5. doi: 10.1109/ICSCT53883.2021.9642669.

[5-48] J. Kennedy and R. Eberhart, "Particle swarm optimization," in Proceedings of ICNN'95

- International Conference on Neural Networks, Perth, WA, Australia, 1995, vol. 4, pp. 1942–1948. doi: 10.1109/ICNN.1995.488968.

[5-49] C. A. C. Coello, G. T. Pulido, and M. S. Lechuga, “Handling multiple objectives with particle swarm optimization,” IEEE Trans. Evol. Comput., vol. 8, no. 3, pp. 256–279, Jun. 2004, doi: 10.1109/TEVC.2004.826067.

[5-50] X.-S. Yang, “Chapter 8 - Particle Swarm Optimization,” in Nature-Inspired Optimization Algorithms (Second Edition), X.-S. Yang, Ed. Academic Press, 2021, pp. 111–121. doi: 10.1016/B978-0-12-821986-7.00015-9.

[5-51] L. Yang, X. Yang, Y. Wu, and X. Liu, “Applied Research on Distributed Generation Optimal Allocation Based on Improved Estimation of Distribution Algorithm,” Energies, vol. 11, no. 9, p. 2363, Sep. 2018, doi: 10.3390/en11092363.

[5-52] H. Zahboune, S. Zouggar, G. Krajacic, P. S. Varbanov, M. Elhafyani, and E. Ziani, “Optimal hybrid renewable energy design in autonomous system using Modified Electric System Cascade Analysis and Homer software,” Energy Convers. Manag., vol. 126, pp. 909–922, Oct. 2016, doi: 10.1016/j.enconman.2016.08.061.

Chapter 6 Analysis of the Implication of the Experts' Opinion on HREM Social Acceptance

Chapter 6 delves into the examination of the impact of the experts' opinion on the social acceptance of the proposed Hybrid Renewable Energy Microgrid (HREM) for a rural agricultural community. The previous chapters have provided a comprehensive overview of the technical aspects of microgrid design and development. However, it is important to also consider the social acceptance of the HREM, as it is crucial for the long-term sustainability of the project. This chapter aims to investigate the influence of the technical assessment and optimization results, or the "experts' opinion," on the social acceptance of the HREM.

6.1. Introduction

Along with the constant evolution of the global energy landscape, the concerns and interests of energy end-users also change. As technology advances and new energy sources become available, consumers are confronted with a plethora of information regarding the availability, utilization, and environmental impact of energy resources. These concerns extend beyond the technical aspects of energy production to the effects of energy consumption on the economy, the environment, social norms, and quality of life as a whole. This demonstrates the significance of considering not only the technical aspects of microgrid development and deployment, but also the socioeconomic and environmental factors that may influence their acceptance by the community. To ensure the microgrid's long-term viability and success, it is imperative to comprehend how the community may perceive and react to it. This necessitates an interdisciplinary approach that takes into account not only the technical aspects, but also the social, economic, and environmental factors that may influence the community's acceptance of the microgrid.

In recent years, the importance of an interdisciplinary approach in addressing current service systems such as utilities, transportation, and communication has been increasingly acknowledged. This approach integrates engineering, social science, and management science to address comprehensively all aspects of the system, including social acceptance of the proposed

solution. [6-1], [6-2]. This method acknowledges that, while engineering is essential to the development of modern infrastructure, there are additional factors that are difficult to analyze, particularly social acceptance. Potential non-technical barriers, such as financial, administrative, organizational, infrastructural, and perceptual barriers, can be identified and addressed by integrating social science and management science into the design and implementation process. This method not only improves the likelihood of successful implementation, but also ensures that the proposed solution aligns with the community's needs and interests.

Management of the electricity systems is a complex task with multiple components, including the management component. Recent research indicates that effective management is crucial to the planning and implementation of capital investment projects intended to address the growing strain on aging electricity systems. This includes managing dynamic pricing and implementing strategies to reduce demand peaks. In addition to this technical aspect, the social component is crucial to comprehending how consumers perceive and respond to energy-related issues. This includes evaluating the cost-benefit relationship and how it can motivate individuals to adopt new norms, such as delaying energy consumption until off-peak hours. In turn, this can influence their lifestyle and behavior [6-3].

Any initiative for development, such as rural electrification through microgrids, must incorporate social, economic, environmental, and management considerations. Taking into account these factors enables funders and project developers to better comprehend the needs of the recipients. This technique also helps identify the obstacles and opportunities that must be overcome for the intervention to be successfully implemented [6-4]. Numerous development or intervention programs have failed because these factors were not taken into account. Acceptance and approval of the type of intervention by community members is influenced by a number of sociocultural factors that, if not properly understood, may have an effect on the project's execution and long-term viability [6-3], [6-5], [6-6]. Consideration of these factors throughout project development facilitates community involvement and ensures that the project is in the best interests of the community. It also considers the project's social implications to ensure that it will have a lasting positive impact on the community.

The examination of social aspects of energy-related issues should be coupled with the

investigation of economic, management, and environmental issues, as they are frequently intertwined and difficult to separate. Identifying the socioeconomic issues that may be affected by the development and implementation of energy-related projects, such as renewable energy projects, is the first step in assessing the social benefits of an idea. The second step involves analyzing the positive or negative effects these projects, such as renewable energy projects, have on these issues.

The implementation of renewable energy projects, such as microgrids, is a complex endeavor involving numerous technical and non-technical factors. Non-technical obstacles, such as financial, administrative, organizational, infrastructural, and perceptual barriers, can have a substantial effect on the overall costs and success of such projects. These obstacles can result in increased costs, implementation delays, and decreased investor returns [6-5], [6-7]. Among these non-technical barriers, perceptual barriers are especially significant because they play a crucial role in determining the community's social acceptance of the microgrid. These obstacles relate to the community's perception, attitude, and comprehension of the microgrid and its potential benefits. Understanding these perceptional barriers is crucial for ensuring the microgrid's long-term viability and success, as it enables the identification and resolution of potential issues that may impede community acceptance.

The social acceptance of a renewable energy project, such as a microgrid, is vital to its successful implementation and long-term viability. This acceptance can be separated into three interconnected dimensions: sociopolitical acceptance, community acceptance, and market acceptance [6-8], [6-9]. Sociopolitical acceptance refers to the degree to which government officials and policymakers support and endorse the project. This includes the government's financial and administrative support for the development and implementation of the project. In contrast, community acceptance refers to the level of support and acceptance from local residents for the location and implementation of the project. This includes the level of community engagement and participation in the development of the project, as well as their perceptions and attitudes toward the project. The third dimension is market acceptance, which refers to the extent to which consumers are willing to adopt the technology and pay for its services. This is typically determined by the consumers' willingness to pay for microgrid services and their perceptions of

the technology's advantages and disadvantages. It is essential to note that a consumer's decision to adopt a technology may not correspond with the level of community acceptance for the project's implementation. This emphasizes the significance of considering all three dimensions of social acceptance to ensure the long-term success and sustainability of the project.

This chapter aims to investigate the acceptance of the Hybrid Renewable Energy Microgrid (HREM) among local residents in Rogongon, Iligan City, Philippines. The study also aims to understand the factors that influence the community's acceptance of the HREM, with a specific focus on the relationship between knowledge, perception, attitude strength, and attitude towards renewable energy and HREM. Additionally, the study will examine the potential role of expert opinion in the form of information dissemination and focused group discussions in influencing the community's acceptance of the HREM. Through a combination of quantitative and qualitative research methods, this study aims to provide a comprehensive understanding of the social acceptance of HREM in the community of Rogongon.

6.2. Methodology

6.2.1 Overall Methodology

This study employs a mixed-methods approach, employing both quantitative and qualitative data collection techniques, to investigate the influence of various factors on the local community's acceptance of the proposed Hybrid Renewable Energy Microgrid (HREM). Figure 6.1 illustrates the overall methodology.

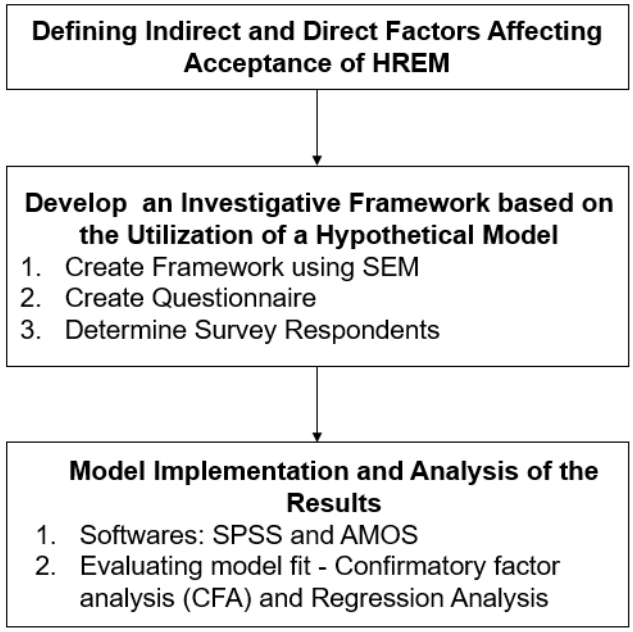

Figure 6.1 Overall Methodology for the Analysis

The overall methodology used in this study consists of three major steps: defining indirect and direct factors influencing HREM acceptance, developing an investigative framework using a hypothetical model, and implementing and analyzing the study's results. Using theories and findings from previous studies on social acceptance of microgrids and renewable energy projects, the first step entails identifying potential factors that may influence HREM acceptance, both directly and indirectly. The second step entails developing an investigative framework based on a hypothetical model, which includes using structural equation modeling (SEM) and developing a questionnaire to survey local residents. The final step is to implement and analyze the study's results using software such as SPSS and AMOS, as well as to evaluate the model fit using confirmatory factor analysis (CFA) and regression analysis. It is also worth noting that the following subsections of the methodology section go into greater detail about each step.

6.2.2 Defining Indirect and Direct Factors based Different Theories About Social Acceptance of Microgrids

In this study, the process of defining the indirect and direct factors influencing the acceptance of the proposed Hybrid Renewable Energy Microgrid (HREM) involved reviewing literature on various theories about social acceptance of microgrids. The NIMBY metaphor is one of the key concepts that emerged from the literature review ("Not in my backyard"). This rational choice theory-based concept proposes that residents support renewable energy development only when it is not built in their immediate vicinity. However, multiple studies have revealed that this hypothesis is insufficient, as it does not fully capture the complexity of local acceptance of microgrids. As a result, academics have criticized the NIMBY explanation for its one-dimensional approach and emphasized the importance of employing a broader range of theoretical concepts when researching the local acceptability of microgrids. The researcher used relational models in this study, which resulted in three concepts for determining the fairness of authority: standing, neutrality, and trust. These ideas were combined with others to investigate the social acceptance of the proposed HREM. [6-10]– [6-13]. This study delves into the concept of trust and fairness in relation to project developers and operators to better understand the factors influencing HREM acceptance. It is critical to note that trust and fairness are essential in ensuring public acceptance of microgrid development projects. According to the "trust, confidence, and cooperation paradigm" (TCC), trust can be broken down into two categories: social trust based on value commonality and confidence based on perceived performance. The incorporation of both of these concepts into this study enables the measurement of citizens' subjective evaluations of the behavior and attitude of plant operators, as well as their knowledge and capacity to respond to the concerns of rural residents. In this study, however, a generic trust measure was used to simplify the model and account for the close correlation between confidence and social trust in the studied population.

This approach is consistent with broader research on justice theories and predictors of microgrid project success, which emphasizes the importance of both procedural and distributive justice in achieving societal and local acceptance of renewable energy projects. The process of earning and maintaining the trust of the inhabitants, as well as providing them with adequate

amounts of knowledge and engagement, is referred to as procedural justice. Distributive justice, on the other hand, refers to the equitable distribution of the consequences of the proposed HREM, such as its perceived benefits and costs, particularly the environmental impact due to construction. As a result, when assessing the acceptability of planned HREM in the local community, it is critical to consider both procedural and distributive justice. The research on justice theories and factors that predict microgrid project success emphasizes the critical role of both procedural and distributive justice in achieving societal and local acceptance of renewable energy projects such as HREM [6-14]- [6-17]. To ensure procedural justice, it is critical to first establish and then maintain community trust by providing clear and accurate information and opportunities for engagement. This will help to boost local residents' trust in the project and its developers. Distributive justice, on the other hand, can be realized by ensuring a fair and equitable distribution of the perceived benefits and costs of the proposed HREM, including its environmental impact. This includes not only the community's direct benefits and costs, but also the indirect effects, such as potential changes to the local environment.

Previous research indicates that a number of factors can influence the local acceptability of planned HREM projects. These variables can be classified as direct or indirect, and they include information provision, involvement options, trust in experts, perceived benefits, perceived costs, and perceived environmental impacts of HREM during the development phase.

Table 6.1, which provides a comprehensive overview of these elements, further categorizes the concepts of procedural and distributive justice. The study aims to develop a comprehensive understanding of the various factors that affect the acceptance of HREM projects, and how they can be effectively managed to achieve a successful outcome, by taking these factors and their potential impact on the community into account.

Table 6.1 Summary of the factors that are presumed to have an impact on the level of acceptance of HREM in the study area

Factors to Consider in Relation to Distributive Justice	**Factors to Consider in Relation to Procedural Justice**
Perceived Benefits	Provision of Information (Experts' Opinion based on Findings from Previous Chapters)
Perceived Costs	Options Available for Participation

Perceived Environmental Impact during Development Phase	Trust in Experts (Researchers and Project Developers)

6.2.3 Creating an Investigative Framework based on the Utilization of a Hypothetical Model

Understanding the factors that influence the acceptance of HREM within a community is one of the primary goals of this chapter. To achieve this, a comprehensive investigative framework was developed and modified from a previous related study in Switzerland [6-21], taking into account both direct and indirect factors. The direct factors, which include perceived benefits of HREM, perceived costs of HREM, and trust in experts, were considered to have a direct impact on the acceptance of HREM. On the other hand, indirect factors, such as the provision of information, the options available for participation, and the perceived environmental impact during construction, were considered to have an indirect influence on the acceptance of HREM. As shown in

Table 6.1 and Figure 6.2, all of these factors were taken into consideration when developing the hypothetical model and the research framework for this study. The hypothetical model was then empirically tested using structural equation modeling (SEM) in order to gain insight into how these direct and indirect factors influence the overall acceptability of HREM within a community.

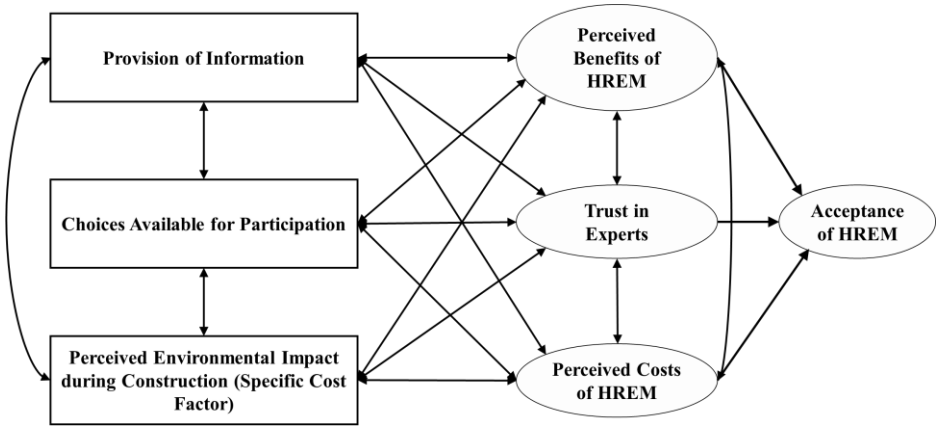

Figure 6.2 A hypothetical model of the factors that influence residents' acceptance of HREM used in the investigation.

6.2.3.1 The Influence of Direct Contributing Factors

Perceived benefits and trust in experts (researchers and project developers) are thought to have a direct positive influence on residents' acceptance of HREM, while perceived costs are thought to have a direct negative influence. This hypothesis is one of the hypotheses expressed in the model. Furthermore, one of the hypotheses that will be tested in this study is the relationship between perceived costs, perceived benefits, and trust in experts. In contrast to these findings, some research suggests that trust has a causal effect on both perceived costs (or risks) and perceived rewards. These studies, on the other hand, consider individuals' trust in authority, such as regulatory organizations, and focus on judgments about potential energy advances [6-18]–[6-20]. In addition, professional advice and used a retrospective approach was sought. Because the emphasis of this study is not on participants' risk perceptions, but rather on their perception of with the costs and benefits of the proposed HREM, a correlational assumption appears more reasonable in this context. Based on the assumptions, the following hypotheses were developed:

H1: There is a positive relationship/influence between perceived benefits and acceptance of HREM.

H2: There is a positive relationship/influence between trust in experts and acceptance of HREM.

H3: There is a negative relationship/influence between perceived costs in experts and acceptance of HREM.

6.2.3.2 The Influence of Indirect Contributing Factors

One more hypothesis that was formulated during the research was that residents' acceptance of HREM would be indirectly affected positively by the reception of information on the HREM from experts and by the participation options that were made available during the planning process, but that local acceptance would be indirectly affected or influenced negatively by the residents' perceptions of the environmental impact that would result from the construction of HREM. On the other hand, the assumption is made that these effects are mediated by trust in experts, perceived benefits, and perceived costs of HREM. The following hypotheses were

formulated based on the assumptions made:

H4: There is an indirect positive relationship/influence between provision of information and acceptance of HREM.

H5: There is an indirect positive relationship/influence between choices available for participation and acceptance of HREM.

H6: There is an indirect negative relationship/influence between perceived environmental impact and acceptance of HREM.

6.2.3.3 Influence of the information's Quality, Amount, and Timeliness, as well as the Opportunities for Participation

The study's hypothetical model serves as the foundation for understanding the factors that influence residents' acceptance of HREM. The model provides a clear and concise representation of the relationships between these factors and acceptance by focusing on the direct effects of perceived benefits, perceived costs, and trust in experts. It is important to note, however, that while the model is simplified, it does not account for other factors such as information provision and participation options. These factors are thought to be important in determining acceptance, so the study investigates them in greater depth using a comprehensive information model and a detailed participation model.

The comprehensive information model used in this research investigates the factors that influence acceptance among participants who have indicated that they have received information. These factors include the quality of the information, the quantity of the information, and the timeliness of the information. The detailed participation model investigates the factors that play a role in a participant's choice regarding whether or not to take advantage of a participation opportunity. These factors include the nature, quantity, and timing of the opportunities that are made available. The research delves deeper into these issues and collects more information in order to achieve the goal of gaining a better understanding of how information and participation choices affect acceptance. The findings imply that there is an indirect but positive impact on the acceptability of high-renewable energy microgrids (HREM) based on the quality, quantity, and timeliness of information and participation choices. This is suggested by the fact that the findings

are positive. The participants in the study who have reported receiving these alternatives will be the focus of the investigation.

6.2.4 Information Provided to Residents and Stakeholders Prior to Household Survey

A series of information dissemination activities were carried out prior to conducting the household surveys in this study as part of the protocol and requirements set by the national government for the pre-feasibility stage of a renewable energy project. This research was carried out in collaboration with an ongoing project funded by the Philippines' Department of Science and Technology (DOST) titled "Development and Installation of Microgrid in a Remote Community," with Mindanao State University - Iligan Institute of Technology (MSU-IIT) as the host university and a counterpart research team from the Philippines for the e-Asia JRP collaboration with Waseda University. Project orientations, open forums, stakeholder meetings, and public presentations are among the activities carried out, as shown in Figure 6.3. Members of the community and beneficiary residents attended and participated in these activities.

The presentations were translated into the participants' native language to ensure that the information provided was understood and grasped. The information disseminated includes the project's objectives and scope, an overview of the planned HREM (Hybrid Hydropower-Solar PV System), presentations on renewable energy systems, benefits and impacts, proposed arrangements and organization for the community HREM, and options for project participation. Furthermore, prior to the household survey, residents provided informed consent to ensure that they were aware of the purpose of the research and survey. Expert opinions based on studies conducted and discussed in previous chapters were used to provide additional information. Table 6.2 summarizes the simplified findings or information that comprise the "expert's opinion."

Table 6.2 Summary of Expert's Opinion based on the findings from Previous Chapters

Chapter Number	Study	Simplified Findings or Information
2	Local-Scale Assessment of Multiple Renewable Energy Sources Using Various GIS Tools and Models	There are locally available renewable energy sources that can be used for electrification of the area.

3	Suitability Analysis of Hybrid Renewable Energies using GIS and Fuzzy-AHP	The proposed HREM will avoid restricted areas and follows the existing regulations stipulated by the government.
4	Optimization of Electric Transmission Line (ETL) Routing for a Renewable Energy-Based Microgrid using LCP Analysis and GIS-MCDA	The proposed distribution line routes of the HREM are optimized will avoid restricted areas and has minimized environmental impact
5	Integrated Optimal Sizing and Operation of Hybrid Renewable Energy Microgrid using Multi-Objective Particle Swarm Optimization (MOPSO)	The renewable energy generating components (PV and microhydropower) will have optimized capacity and will provide stable supply of electricity

Figure 6.3 Photographs of activities conducted in the study area

6.2.5 Description of the Household Survey Questionnaire

The household survey questionnaire used in this study aims to identify and evaluate a wide range of factors that may influence local community acceptance of the proposed HREM. The questionnaire was developed and modified from a previous study on renewable energy plant acceptance in Switzerland [6-21]. The questionnaire collects responses from participants using a six-point Likert scale, as shown in Figure 6.4. The questionnaire is based on previous research on

social and community acceptance of microgrids and renewable energy projects in various countries, such as wind power, solar power, and micro hydropower. Table 6.3 summarizes the various components of the questionnaire. The survey's goal is to collect data on the availability of information and participation options throughout the HREM's planning and development process. The questionnaire also asks about perceived benefits, costs, trust in experts, the environmental impact of HREM construction, and the quality, quantity, and timing of information and participation options.

A detailed information model and a detailed participation model are also included in the questionnaire, with the goal of gaining a better understanding of the impact of information and participation options on acceptance. The detailed information model investigates the quality, quantity, and timing of information provided to residents, whereas the detailed participation model investigates the quality, quantity, and timing of participation options available to residents.

Table 6.3 Formulated questionnaire based on the selected indirect and direct factors

ITEM PER SCALE
Main Model
Acceptance of HREM **(6-point Likert scale)**
① I'm delighted that an HREM is being considered for development in my community.
② I support the proposed HREM and will voluntarily participate in the protection and maintenance of it.
③ How do you rate the proposed HREM?
Perceived benefits of HREM **(6-point Likert scale)**
④ I believe the proposed HREM will improve my standard of living.
⑤ I believe the proposed HREM will provide an affordable and reliable electricity.
⑥ The proposed HREM makes me feel good, because it's environmentally friendly.
⑦ I think the proposed HREM is beneficial to our livelihood.
Perceived costs of HREM **(6-point Likert scale)**
⑧ I think the HREM will impair the quality of living in the community.
⑨ The proposed HREM will hurt me financially or it is not affordable.
⑩ I think the proposed HREM in the community will spoil the natural landscape.
⑪ I think the proposed HREM will deter the electricity connection from local distribution company.
Trust **(6-point Likert scale)**
⑫ The experts treats and involves me fairly.
⑬ The experts are experienced and expert enough to ensure a safe and successful construction of HREM.
⑭ The experts appreciates the local residents' concerns.
⑮ The experts are knowledgeable on renewable energy and HREM.
Provision of Information **(0 'no', 1 'yes')**
⑯ Did you get information on the HREM from the people responsible (experts) during the pre-feasibility and planning phase?
Options for Participation **(-1 'no options provided', 0 'any options provided')**
⑰ What participations options were you given during the planning of the HREM?
Perceived Environmental Impact of HREM Construction **(0 'no', 1 'yes')**
⑱ Do you think the construction of HREM will severely damage the local environment?

Detailed Information Model

Quality of the information **(6-point Likert scale)**

① All of the advantages and disadvantages of the HREM were honestly described in the material/project presentation that was supplied.

② I think the information was fair and accurate.

③ The information has been presented in a manner that is easy to comprehend.

④ I believe that the information that was provided to me was correct at all times.

Quantity of the information **(1 'not enough' 2 'enough')**

⑤ Were you provided with an adequate amount of information?

Timing of the Information (1 'not soon enough', 2 'early enough')

⑥ Do you believe that information on the plans for an HREM in your community was communicated to you in a timely manner?

Strongly Disagree	Disagree	Slightly Disagree	Slightly Agree	Agree	Strongly Agree
1	2	3	4	5	6

50% Negative **50% Positive**

Figure 6.4 Six point Likert scale used to rate the items in the questionnaire

6.2.6 Description of the Surveyed Household Respondents

The survey's sample population included all people who resided in areas that would be electrified by the HREM. The questionnaire was used to collect the addresses of these households. Participants in the survey were asked to provide feedback on the planned HREM development and to rate their experiences with the planning and development process retrospectively. To ensure a representative sample, 55 residents from various households were chosen at random from a pool of those who responded to the survey and agreed to participate. To facilitate understanding and response, the questionnaires were translated into Bisaya, the native language of the study area.

It is important to note that the analysis only included responses from survey participants who were aware of the planned HREM development in their community prior to the survey and who had been residing at their current address prior to the announcement of the planned HREM development. This was done to ensure that the responses came from people who understood the proposed project and its potential effects on their neighborhood. The survey's sample population consisted of an estimated 105 households in the study area that would be electrified by the proposed HREM. This sample size was deemed adequate for providing a complete picture of the community's perceptions and attitudes toward the proposed HREM development.

6.2.7 Profile of the Survey Participants

The study's sample included 55 residents from the immediate vicinity of the proposed HREM development. The sample was carefully chosen to represent the population in terms of gender, age, socioeconomic status, and occupation.

The sample included 35 females (63.6% of the total) and 22 males (36.4%). According to Figure 6.5 and Figure 6.6, the majority of respondents were young adults aged 18 to 30. The sample also had a relatively typical socioeconomic status distribution for the population, with households in the home survey sample ranging in size from 4 to 7 people.

However, based on data on professions and occupations, the sample appeared to include a disproportionate number of young people and those with an elementary level of education. This is important to consider when interpreting the study's findings because it may affect the generalizability of the findings.

All of the interviewees were involved in agricultural activities, primarily subsistence farming, or had family members who were. Furthermore, more than 80% of the interviewees had family members working in nearby cities or urbanized areas, providing financial support through remittances. This is important to consider when interpreting the study's findings because it may affect the community's reliance on and perception of the HREM project.

Overall, the sample was thought to be a fairly typical representation of the population of Rogongon, a rural agricultural community in Iligan City, Philippines. The sample size and composition were determined to be adequate for providing a representative snapshot of the community's attitudes and perceptions of the proposed HREM development. It is important to note, however, that the sample may not be perfectly representative of the entire population due to biases and limitations in the sampling method used. For example, the sample may over- or under-represent certain demographic groups. Furthermore, the sample size of 55 respondents may be considered small and may not adequately represent the community's diversity of opinions and experiences. As a result, the findings of this study should be interpreted with caution and should not be generalized to the entire population without additional research.

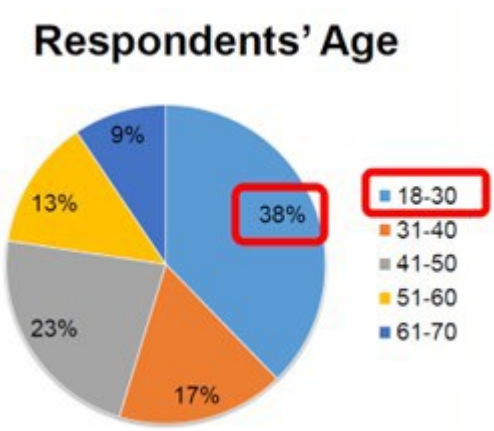

Figure 6.5 Age Group Distribution of Survey Respondents

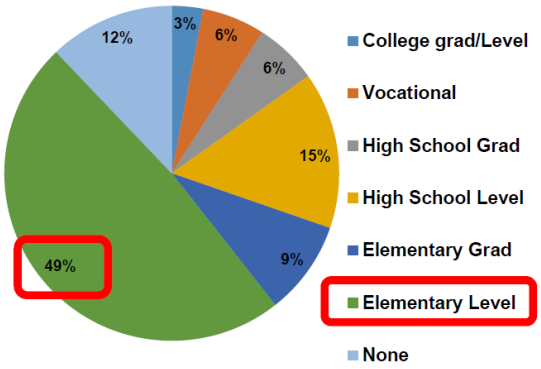

Figure 6.6 Educational Attainment Distribution of Survey Respondents

6.2.8 Model Implementation and Analysis of the Data

As shown in Figure 6.7, SPSS Amos 28 was used to perform structural equation modeling (SEM) in order to validate the proposed model. The structural equation modeling, or SEM, statistical analysis process allows you to validate the data fit of previously established models. The technique also includes confirmatory factor analysis (also known as CFA) and regression analysis. CFA is used to validate measurements of latent components, whereas regression analysis is used to estimate the pathways that connect the latent constructs [6-22]. The t-tests were run in SPSS 28 to see if there was a statistically significant difference in mean values.

The diagram's notation is shown in Figure 6.8. The SEM is made up of indicators, latent

variables, and observed variables. Latent variables are variables that cannot be directly observed or measured and must instead be inferred indirectly from other observable variables using a mathematical model. These observable variables can be observed directly. The implemented main model includes four latent variables: perceived benefits, trust in experts, perceived costs, and acceptance of HREM, as well as three observed variables: provision of information, participation options, and perceived environmental impact.

The diagram for measuring common factor loadings is shown in Figure 6.9. The factor loadings are calculated to determine whether an indicator is acceptable or not. Factor loading is defined as the correlation coefficient between the variable and the factor. The proportion of variation explained by a variable on a specific factor is referred to as factor loading. A factor loading of 0.5 or greater in the SEM method indicates that the factor adequately removes variation from the variable.

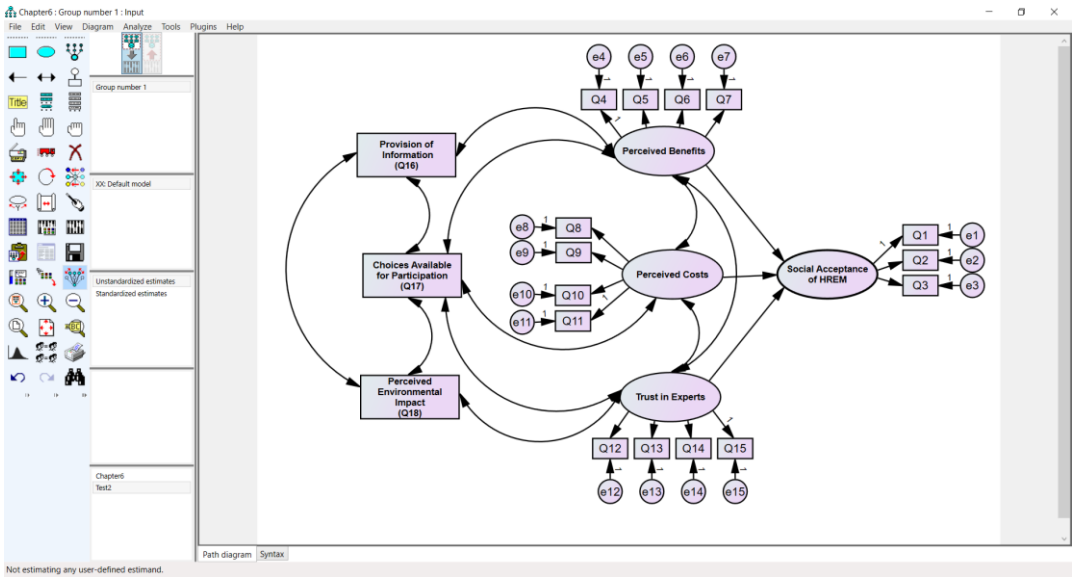

Figure 6.7 Educational Attainment Distribution of Survey Respondents

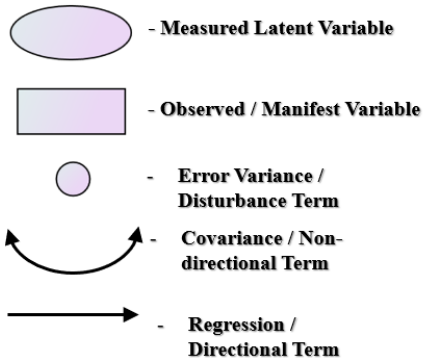

Figure 6.8 Diagram Notation in SPSS Amos 28

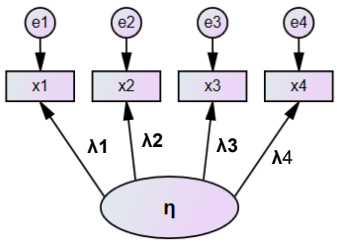

λ = Factor Loadings
= correlation between factor & indicator

Figure 6.9 Diagram for Measuring Common Factor Loadings

6.3. Results of the Analysis

6.3.1 Survey Results

After conducting information dissemination activities and interviewing several households, the household survey results were analyzed and tabulated. Table 6.4 summarizes the mean, standard deviation, and standard factor loadings calculated from the survey responses. The table breaks down the questionnaire items by scale, complete with averages, standard deviations, and factor loadings based on standardization.

Acceptance of HREM, perceived benefits of HREM, perceived costs of HREM, and trust are all latent variables in the main model. The three observed variables are information provision,

participation options, and perceived environmental impact of HREM construction.

According to the findings, the mean for HREM acceptance is 4.96, indicating a positive attitude toward the proposed HREM development. The mean for perceived HREM benefits is 4.88, indicating a favorable attitude toward the HREM's potential benefits. The mean for perceived HREM costs is 2.63, indicating a neutral to slightly negative attitude toward the potential HREM costs. The mean for trust in experts is 5.03, indicating a positive attitude toward the HREM development experts. Additionally, the results also show that the experts provided information on the HREM to the majority of the respondents during the pre-feasibility and planning phases, and that options for participation were provided during the HREM planning. The majority of respondents did not believe that the construction of HREM would have a significant impact on the local environment.

The detailed information model includes two latent variables: information quality and information quantity. The results show that the mean for information quality is 4.50, indicating a favorable attitude toward the information provided. The majority of respondents felt they had received adequate information about the HREM. Furthermore, survey results show a relatively positive attitude toward the proposed HREM development, with the majority of respondents supporting the project and believing that it will improve their standard of living by providing affordable and reliable electricity. The perceived benefits of the HREM, as measured by survey items 4-7, had an average mean of 4.88, indicating that respondents generally believed the HREM would improve their lives.

The perceived costs of the HREM, as measured by items 8-11, had an average mean of 2.63, indicating that respondents were concerned about the project's potential negative consequences. However, their concerns were not as strong as their support for the HREM's benefits. The average mean of the trust in experts, as measured by items 12-15, was 5.03, indicating that respondents generally trusted the experts involved in the HREM's planning and development. The findings also revealed that the majority of respondents were given information about the HREM during the pre-feasibility and planning phases, as well as options for participation. However, a sizable proportion of respondents believed that the construction of HREM would severely harm the local environment.

Overall, these findings indicate that, while some people are concerned about the HREM's potential negative effects, the vast majority of the surveyed community supports the project and believes it will improve their lives.

Table 6.4 Items in the questionnaire broken down by scale, complete with averages, standard deviations, and factor loadings according to standardization

ITEM PER SCALE	MEAN ($\bar{x}$)	STANDARD DEVIATION (*S.D.*)	STANDARDIZED FACTOR LOADINGS (λ)
Main Model			
Acceptance of HREM **(6-point Likert scale)**			
① I'm delighted that an HREM is being considered for development in my community.	4.82	0.80	0.77
② I support the proposed HREM and will voluntarily participate in the protection and maintenance of it.	4,98	0.85	0.68
③ How do you rate the proposed HREM?	5.07	0.84	0.88
Perceived benefits of HREM **(6-point Likert scale)**			
④ I believe the proposed HREM will improve my standard of living.	4.87	0.75	0.74
⑤ I believe the proposed HREM will provide an affordable and reliable electricity.	4.96	0.88	0.68
⑥ The proposed HREM makes me feel good, because it's environmentally friendly.	4.69	0.72	0.81
⑦ I think the proposed HREM is beneficial to our livelihood.	4.98	0.78	0.54
Perceived costs of HREM **(6-point Likert scale)**			
⑧ I think the HREM will impair the quality of living in the community.	5.02	0.71	0.85
⑨ The proposed HREM will hurt me financially or it is not affordable.	1.45	0.50	0.73
⑩ I think the proposed HREM in the community will spoil the natural landscape.	2.00	0.82	0.56
⑪ I think the proposed HREM will deter the electricity connection from local distribution company.	2.05	0.83	0.63
Trust **(6-point Likert scale)**			
⑫ The experts treats and involves me fairly.	5.07	0.79	0.86
⑬ The experts are experienced and expert enough to ensure a safe and successful construction of HREM.	5.02	0.78	0.89
⑭ The experts appreciates the local residents' concerns.	4.93	0.77	0.92
⑮ The experts are knowledgeable on renewable energy and HREM.	5.11	0.83	0.86
Provision of Information **(0 'no', 1 'yes')**			
⑯ Did you get information on the HREM from the people responsible (experts) during the pre-feasibility and planning phase?	0.87	0.34	
Options for Participation **(-1 'no options provided', 0 'any options provided')**			
⑰ What participations options were you given	−0.13	0.34	

during the planning of the HREM? ***Perceived Environmental Impact of HREM Construction* (0 'no', 1 'yes')** ⑱ Do you think the construction of HREM will severely damage the local environment?	0.56	0.50	
Detailed Information Model ***Quality of the information* (6-point Likert scale)** ① All of the advantages and disadvantages of the HREM were honestly described in the material/project presentation that was supplied.	4.12	0.71	0.87
② I think the information was fair and accurate.	4.57	0.69	0.90
③ The information has been presented in a manner that is easy to comprehend.	4.67	0.82	0.77
④ I believe that the information that was provided to me was correct at all times.	4.63	0.81	0.76
***Quantity of the information* (1 'not enough' 2 'enough')** ⑤ Were you provided with an adequate amount of information?	1.87	0.33	0.85
Timing of the Information (1 'not soon enough', 2 'early enough') ⑥ Do you believe that information on the plans for an HREM in your community was communicated to you in a timely manner?	1.89	0.36	

6.3.2 Analysis of Community Acceptance towards the Proposed HREM Development

According to the survey and analysis results, a significant percentage of the surveyed residents are open to the idea of HREM implementation. Respondents to the questionnaire were asked to rate how well the planned HREM would work in their community as a whole on a scale of 1 (strongly disagree) to 6 (strongly agree). The mean response was 4.96, with a standard deviation of 0.83, indicating that the proposed HREM has relatively high local acceptability in the study area. This is a significant finding because it indicates that the community is open to the concept of HREM development. Furthermore, there are significant differences in acceptance levels between local residents who perceive a negative environmental impact of HREM ($\bar{x}$ = 4.71, *S.D.* = 0.79) and those who do not ($\bar{x}$ = 5.08, *S.D.* = 0.85) (t = -8.86, p =.0001, d =.65). These differences are significant because they show that residents who do not perceive a negative environmental impact from HREM are more accepting of it. This suggests that the perceived

environmental impact of HREM has a significant impact on the proposed development's local acceptance.

6.3.3 Evaluation of the Model's Fit and Factors Affecting HREM Acceptance

The Confirmatory Factor Analysis (CFA) results and model fitness evaluation show that the main model hypothesized for the study has a good fit and accounts for a significant portion of the variation in the acceptability of the proposed HREM in the local community. Various fit statistics, such as the p-value, Root Mean Square Error of Approximation (RMSEA), and Comparative Fit Index, were used to assess the model's fit (CFI). The values of these fit statistics indicate that the model has a good fit, with a p-value of 0.0001, RMSEA of 0.046, and CFI of 0.963. This suggests that the model is a good representation of the data and that the relationships between the variables in the model are supported by the data. Figure 6.10 shows the SEM procedure for the main model, which illustrates that acceptance, perceived benefits, perceived costs, and trust all have considerable and significant factor loadings ($\lambda > .51$) in the CFA. These factor loadings indicate the degree to which the variables in the model are related to the factors they represent. Table 6.4 presents the standard loads that are assigned to each item of the questionnaire, providing further detail on the relationships between the variables in the model. Overall, the CFA findings and assessment of the model's fitness show that it is a good representation of the data and the relationships between the variables in the study and offer strong support for the main model.

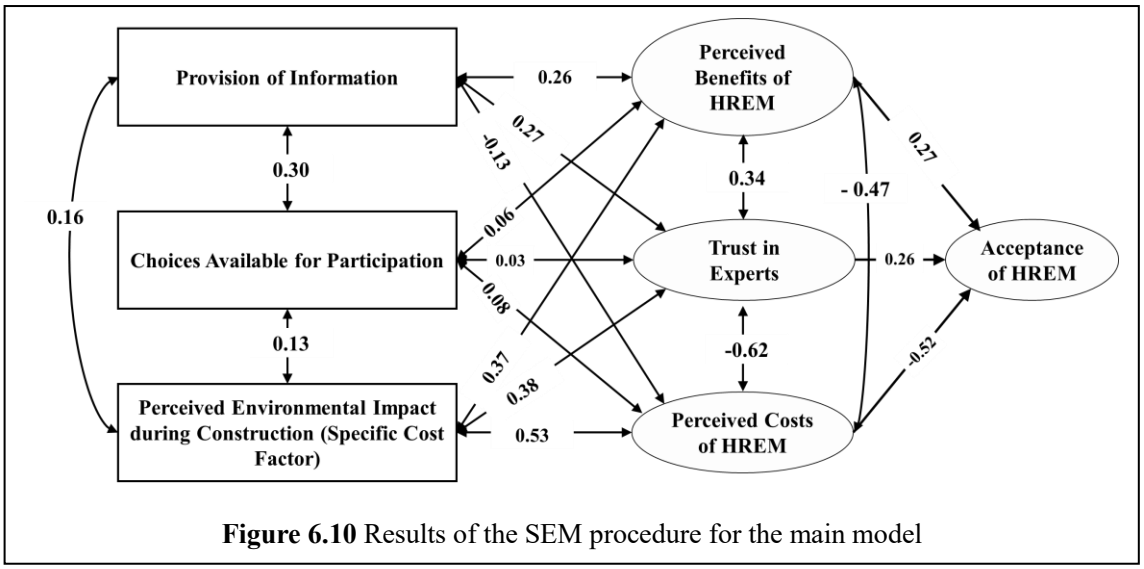

Figure 6.10 Results of the SEM procedure for the main model

6.3.4 Influence of trust in experts and perceived costs and benefits of HREM

According to the findings of the Confirmatory Factor Analysis (CFA), there is a significant correlation between the local community's acceptance of the proposed development of a Hybrid Renewable Energy System (HREM) and trust in the technical knowledge of experts, as well as the perceived benefits and costs of the HREM. Figure 6.10, which presents information on the model's standard structural parameters, illustrates the correlation between these two variables very clearly. The standardized regression weights of the direct factors, which include perceived benefits (β = 0.27) and perceived costs (β = -0.52), as well as trust in experts β (= 0.26), are all statistically significant (p 0.001) and are in line with what was anticipated. A positive correlation (β = 0.34) was found between trust in experts and perceived benefits, while a negative correlation (β = -0.62) was found between trust in experts and perceived costs. There was also discovered to be a negative correlation between the perceived benefits and the perceived costs (β = -0.47). In addition, it was found that the direct factors have a robust and significant intercorrelation, which suggests that trust in experts has a positive relationship with perceived benefits (β = 0.34) and a negative relationship with perceived costs (β = -0.6). This was found to be the case as a result of the fact that the direct factors have a strong and significant intercorrelation.

These findings shed light on the factors that influence HREM acceptance in the local community. They contend that a positive perception of the benefits of HREM, as well as high levels of trust in the project's experts, can lead to greater acceptance of the proposed HREM development. However, a negative perception of the costs of HREM, as well as a lack of trust in the experts, can lead to lower acceptance. This data can be used to guide future efforts to increase support for renewable energy projects. Policymakers and project developers, for example, could focus on raising public awareness of the benefits of HREM and on fostering trust and engagement with the local community. Furthermore, they could work to mitigate any negative perceptions of HREM costs, such as concerns about environmental impact or economic costs. Overall, these findings emphasize the importance of taking into account public perceptions and trust in experts when planning and implementing HREM projects.

6.3.5 Influence of Perceived Environmental Impact on HREM Acceptance

Based on the results of this study, the perception of the environmental impact of the proposed HREM development is an important factor in shaping community acceptance of the project. According to the data, the perception of environmental impact has a direct influence on key acceptance factors such as perceived benefits ($\beta = 0.37$), perceived costs ($\beta = 0.53$), and trust in experts ($\beta = 0.38$) (all $p < 0.001$). Furthermore, the study discovered that environmental impact has an indirect effect on acceptance by shaping perceptions of perceived benefits, perceived costs, and trust in experts, with an overall impact of $\beta = 0.49$ ($\beta = 0.28$ via perceived costs, $\beta = 0.11$ via perceived benefits, and $\beta = 0.11$ via trust in experts, all $p < 0.001$). These findings emphasize the importance of addressing perceived negative environmental impacts in order to increase local community support for the proposed HREM development. Future efforts to increase support can be better targeted and more effective if we understand the role that perception of environmental impact plays in shaping perceptions of the proposed HREM development.

6.3.6 Influence of Information Provision and Participation Options on HREM Acceptance

Results of the analysis show that the provision of information to the residents has a significant and positive effect on acceptance, as it influences perceptions of perceived benefits ($\beta = 0.24$, $p < 0.001$), perceived costs ($\beta = 0.11$, $p < 0.05$), and trust in experts ($\beta = 0.26$, $p < 0.001$). This suggests that providing residents with clear and accurate information about the proposed HREM development could help increase support for the project. This is an important finding because it emphasizes the importance of effective communication strategies in promoting community-based sustainable energy projects. Clear and accurate information can help residents understand the potential benefits and costs of the proposed HREM development, as well as boost their trust in the project's experts and decision-makers.

According to the findings of the study, the dissemination of information has a substantial and indirect impact on the degree to which members of the community are willing to accept the proposed HREM development. It was discovered that the impact of information on acceptance was significant, with a β value of 0.21 (p 0.001) for the statistic. In addition, the study discovered that trust in experts, perceived costs, and perceived benefits all have indirect effects on acceptance, with β values of 0.07 ($p < 0.05$), 0.07 ($p < 0.001$), and 0.07 ($p < 0.001$), respectively. These values were based on the statistical significance of the relationship between each variable and acceptance. These findings suggest that residents are more likely to agree to the proposed HREM development if they have access to accurate and readily available information about the planned HREM development and how it may impact both them and their neighborhood. Additionally, these findings suggest that residents are more likely to oppose the proposed HREM development if they do not have access to this information. This highlights how important it is to provide residents with information that is not only clear but also factual in order to build trust, confidence, and support for proposed HREM developments.

Other findings of this study, on the other hand, does not support the hypothesis that an indirect impact of options for participation influences HREM acceptability. The influence that options for participation have on perceived benefits is a β value of 0.06, which is not statistically significant. In addition, the impact or influence that it has on perceived costs is a β value of 0.08, which is a value that is not significant. This suggests that, while providing information may have a positive impact on perceptions of benefits and trust in experts related to the proposed HREM

development, it may not have a significant impact on perceived costs. However, it is important to note that even a minor change in perceived costs can have a significant impact on overall acceptance. It is also worth considering the possibility of providing information on cost-cutting measures or addressing cost-related concerns in the community.

Furthermore, the lack of a significant effect of participation options on acceptance emphasizes the importance of providing residents with clear and accurate information in order to promote support for sustainable energy projects. Effective communication and engagement strategies can help address misconceptions and concerns, as well as increase understanding of the proposed HREM development's potential benefits and costs. This can eventually lead to a more informed and supportive community, as well as a higher likelihood of success for local sustainable energy projects.

6.3.7 Influence of Provision of Information and Options for Participation on HREM Acceptance

The term "timeliness" relates to the time frame during which one would anticipate information to be accessible and readily available. When referring to information, timeliness may be defined as the amount of time that elapses between when it is anticipated that the information will be available and when it is really accessible for use.

Since it was found that the participation choices in the primary model did not have a substantial affect, the comprehensive study of time, quality, and quantity was carried out only for the purpose of providing information. During the period of pre-feasibility and planning, there were a total of 55 persons who received project information about the planned HREM from experts. These participants were given the task of evaluating not just the quantity of information that was provided but also the timing at which it was presented as well as the level of accuracy of the information. Because the original distributions of timing and quantity contained floor effects, these variables needed to be recoded (23.6% of respondents claimed to have received not enough information, 76.4% just the right amount, and only 0.7% reported receiving too much information; 12.7% of respondents claimed to have received information too late, and 83.6% at the right time, and only 3.6% claimed to have received information too early). The number of participants who

reported to have received an excessive quantity of information or to have received the material too early was eliminated from the analysis, which brought the total number of participants in the sample down to N=13. The number of participants who reported to have received the material too early was also eliminated from the analysis. The factors were then split into two groups: time, which was categorized as "not soon enough" or "early enough," and amount, which was categorized as "not enough" or "enough" (quantity).

The data are well represented by the model ($p = 0.4067$, RMSEA = 0.016, and CFI = 0.995), and the model accounts for 58.2% of the variance in the degree to which the local community accepts the HREM. While the notion of acceptability and the quality of information are both complicated and made up of a number of different aspects, the concepts of information quantity and information timeliness are each comprised of a single detail. According to the findings of the confimatory factor analysis, both the acceptability and information quality constructs had substantial and significant factor loadings, with λ values that were larger than 0.72 (p 0.001 to be exact). However, neither the amount of information presented nor the time of its presentation had a significant influence on acceptance with a β value of 0.06. Nor did the quantity of information presented have a significant impact on acceptance, with a β value of 0.02. On the other hand, the quality of the information had a substantial influence on HREM acceptance (β value of 0.72, with p less than 0.001), and it is the only standardized structural parameter that has a significant impact on the way in which the local community responds to the proposed HREM.

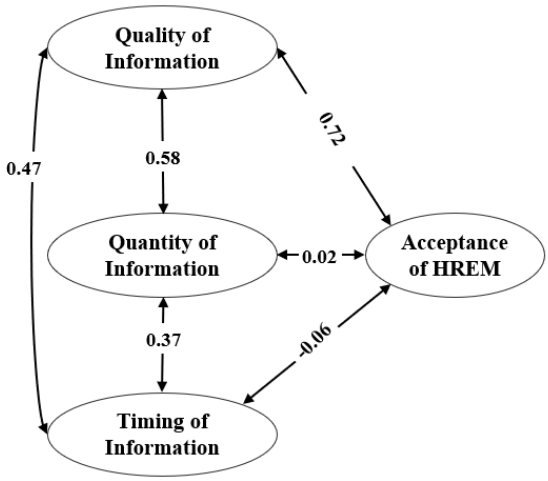

Figure 6.11 Results of the SEM procedure for the detailed information model

6.4. Overall Discussion of the Results of the Analysis

Table 6.5 provides a concise summary of the investigation's findings. The community's level of trust or confidence in the experts or researchers conducting the study will be one of the most influencing factors in determining how well the planned HREM will be received in the community. Consideration must also be given to the HREM's perceived benefits and associated costs. The inverse relationship between perceived benefits and perceived costs is not unexpected. Nonetheless, it is noteworthy to discover that trust in the expertise of project developers and researchers is correlated with both of these variables and should be investigated further. Higher levels of perceived benefits are positively correlated with higher levels of trust, whereas higher levels of perceived costs are negatively correlated with lower levels of trust. Consequently, ensuring fairness in the distribution of both positive and negative HREM outcomes can foster trust and acceptance, whereas failing to do so can erode trust. Additionally, acceptance can be promoted by ensuring the equitable distribution of both positive and negative HREM outcomes. On the other hand, individuals with a higher level of trust in the authorities are more likely to view the HREM's benefits and costs favorably. A lack of community trust may lead to an overestimation of the HREM's cost-benefit ratio. On the other hand, a sufficient level of community trust may act as a buffer against negative outcomes and a motivator for positive outcomes. The importance of trust in gaining acceptance should not be minimized, despite the

fact that it is not the most important variable.

Table 6.5 Summary of correlation between different variables

Variable 1		Variable 2		β-value	Interpretation	Remarks
Name	**Type**	**Name**	**Type**			
Perceived Benefits	Latent	Acceptance of HREM	Latent	0.27	Significant Positive Correlation	H_1 is supported
Trust in Experts	Latent	Acceptance of HREM	Latent	0.26	Significant Positive Correlation	H_2 is supported
Perceived Costs	Latent	Acceptance of HREM	Latent	- 0.52	Significant Negative Correlation	H_3 is supported
Provision of Information	Observed	Acceptance of HREM	Latent	0.2	Significant Positive Correlation	H_4 is supported
Choices Available for Participation	Observed	Acceptance of HREM	Latent	0.01	Not Significant Indirect Positive Correlation	H_5 is not supported
Perceived Environmental Impact	Observed	Acceptance of HREM	Latent	0.49	Significant Indirect Negative Correlation	H_6 is supported

Individuals who hold negative views on the potential environmental impact of the proposed HREM exhibit higher levels of perceived costs and lower levels of perceived benefits. This is in comparison to individuals who do not believe they are affected by the potential environmental impact of the proposed HREM. The results of the study lend credence to two separate findings and conclusions. It is possible to draw the conclusion, from a psychological point of view, that the perception of an impact on the environment leads to the belief that there must be costs and, as a result of reactance, that there cannot be significant benefits. This could be due to the widespread belief that environmental damage will have a negative impact on businesses and their bottom lines. This perception then leads to larger reported spending and fewer benefits, even though the actual levels of costs and benefits are lower. This occurs despite the fact that the actual levels of both costs and benefits are lower.

The community's acceptance of the HREM was significantly influenced, in a positive way, by the information that was gathered. Compared to respondents who claimed they had not been made aware, those who claimed to have been informed by those involved in the planning and development process had higher levels of perceived benefits and lower levels of perceived costs.

This demonstrates the significance of effectively communicating information throughout the entire planning and development process in order to raise awareness of the HREM's advantages and mitigate concerns regarding its potential expenses. Those respondents who were given information had a greater likelihood of having trust in the professionals compared to those who were not given information, which led to an increase in trust overall. However, in comparison to the impact on perceived benefits and trust in the plant operator, the effect of received information on perceived costs was much less significant and, in some cases, even detrimental. This suggests that the information provided may not contain sufficient detail about the costs associated with the HREM, or that local residents may not trust this information as much as they do information about the benefits of the proposed microgrid, as they consider it to be less objective. Alternatively, this suggests that the information may not contain sufficient detail about the costs associated with the HREM.

6.5. Policy-making Implications

Major decisions in the Philippines, such as increasing rural electrification, promoting microgrids, and exploitation of energy, are influenced by energy policymakers' decisions. As the results of this study show the importance of provision of information to local residents, policies should be made and promoted in providing education and information dissemination to target rural areas that need to be electrified. Since most of the residents are likely to have lower educational attainment, specialized approach should be done in order to effectively provide renewable energy education them.

The results also show that there is a high significant negative correlation between “Perceived Cost” and “Acceptance of HREM” which means that residents are more concerned about the costs compared to the other factors. Thus, the government should provide subsidy for this rural electrification projects such as HREMs. Furthermore, different financing schemes and models should also be introduced to lower the overall cost of installation and operation of such projects.

6.6. Summary

The results of this investigation showed that both hypothetical models that were examined were a good match for the data. Due to the large percentage of variation explained (83.6%), it can be deduced that while developing the main model, no significant factor playing a role in determining local acceptability was overlooked. Furthermore, the findings of this study, with the notable exception of the non-existent influence of participation choices, are consistent with the findings of prior quantitative studies. The discovery and discussion of connections between elements that influence local acceptability is one of the innovative aspects of this study. It was found that structural equation modeling was a reliable method for identifying such correlations. This made it possible to conduct an in-depth investigation into the ways in which various factors, such as trust in experts, perceived benefits and costs, as well as the perceived environmental impact, information, and participation, influence both one another and local acceptance.

6.7. Chapter 6 References

[6-1] R. C. Larson, "Service science: At the intersection of management, social, and engineering sciences," *IBM Syst. J.*, vol. 47, no. 1, pp. 41–51, 2008, doi: 10.1147/sj.471.0041.

[6-2] B. Hefley and W. Murphy, Eds., *Service Science, Management and Engineering Education for the 21st Century*. Boston, MA: Springer US, 2008. doi: 10.1007/978-0-387-76578-5.

[6-3] F. Norouzi, T. Hoppe, L. R. Elizondo, and P. Bauer, "A review of socio-technical barriers to Smart Microgrid development," *Renew. Sustain. Energy Rev.*, vol. 167, p. 112674, Oct. 2022, doi: 10.1016/j.rser.2022.112674.

[6-4] A. Rodriguez Zabala, D. López-García, S. X. Carvajal-Quintero, and A. Arango Manrique, "A Comprehensive Review of Sustainability in Isolated Colombian Microgrids," *Tecnura J.*, vol. 25, no. 70, pp. 126–145, Oct. 2021, doi: 10.14483/22487638.18619.

[6-5] A. Boche, C. Foucher, and L. F. L. Villa, "Understanding Microgrid Sustainability: A Systemic and Comprehensive Review," *Energies*, vol. 15, no. 8, p. 2906, Apr. 2022, doi: 10.3390/en15082906.

[6-6] M. Soshinskaya, W. H. J. Crijns-Graus, J. M. Guerrero, and J. C. Vasquez, "Microgrids: Experiences, barriers and success factors," *Renew. Sustain. Energy Rev.*, vol. 40, pp. 659–672, Dec. 2014, doi: 10.1016/j.rser.2014.07.198.

[6-7] A. Saxena, G. M. Patil, N. Kumar Agarwal, A. Singh, A. Prakash, and K. Sharma, "Environmental and Social Aspects of Microgrid Deployment- A Review," in *2021 IEEE 8th Uttar Pradesh Section International Conference on Electrical, Electronics and Computer Engineering (UPCON)*, Dehradun, India, Nov. 2021, pp. 1–5. doi: 10.1109/UPCON52273.2021.9667612.

[6-8] M. Wolsink, "The research agenda on social acceptance of distributed generation in smart grids: Renewable as common pool resources," *Renew. Sustain. Energy Rev.*, vol. 16, no. 1, pp. 822–835, Jan. 2012, doi: 10.1016/j.rser.2011.09.006.

[6-9] M. Wolsink, "Wind Powerwind power: Basic Challenge Concerning Social Acceptancewind powersocial acceptance," in *Encyclopedia of Sustainability Science and Technology*, R. A. Meyers, Ed. New York, NY: Springer New York, 2012, pp. 12218–12254. doi: 10.1007/978-1-4419-0851-3_88.

[6-10] M. Wolsink, "Wind power implementation: The nature of public attitudes: Equity and fairness instead of 'backyard motives,'" *Renew. Sustain. Energy Rev.*, vol. 11, no. 6, pp. 1188–1207, Aug. 2007, doi: 10.1016/j.rser.2005.10.005.

[6-11] R. Wüstenhagen, M. Wolsink, and M. J. Bürer, "Social acceptance of renewable energy innovation: An introduction to the concept," *Energy Policy*, vol. 35, no. 5, pp. 2683–2691, May 2007, doi: 10.1016/j.enpol.2006.12.001.

[6-12] K. Schumacher, "Public acceptance of renewable energies – an empirical investigation across countries and technologies".

[6-13] P. Devine-Wright and B. Wiersma, "Understanding community acceptance of a potential offshore wind energy project in different locations: An island-based analysis of 'place-technology fit,'" *Energy Policy*, vol. 137, p. 111086, Feb. 2020, doi: 10.1016/j.enpol.2019.111086.

[6-14] B. R. Upreti, "Conflict over biomass energy development in the United Kingdom: some observations and lessons from England and Wales," *Energy Policy*, vol. 32, no. 6, pp. 785–

800, Apr. 2004, doi: 10.1016/S0301-4215(02)00342-7.

[6-15] N. Simcock, “Procedural justice and the implementation of community wind energy projects: A case study from South Yorkshire, UK,” *Land Use Policy*, vol. 59, pp. 467–477, Dec. 2016, doi: 10.1016/j.landusepol.2016.08.034.

[6-16] N. Kluskens, V. Vasseur, and R. Benning, “Energy Justice as Part of the Acceptance of Wind Energy: An Analysis of Limburg in The Netherlands,” *Energies*, vol. 12, no. 22, p. 4382, Nov. 2019, doi: 10.3390/en12224382.

[6-17] U. Liebe, A. Bartczak, and J. Meyerhoff, “A turbine is not only a turbine: The role of social context and fairness characteristics for the local acceptance of wind power,” *Energy Policy*, vol. 107, pp. 300–308, Aug. 2017, doi: 10.1016/j.enpol.2017.04.043.

[6-18] L. Liu, T. Bouman, G. Perlaviciute, and L. Steg, “Effects of trust and public participation on acceptability of renewable energy projects in the Netherlands and China,” *Energy Res. Soc. Sci.*, vol. 53, pp. 137–144, Jul. 2019, doi: 10.1016/j.erss.2019.03.006.

[6-19] P. Dirksmeier and L. Tuitjer, “Do trust and renewable energy use enhance perceived climate change efficacy in Europe?,” *Environ. Dev. Sustain.*, May 2022, doi: 10.1007/s10668-022-02421-4.

[6-20] C. Büscher and P. Sumpf, “‘Trust’ and ‘confidence’ as socio-technical problems in the transformation of energy systems,” *Energy Sustain. Soc.*, vol. 5, no. 1, p. 34, Dec. 2015, doi: 10.1186/s13705-015-0063-7.

[6-21] M. Soland, N. Steimer, and G. Walter, “Local acceptance of existing biogas plants in Switzerland,” Energy Policy, vol. 61, pp. 802–810, Oct. 2013, doi: 10.1016/j.enpol.2013.06.111.

[6-22] R. B. Kline, *Principles and practice of structural equation modeling*, 3rd ed. New York: New York: Guilford Press.

Chapter 7 Conclusions

This chapter summarizes the conclusions and main achievements of this thesis

7.1. Summary and Main Achievements of this Thesis

A local scale assessment of multiple renewable energy resources (solar, wind, and hydro) was done using various GIS tools, models, and algorithms which include r.sun, SWAT, head algorithm and WRF. The results show that the study area has high solar energy potential in the coastal areas. Results also show that the western part of the study area has high wind energy potential while several potential hydro energy sites were identified. As a result, the first issue was addressed.

A comprehensive and integrated methodology for determining suitable sites for single type and hybrid renewable energy systems was created using GIS and Fuzzy-Analytic Hierarchy Process (AHP). The single type of renewable energy systems that were considered were solar-photovoltaic (PV), wind power, and hydropower systems. The hybrid renewable energy systems that were considered are hybrid wind solar-PV and hydropower solar-PV. The identified sites were also mapped and analyzed. As a result, the second issue was solved.

An alternative method of ETL routing was done by utilizing a modified EPRI-GTC methodology and applying needed changes based on the available data and review of the study area, The ETL routing process was also influenced by related works, which introduced a weighted ranking system and a suitability index for geographic factors. The results produced three alternative routes based on three perspectives: the built environment, natural environment, and engineering environment, after applying the Least Cost Path (LCP) algorithm of ArcGIS. The alternative routes are then overlaid based on a simple combined perspective to create the final route. Moreover, the alternative routes were evaluated to provide secondary routes and the routes developed from an engineering perspective were nominated. As a result, the third issue was addressed.

A comprehensive modeling of HREM was done and integrated methodology of optimal sizing and operation of HREM was developed by utilizing a modified multi-objective particle swarm optimization (MOPSO) algorithm that is capable of simultaneous optimization of multiple

conflicting objectives with several constraints and a proposed multi-case power management strategy. As a result, the fourth issue was solved.

Several indirect and direct factors affecting the acceptance of HREM were investigated and analyzed using a hypothetical framework that was developed. The implications of expert's opinion (formed from results of from Chapters 2 to 5) on acceptance of HREM was also investigated and analyzed. Results from the analysis can aid policymakers in improving acceptance of microgrid projects in unelectrified rural agricultural areas.

7.2. Future Works and Recommendations

In order to improve the country's electrification while minimizing the burden on the communities, it is advised that geospatial tools and high-resolution datasets be used to assess the hydropower resources specific to other hydropower systems, particularly pumped hydropower systems. These emerging technologies harness existing resources like water and gravity.

An accurate estimate of the wind resource is essential for the construction of wind farms. A good NWP model is necessary since wind is such a sensitive meteorological variable. It is suggested that you enhance your wind estimate by using the most recent WRF model. It would be preferable if the processing took into account climatological data spanning 30 years in order to investigate the wind variability in the Philippines in more detail. Additionally, the accuracy of wind assessment may be increased by using more recent land data, higher resolution topographic data, and data assimilation in the WRF model. For more sophisticated methods, the parameters within the parameterization scheme may be changed to be more appropriate with the climate in the Philippines.

The geographical models may also assist with the regulatory procedure and the expansion of renewable energy in the province. In addition, policymakers and pertinent organizations may utilize the data generated by this study to manage, plan, and develop renewable energy resources. In addition to providing a current and reliable pre-feasibility study background for possible investors, this will most importantly benefit power users, especially those who live in remote areas without access to energy.

For the alternative method for ETL routing presented in this research, potential flaws and

weaknesses can be uncovered with a review scrutinizing the results of the study. Furthermore, assessments for applicability of the alternative method can be done through more case studies. Also, high accuracy and up-to-date spatial data, including satellite images can be used to ensure maximum accuracy of the routes created.

The results of this study demonstrate the importance of providing information and encouraging participation in addition to location and close proximity in influencing community acceptance of HREM. This is in addition to the crucial technical indicators of suitable sites. In doing so, the research emphasizes how community and sociopolitical aspects of social acceptability are interdependent. Future study should examine these interdependencies, especially in light of judgments of the efficacy of different social science approaches (focus groups, surveys) as sources of information regarding public acceptability to support policy change.

Additionally, investigating and developing techniques for handling other uncertainty factors in the design and optimization of HREMs, as well as microgrid stability, might prove important. This work's important findings and contributions can be used for future studies in the area of developing deep learning or artificial neural network algorithms for a more flexible solution to the optimization issue. Furthermore, more research into techniques to enhance the reliable and economically justifiable use of diverse renewable energy sources in microgrids and power systems could also be the focus of future studies. More study is required to find the most effective strategy to employ excess RE in off-grid HREMs.

Overall, the proposed framework for design and assessment of HREM using various GIS and optimization techniques is comprehensive covering multiple processes and considering social, environmental, technical, and economic aspects. The framework can serve as a reference for island microgrids assessments and can be replicated to other HREM sites. Other types of HREM can also be used in the framework. Furthermore, the study’s results will be valuable in the management of renewable energy resources, planning and development, and rural electrification.

ACKNOWLEDGMENT

As I embark on the next chapter of my life, I look back on my journey through my doctoral program with immense gratitude for the many people who have supported and encouraged me along the way.

My advisor, Professor Yosuke Nakanishi of Waseda University, deserves special recognition for his unwavering guidance, invaluable insights, and constant motivation. His kind and accepting nature, patience, and understanding made him the perfect mentor, and I am forever grateful for the opportunity to have learned from him.

I am also deeply grateful to the panel members of my dissertation, Professors Takashi Nozu and Hiroshi Onoda, for their valuable input, constructive feedback, and expert guidance that helped shape and improve my research. I am also thankful to the Power System and Environment Lab at the Graduate School of Environment and Energy Engineering at Waseda University for providing me with a rich and enlightening experience. I would like to extend my gratitude to Prof. Shinichi Iwamoto, Prof. Hiroshi Takamori, Prof. Kenji Iba, Dr. Kazuaki Iwamura, Ms. Chie Hanaoka and Yining "Steven" Chen for sharing their expertise, guiding me throughout the conduct of my research, and for their contributions in the lab's efforts. I am also grateful for the friendships I made in the laboratory, who supported me throughout my research.

I am also grateful to my colleagues at the Department of Electrical Engineering and Technology (DEET) at the College of Engineering and Technology, Mindanao State University—Iligan Institute of Technology, particularly Professors Noel Estoperez, Anacita Tahud, and Karl Martin Aldueso, for taking on my responsibilities and providing guidance, emotional and moral support, and financial assistance while I pursued my education in Japan. I am also thankful to the Ministry of Education, Culture, Sports, Science and Technology of Japan (MEXT), the Department of Science and Technology – Engineering Research and Development for Technology – Faculty Development Program (DOST-ERDT FDP) Foreign PhD Scholarship and the e-Asia Joint Research Program for awarding me a scholarship that helped me cover the costs of my Doctor of Philosophy program and living expenses in Japan. I also appreciate Mindanao State University-Iligan Institute of Technology for allowing me to study abroad while being employed

by them.

I would like to express my sincerest gratitude to my family and friends in the Philippines for their unconditional love, support and encouragement throughout this journey. My parents, Rufino and Rosalinda Tarife, and grandparents, Vicente and Nenita Pelos, have been my constant source of inspiration and support. I would also like to thank my close friends Henrik Rossmann, Shara Astillero, Kento Fujimori, and Jennica Fujimori for being my support system and listening ear during my time in Japan. They have truly become my second family and I am forever grateful for their love and support. This dissertation would not have been possible without the support and encouragement of all of these people and for that, I am eternally grateful.

Lastly, I would also like to give thanks to my Lord and savior Jesus Christ and the Almighty Father for giving me the strength and guidance to finish this journey. I couldn't have done this without Your grace and guidance.